AD-A061 823 COLD REGIONS RESEARCH AND ENGINEERING LAB HANOVER N H F/G 14/5
ESTUARINE PROCESSES AND INTERTIDAL HABITATS IN GRAYS HARBOR, WA--ETC(U)
JUL 78 L W GATTO IAO-CWP-S-75-9
UNCLASSIFIED CRREL-78-18 NL

1 OF 2
AD
A061823

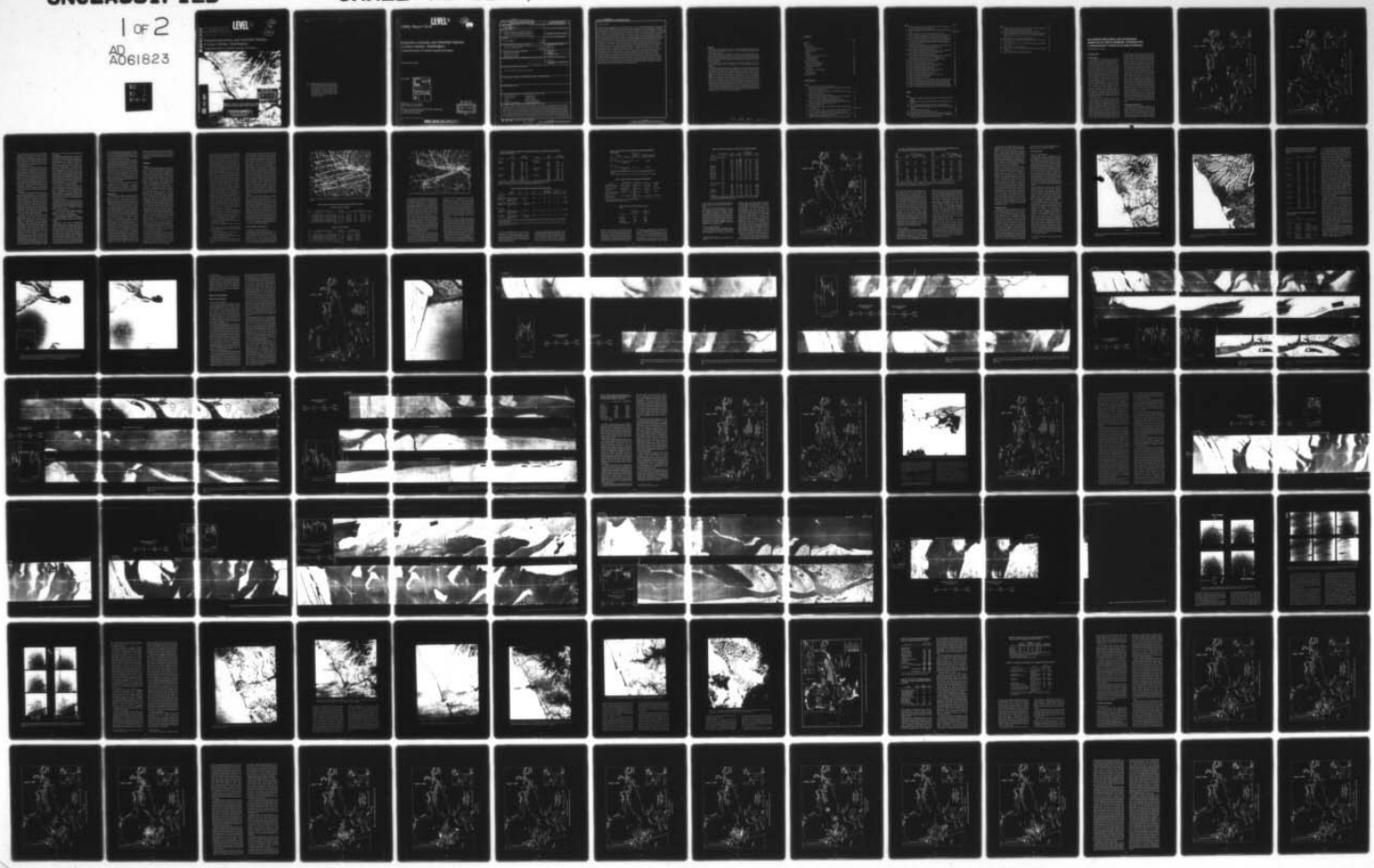

CRREL REPORT 78-18

LEVEL II

12

U S ARMY CORPS OF ENGINEERS

Estuarine processes and intertidal habitats in Grays Harbor, Washington

A demonstration of remote sensing techniques

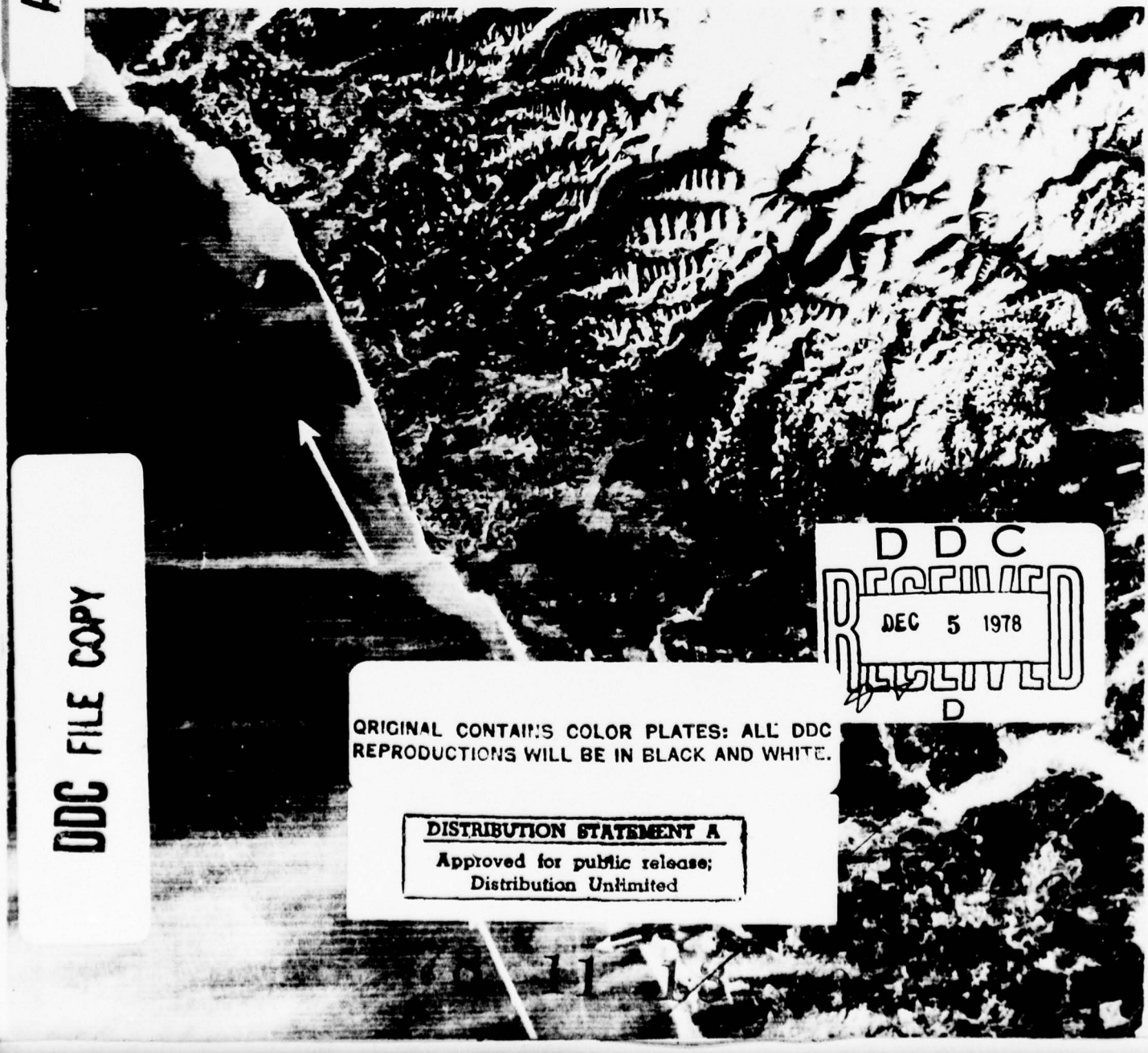

Cover: *LANDSAT-1 band 5 image of Grays Harbor and the northwestern coast of Washington taken on 26 January 1973. Note the northerly transport of suspended particulates by the Davidson current. Northern part of Willapa Bay is in the south central part of the image. Snow covered Olympic Range in north central part.*

LEVEL II

12

CRREL

CRREL Report 78-18

Estuarine processes and intertidal habitats in Grays Harbor, Washington

A demonstration of remote sensing techniques

Lawrence W. Gatto

July 1978

Prepared for
DIRECTORATE OF CIVIL WORKS
OFFICE, CHIEF OF ENGINEERS
By
COLD REGIONS RESEARCH AND ENGINEERING LABORATORY
U.S. ARMY CORPS OF ENGINEERS
HANOVER, NEW HAMPSHIRE

Unclassified

SECURITY CLASSIFICATION OF THIS PAGE (When Data Entered)

REPORT DOCUMENTATION PAGE

READ INSTRUCTIONS BEFORE COMPLETING FORM

1. REPORT NUMBER: CRREL Report 78-18	2. GOVT ACCESSION NO.
3. RECIPIENT'S CATALOG NUMBER	
4. TITLE (and Subtitle): ESTUARINE PROCESSES AND INTERTIDAL HABITATS IN GRAYS HARBOR, WASHINGTON / A Demonstration of Remote Sensing Techniques	5. TYPE OF REPORT & PERIOD COVERED
	6. PERFORMING ORG. REPORT NUMBER
7. AUTHOR(s): Lawrence W. Gatto	8. CONTRACT OR GRANT NUMBER(s)
9. PERFORMING ORGANIZATION NAME AND ADDRESS: U.S. Army Cold Regions Research and Engineering Laboratory, Hanover, New Hampshire 03755	10. PROGRAM ELEMENT, PROJECT, TASK AREA & WORK UNIT NUMBERS: IAO - CWP-S-75-9; IAO - CWR-S-74-16
11. CONTROLLING OFFICE NAME AND ADDRESS: Directorate of Civil Works, Office, Chief of Engineers, Washington, D.C. 20314	12. REPORT DATE: July 1978
	13. NUMBER OF PAGES: 85
14. MONITORING AGENCY NAME & ADDRESS (if different from Controlling Office): 116p.	15. SECURITY CLASS. (of this report): Unclassified
	15a. DECLASSIFICATION/DOWNGRADING SCHEDULE

16. DISTRIBUTION STATEMENT (of this Report)

Approved for public release; distribution unlimited.

17. DISTRIBUTION STATEMENT (of the abstract entered in Block 20, if different from Report)

18. SUPPLEMENTARY NOTES

19. KEY WORDS (Continue on reverse side if necessary and identify by block number)

Aircraft photography	Ground truth data
Data acquisition	Intertidal habitats
Ecology	LANDSAT imagery
Estuaries	Remote sensing techniques
Grays Harbor, Washington	Water surface circulation

20. ABSTRACT (Continue on reverse side if necessary and identify by block number)

The primary objective of this project was to demonstrate the utility of remote sensing techniques as an operational tool in the acquisition of data required by the U.S. Army Corps of Engineers, Seattle District, in the Grays Harbor dredging effects project, and related projects. Aerial imagery was used to map surface circulation and suspended sediment patterns near the hopper dredge pump site at the harbor entrance and near pulpmill outfalls in Aberdeen, and to map the areal distribution and extent of intertidal habitats. The surface circulation maps prepared from the aerial photographs and thermal imagery compared favorably with the large-scale circulation patterns observed in the Grays Harbor hydraulic model at the U.S. Army Engineer Waterways Experiment Station. Of the imagery provided

DD FORM 1 JAN 73 1473 EDITION OF 1 NOV 65 IS OBSOLETE

Unclassified

SECURITY CLASSIFICATION OF THIS PAGE (When Data Entered)

20. Abstract (cont'd)

by NASA, the thermal imagery was more useful than the color or color infrared (CIR) photographs for mapping circulation, while the CIR photographs were more useful than the thermal imagery or the color photographs for mapping intertidal habitats. Current velocities estimated from dye dispersion patterns and drifting dye drogues were comparable at some locations to velocities measured by in situ current meters and in the hydraulic model. Based on a cursory evaluation of LANDSAT-1 imagery acquired in January, February, and October 1973, it had limited utility in providing data on surface circulation patterns in Grays Harbor. The areal distribution and extent of nine wetland vegetation types, dune vegetation, and three types of eelgrass were mapped using primarily aerial CIR photographs and ground surveys. Color photographs were also used for areas not covered by the CIR photographs. Wetland vegetation types mapped were: low silty marsh, low sandy marsh, sedge marsh, high immature marsh, high mature marsh, salt marsh, diked pasture, freshwater marsh, and wooded swamp. Undiked salt marsh (first five types) covered 5540 acres (22.3 km^2) in Grays Harbor. Dominant salt marsh plants include *Triglochin maritimum, Salicornia virginica, Deschampsia caespitosa, Carex lyngbyei,* and *Distichlis spicata.* The eelgrass beds mapped were *Zostera noltii* (narrow-bladed), "dense" *Z. marina* (broad-bladed) and "sparse" *Z. marina.* "Dense" and "sparse" *Z. marina* covered 5540 (22.3 km^2) and 5450 acres (22 km^2), respectively, in 1975; *Z. noltii* covered 680 acres (2.74 km^2). Most eelgrass occurred in North Bay. However, "dense" *Z. marina* beds were significant on both Mid-Harbor Flats and Whitcomb Flats. *Z. noltii* also occurred along South Channel and west of John's River. *Z. noltii* occurred at much higher intertidal elevations than did *Z. marina,* forming a band of vegetation between lower *Z. marina* and higher salt marsh vegetation. The substrate where the *Z. noltii* is found is usually softer with more silt and loam than the substrate where *Z. marina*, which is firmer with predominantly sand, is found. In spite of the limitations of remote sensing techniques, they have important advantages compared with ship surveys. Based on project requirements, remote sensing techniques should be considered reliable tools to augment conventional data acquisition techniques in operational Corps of Engineers projects.

PREFACE

This report was prepared by Lawrence W. Gatto, Research Geologist, Earth Sciences Branch, Research Division, U.S. Army Cold Regions Research and Engineering Laboratory.

The work was funded by the Office of Chief of Engineers, Washington, D.C., under two Intra-Army Orders: CWR-S-74-16, *Initiate an Investigation of Estuarine Processes and Intertidal Habitats in Grays Harbor;* and CWP-S-75-9, *Demonstrate the Use of Remote Sensing for Operation and Maintenance of Navigation Facilities* (Work Unit 31094).

The technical content of this report was reviewed by William Lucas, Dr. Frederick Weinmann, and John Erlandson of the Seattle District, Corps of Engineers.

The author expresses appreciation to William Lucas, Project Planning Section, Dr. Frederick Weinmann, Environmental Resources Section, Planning Branch, and John Erlandson, Chief, Survey Branch, Engineering Division, Seattle District, North Pacific Division, Corps of Engineers, for technical review and many helpful suggestions. The author also expresses appreciation to Dr. Harlan McKim, CRREL, for assistance in formulating project objectives, and for initial project coordination with Seattle District personnel; to Dr. Harlan McKim and Thomas Marlar, also of CRREL, and Eric Nelson and William Lucas, Seattle District, for assistance during the dye studies and the low altitude photographic mission; to Dave Schuldt, Dr. Frederick Weinmann and Eric Nelson for assistance in project coordination; and to Eleanor Huke for assistance in preparation of illustrations.

CONTENTS

ILLUSTRATIONS

TABLES

ESTUARINE PROCESSES AND INTERTIDAL HABITATS IN GRAYS HARBOR, WASHINGTON
A Demonstration of Remote Sensing Techniques

Lawrence W. Gatto

INTRODUCTION

Site description

Grays Harbor is a large tidal estuary located on the Pacific coast of Washington approximately 145 km (90 mi) southwest of Seattle (Fig. 1). It is 29 km (18 mi) long from Aberdeen to Point Brown, and 21 km (13 mi) wide from the north shore of North Bay to the south shore of South Bay. Tides are mixed, with two uneven high and low tides each lunar day. Mean and diurnal tidal ranges are 2.1 and 2.7 m (6.9 and 9.0 ft), respectively, at Point Chehalis (National Ocean Survey 1973 and 1974). These values increase to 2.4 and 3.1 m (7.9 and 10.1 ft) at Aberdeen. Maximum spring high tide at Aberdeen is 3.8 m (12.5 ft); maximum spring low tide, −0.6 m (−2.1 ft). The estuary is usually partially mixed (Barrick 1976), with a significant difference between surface and bottom salinity concentrations but no distinct saltwater wedge. Harbor water is generally well mixed after extended periods of low freshwater discharge (usually from May to October) but stratified during periods of high discharge (mid-October through April) (Beverage and Swecker 1969).

Flow reversal of the Chehalis River occurs locally because of tidal action and saltwater intrusion extends several miles upstream from Montesano [which is approximately 16 km (10 mi) east of Aberdeen]. The farthest saltwater intrusion during low stream discharge is just upstream from the Montesano bridge on Highway 107. Intrusions when river flows are greater than 1400 m^3/sec (50,000 ft^3/sec) extend only to Cosmopolis. Salinity concentrations just east of the mouth of the Wishkah River vary from 0.0 parts per thousand (ppt) (total salt) at lower low water (LLW) to about 10.0 to 12.0 ppt at higher high water (HHW) (Beverage and Swecker 1969). The horizontal density gradient from the entrance to the upstream limits is fairly uniform. The surface salinities in the harbor entrance generally average about 1.0 to 2.0 ppt lower than the bottom salinities, while near the upstream limits of saltwater intrusion, the surface salinities average about 3.0 to 5.0 ppt lower than the bottom salinities (Brodgon 1972a).

Local climate is moist maritime, with mild dry summers and cool wet winters. Average daily temperatures in July range from 10° to 21.1°C (50° to 70°F), and in January, from 1.1° to 7.2°C (34° to 45°F). Average annual temperature is 10°C (50.5°F). Southwest and west winds prevail and occasionally exceed 64 km/hr (40 mph). Normal annual precipitation ranges from 178 to 254 cm (70 to 100 in.), and approximately 78% of the precipitation occurs from September through March. The number of clear, or partly cloudy, days each month is 4 to 7 in winter, 8 to 15 in spring and fall, and 15 to 20 in summer. The amount of sunshine received is approximately 20% in winter, 30 to 50% in spring and fall, and 50 to 65% in summer. Frequently in summer and fall, low clouds or fog move inland from the ocean at night and dissipate by the following noon.

Background and objectives

Authority for maintaining the navigability of the turning basins and channels leading to and within the harbor was given to the Seattle District, Corps of Engineers, through the Rivers and Harbors Act of 1935 (and later modifications). Annual maintenance dredging is required to ensure navigability in the channels leading to

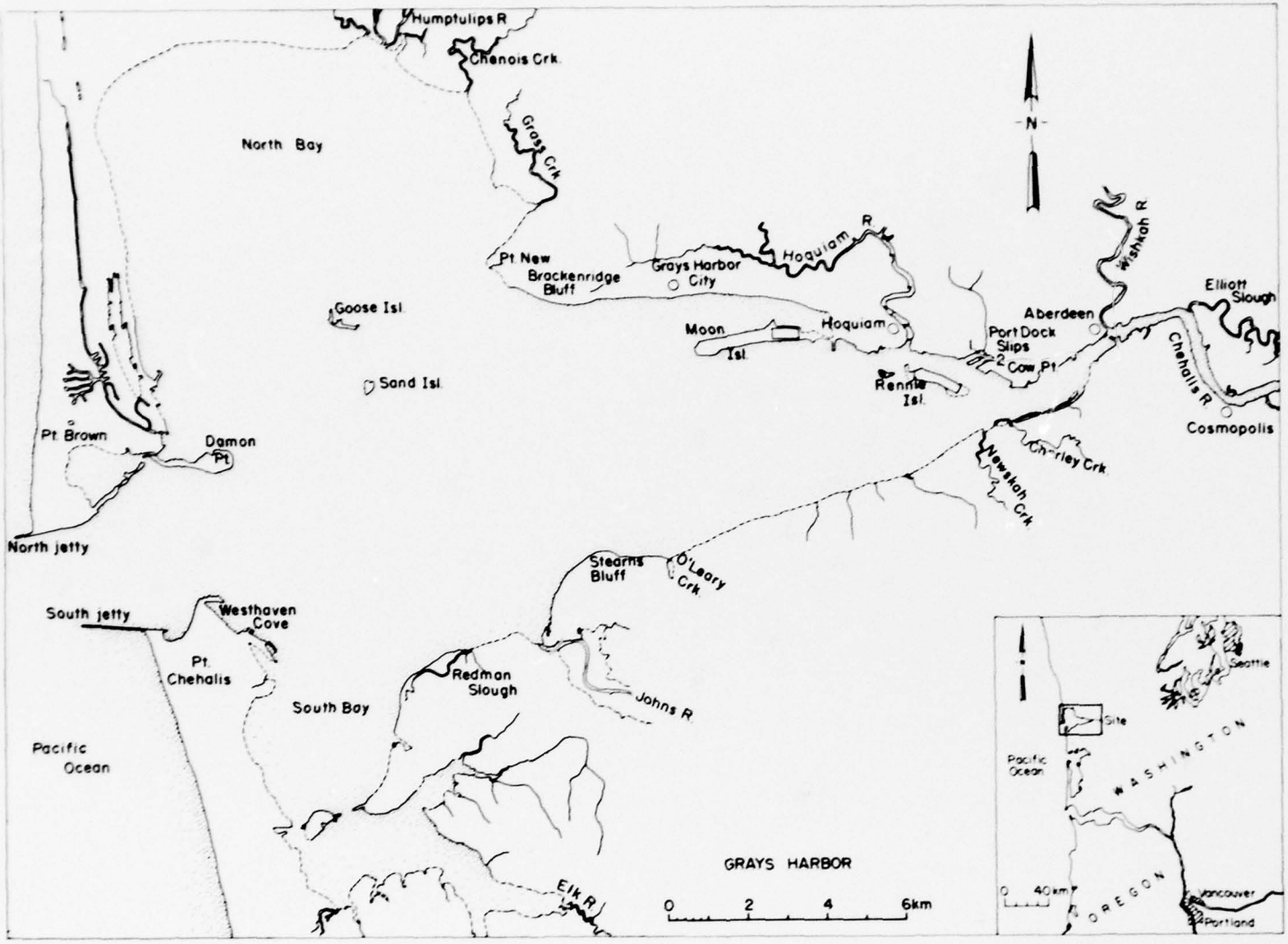

Figure 1a. Location map, Grays Harbor, Washington.

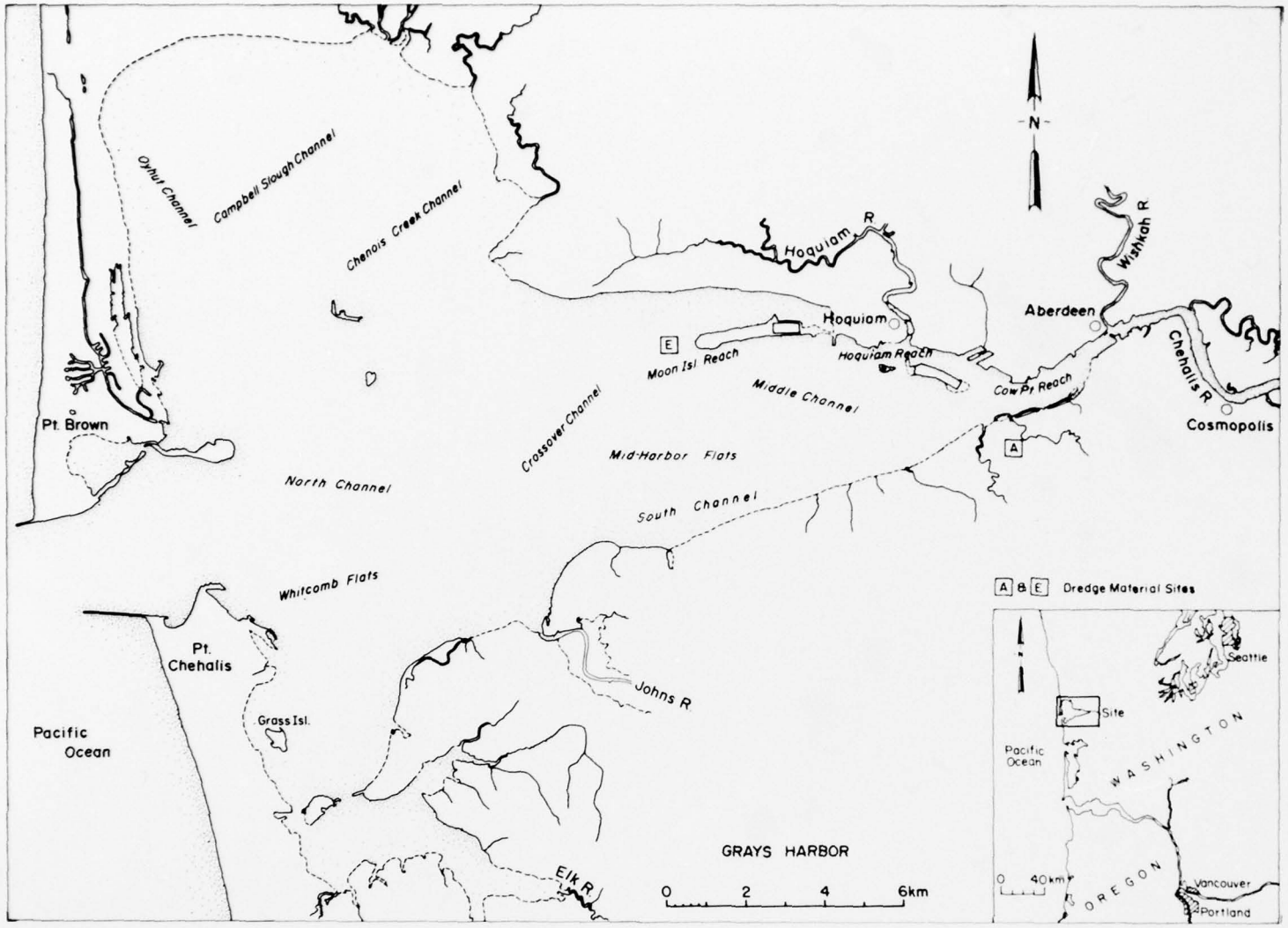

Figure 1b. Location map, channels and shoals, Grays Harbor, Washington.

Hoquiam, Aberdeen and Cosmopolis. Dredging is also necessary about every 15 years in the Westhaven Cove channels (U.S. Army Corps of Engineers 1975). The Corps of Engineers also provides for the construction and maintenance of, and improvements to, harbor entrance jetties, revetments, groins, and breakwaters (U.S. Army Corps of Engineers 1971).

Assessments of the potential impacts that these operational and maintenance activities will have on the Grays Harbor environment have been prepared for evaluation by local, state and federal agencies (U.S. Army Corps of Engineers 1975). The maintenance dredging activities were adopted in 1972 as the most acceptable alternatives and were considered temporary and part of an interim short-range plan. This plan was abandoned after the 1975-1976 dredging season, when studies on current dredging effects were completed. Subsequently, an up-dated Environmental Impact Statement was prepared before the formulation of the long-range dredging project.

From 1972 to 1974 personnel of the U.S. Army Cold Regions Research and Engineering Laboratory conducted a remote sensing research project in Cook Inlet, Alaska (Gatto 1976). The overall objective of this project was to determine the feasibility of using data acquired by satellite and aircraft to map surface water circulation patterns, and sediment and tidal flat distributions. The results of this and other investigations verified the utility of remote sensing techniques in performing these tasks (Cameron 1952, 1962, 1965; Keller 1963; Ramey 1968; Duhaut 1972; Meyer and Welch 1975).

Lillesand et al. (1975) reported that aerial photographs, when used in conjunction with limited ground truth data, can be used to measure and delineate waste distributions as reliably as conventional surface measuring techniques and in more detail. Welch and Munday (1977) discuss the advantages of using aerial photographs to describe circulation patterns in tidal estuaries. Areas of high shear and convergence in the surface waters can be delineated using typical surface signatures, i.e., a color boundary or line of foam, that are easily recognizable and coherent when viewed from an aircraft. But the same patterns can be virtually unrecognizable from surface vessels. Dye-emitting drogues photographed from aircraft are also useful. The role of surface vessels is reduced to providing vertical hydrographic profiles and precise position markers for resulting aerial photographs.

For mapping intertidal habitats, Cowardin and Myers (1974) reported that proper timing of aircraft flights, use of multispectral photographs, and knowledge of the ecology of the area were essential for remote wetland mapping. In discriminating species of salt marsh vegetation, color infrared photographs is of special value (Hefner et al. 1974). Color infrared and "true" color photographs were used by Stroud and Cooper (1968) to map salt marsh species in an Atlantic coast salt marsh. However, Keller (1963) concluded that aerial photographs (type of film not specified) were not adequate for the mapping of eelgrass distribution in Humboldt Bay, California, since beds of green algae (*Ulva* sp. and *Enteromorpha* sp.) are not distinguishable from eelgrass beds in the photographs.

To facilitate technology transfer, this demonstration project was initiated using Grays Harbor, Washington, as the test site. Grays Harbor was selected because the Seattle District, Corps of Engineers, has several studies of this harbor underway; oceanographic baseline data are available; and the harbor is especially important since future coastal zone development is expected to increase.

The primary objective of this project was to demonstrate the utility of remote sensing techniques in acquisition of data required for studies of dredging effects and related projects by the Seattle District, Corps of Engineers. Specific project objectives were to:

1. map circulation and sediment distribution patterns and relate these patterns to dredge material movement and redeposition
2. map distribution of intertidal habitats
3. monitor pulpmill effluents near Aberdeen and relate their dispersion to surface circulation patterns.

Objectives 1 and 3 were accomplished by mapping the surface currents at and near the hopper dredge dump site at the harbor entrance and at the eastern end of the harbor where pulpmill effluents are dumped at the mouth of the Chehalis River. Because NASA aircraft missions were flown at times when dredging and pulpmill effluent dumping were not underway, the circulation and sediment patterns analyzed were not related to these activities. Instead, uranine dye was used as a tracer to analyze surface circulation patterns at and near the dump site; this dye was used to simulate the movement

of the suspended sediment plume which normally is formed during dumping operations. Similar dye studies at the pulpmill outfall could be used to show dispersion patterns that would likely form when the effluent is released.

Seattle District personnel consider it doubtful that a significant sediment plume is formed during hopper dredge dumping operations. In addition, because there are differences between the behavior of dyes and that of sediment in water there may not be a close comparison between the dispersion of the dye and of fine grained sediment. Also, brown sediment is not as distinct in water as the green uranine dye, and may not be as easily traced. This shortcoming may be solved by applying dye to the sediment in the hopper dredge and monitoring the dyed sediment once it is released.

The products derived using remote sensing techniques were evaluated for accuracy, reliability, and cost effectiveness as compared with conventional data products. In addition, Seattle District personnel assessed the remote sensing data products for this operational utility.

Project history

In January 1974, CRREL representatives met with personnel from the Environmental Resources Section, Seattle District, Corps of Engineers. Previous remote sensing activities at CRREL and the possible utility of remote sensing techniques for District projects were discussed; i.e., in determining circulation patterns in small boat harbors, in detecting beach erosion, and in monitoring dredge spoils. A site specific application, tracing sediment movement along Ediz Hook north of Port Angeles Harbor (sediment is derived from the foot of sea cliffs and the Elwha River located west of the hook), was also discussed. Investigations in Grays Harbor, however, were specifically identified as having high priority. It was considered that aerial imagery might be used in determining the source of sediment ($\cong 1.528 \times 10^6$ m^3/yr) ($\cong 2 \times 10^6$ yd^3/yr) deposited in Grays Harbor channels; in detecting the migration of the navigation channels; in delineating areas of deposition and possible dredge material disposal sites; in monitoring sediment movement during various tidal stages; in mapping intertidal habitats, surface circulation patterns, and dispersion of pulpmill effluents discharged near Aberdeen; and in tracing sediment movement near the north jetty at the entrance to Grays Harbor, and near the Westhaven small boat basin near Port Chehalis. As a result of these discussions, the three previously mentioned objectives were selected and this cooperative demonstration project was developed.

APPROACH

General

NASA provided aircraft support commencing in July 1974. Ground truth data for analyzing harbor circulation patterns were collected by personnel from Grays Harbor College (under contract), the Seattle District and CRREL; and for analyzing intertidal habitats, by personnel from Washington State Department of Game (under contract). Data analysis began with receipt of photographic data products from NASA. The utility assessment by District personnel was accomplished in two man-months.

Initially, a review was made of current literature and unpublished reports pertaining to the oceanography of Grays Harbor. Oceanographic and bathymetric data and historical aerial photographs were obtained from the Seattle District, Grays Harbor College, NASA, and other state and federal agencies. Temperature, salinity and suspended sediment distribution and surface circulation maps were prepared from ground truth data acquired in July 1974 and from aircraft imagery, respectively. The temperature, salinity and sediment maps were used to characterize water types and circulation patterns, and were compared with interpretations from aircraft and satellite imagery.

Field surveys and vegetation sampling along transects were done to provide the ground truth data for mapping the intertidal habitats. NASA NP-3A imagery and low altitude aircraft photographs were used to analyze surface circulation patterns, wave refraction/reflection, longshore currents, surface water color changes, nearshore bathymetry, tidal flat morphology, intertidal habitats and thermal patterns. The utility of LANDSAT-1 imagery for monitoring seasonal water movements and regional circulation patterns was evaluated.

The general definition of wetlands used in this study was any area inundated, at some time during the year, by nonflood waters. A further restriction was that only those vascular plants occurring in the intertidal range were considered. Salt marshes and eelgrass are important wetland vegetative types in Grays Harbor.

Salt marshes are beds of rooted vegetation which are alternately inundated and drained by the rise and fall of the tide (Cooper 1974, p. 55). Species composition on this tide-stressed environment is controlled by several factors including elevation (dictating period of exposure), sediment characteristics, salinity, drainage, and temperature. During previous studies (Messmer 1971; MacDonald and Barbour 1974), salt marsh vegetation was mapped for limited areas of the harbor and separated into two zones. In the lower zone of short 10-20-cm (3.93-7.86-in.) vegetation, *Salicornia virginica* was predominant and *Jaumea carnosa*, *Triglochin maritimum*, *Distichlis spicata*, *Plantago maritima*, and *Glaux maritima* were found in order of decreasing frequency of occurrence. In the high zone, *Deschampsia caespitosa* was predominant with *J. carnosa*, *S. virginica*, *D. spicata*, *Atriplex patula*, *P. maritima*, *Lasthenia* sp., *Cuscuta salina*, *Lilaeopsis occidentalis*, *Juncus lesueurii*, *Carex lyngbyei*, and *Potentilla egedii* found with decreasing frequency.

Two species of eelgrass are found in Grays Harbor, *Zostera marina* and *Z. noltii* (European eelgrass). They are visually separable entities. *Z. marina* beds are further divided into "dense" and "sparse" beds. Only "dense" beds were quantitatively sampled, as statistics obtained from "sparse" beds would have been so variable as to render them meaningless. Visually, "sparse" eelgrass beds were an order of magnitude less dense than "dense" *Z. marina* beds as determined during field surveys in May 1975.

Zostera marina is a perennial, monocotyledonous plant which is especially important in more protected estuarine waters. Thayer et al. (1975) list the following benefits of *Z. marina*:

1. has high growth rates, 300-600 g dry wt/m^2/yr, not including root production
2. supports epiphytic organisms with biomass equalling that of eelgrass
3. is a major contributor to the detritus food chain
4. produces organic matter by decaying which initiates sulphate reduction reaction important to the sulphur cycle
5. reduces sediment erosion and shifting
6. retards currents with its leaves
7. absorbs phosphorus and nitrogen and returns these nutrients to water
8. is used by man as fuel, in packing and upholstering, and for insulation, fodder and fertilizer.

Thomas and Duffy (1968) and Waddel (1964) also noted that, in addition to providing the basis for estuarine food chains, eelgrass and salt marsh vegetation help stabilize estuarine bottoms. Removal of eelgrass in some locations would result in the release of accumulated sediment which could cause serious damage to neighboring oyster beds. The stabilization by eelgrass helps create habitats for a variety of fishes, shellfish, crabs and other invertebrates. Watertowl and shorebirds, in particular, find salt marshes to be excellent resting and feeding areas. Phillips (1974) provided an excellent summary of ecological factors affecting eelgrass vegetative and reproductive growth and of the plant's life history. Parker (1975) stated that weather conditions, chemical pollution, turbidity from dredging, oyster culture, and rate of siltation were important factors that cause changes in eelgrass distribution and density. Data on distribution, areal extent, and density of eelgrass and salt marshes are prerequisite to assessing changes in the wetland system brought about by environmental alterations such as dredging.

The intertidal habitat mapping was performed under contract with personnel at the Washington State Department of Game. All information regarding this is taken from a report prepared by that department (Smith et al. 1976). That report contains detailed descriptions of the field sampling methods used during the ground surveys, of the species composition of and historical changes in the distribution of the intertidal habitats, and of the areas for future research. Remote sensing techniques were an integral part of mapping all the intertidal habitats and marshland vegetation within Grays Harbor. This mapping effort, in itself, is a good demonstration of the utility of remote sensing techniques used in concert with other data-gathering methods to accomplish overall study objectives.

Aircraft imagery and sensor data

Chronology of air photo acquisition

Photographic missions 283 and 305 were conducted with the NASA Earth Observations Aircraft NP-3A (Earth Survey-1) on 12-13 July 1974 and 10 April 1975, respectively. Six daylight flight lines (Fig. 2; Table 1) totalling 153.4 km (95.3 mi) were flown at an approximate altitude of 3636 m (12,000 ft) from 1419 to 1503 hr (PDT)

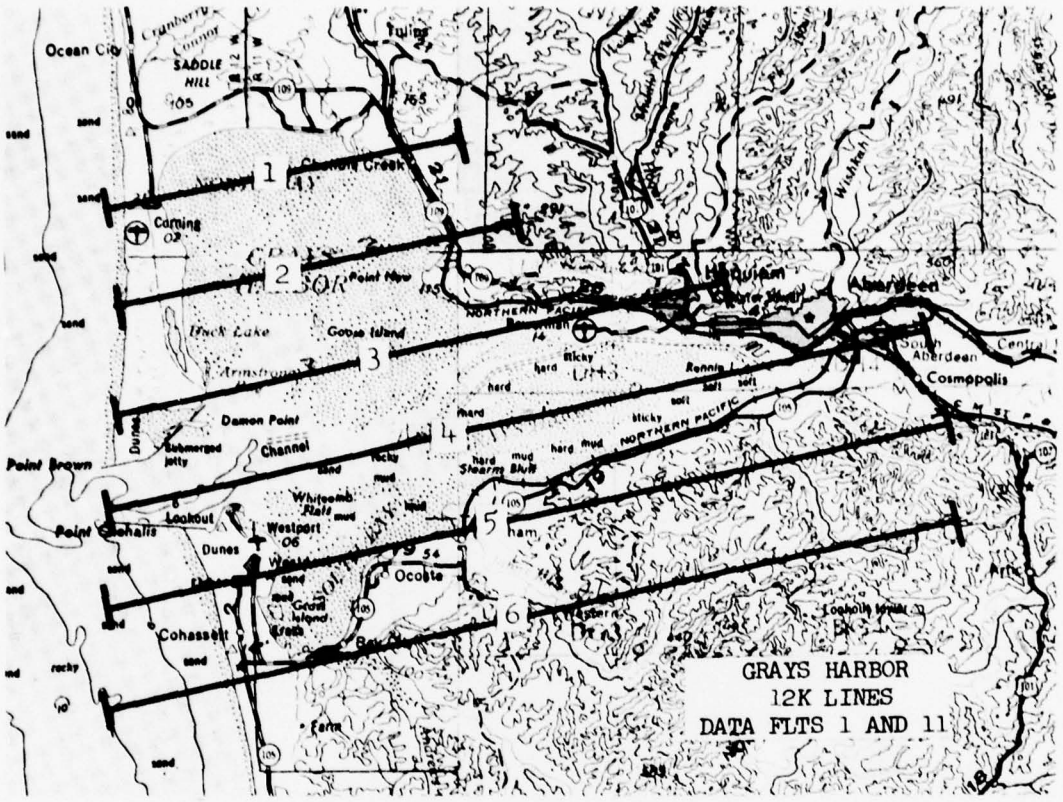

Figure 2. Approximate locations of flight lines for daylight NASA NP-3A aircraft missions 283 and 305.

Table 1. Flight line coordinates, mileage and times flown, NASA aircraft flights.

Day Lines: 3636 m (12,000 ft)

Line	*Approximate coordinates*		*Mileage*		*Time (PDT)*			
no.	*West end*	*East end*	*(km)*	*(mi)*	*13 July 74*	*Frame nos.*	*10 April 75*	*Frame nos.*
1	47°01.0'N/124°10.5'W	47°02.4'N/124°00.0'W	14.8	9.2	1419-1421	1-8	1308-1310	1-11
2	46°59.0'N/124°10.3'W	47°00.6'N/123°58.0'W	16.6	10.3	1426-1428	9-18	1322-1324	29-38
3	46°56.8'N/124°10.3'W	46°59.5'N/123°52.0'W	24.0	14.9	1433-1436	19-31	1335-1338	59-70
4	46°54.8'N/124°10.5'W	46°58.5'N/123°45.9'W	31.4	19.5	1441-1446	32-49	1314-1319	12-28
5	46°52.8'N/124°10.5'W	46°56.5'N/123°45.0'W	33.3	20.7	1450-1454	50-67	1328-1333	39-58
6	46°50.7'N/124°10.5'W	46°54.4'N/123°45.0'W	33.3	20.7	1458-1503	68-85	1341-1346	71-91
		Total	153.4	95.3				

Night Lines: 909 m (3000 ft)

Line	*Approximate coordinates*		*Mileage*		*Time (PDT)*	
no.	*West end*	*East end*	*(km)*	*(mi)*	*12-13 July 74*	*10 April 75*
21	47°01.7'N/124°09.5'W	47°00.5'N/124°00.0'W	12.9	8.0	2347-2350	2203-2206
22	47°00.8'N/124°09.5'W	46°59.7'N/124°00.0'W	12.9	8.0	2356-2358	2209-2211
23	47°00.0'N/124°09.0'W	46°57.7'N/123°51.4'W	22.2	13.8	0005-0010	2156-2201
24	46°53.9'N/124°06.0'W	46°58.6'N/123°45.6'W	27.7	17.2	0017-0022	2148-2154
25	46°52.9'N/124°06.1'W	46°54.5'N/123°58.8'W	9.2	5.7	0028-0033	2144-2145
		Total	84.9	52.7		

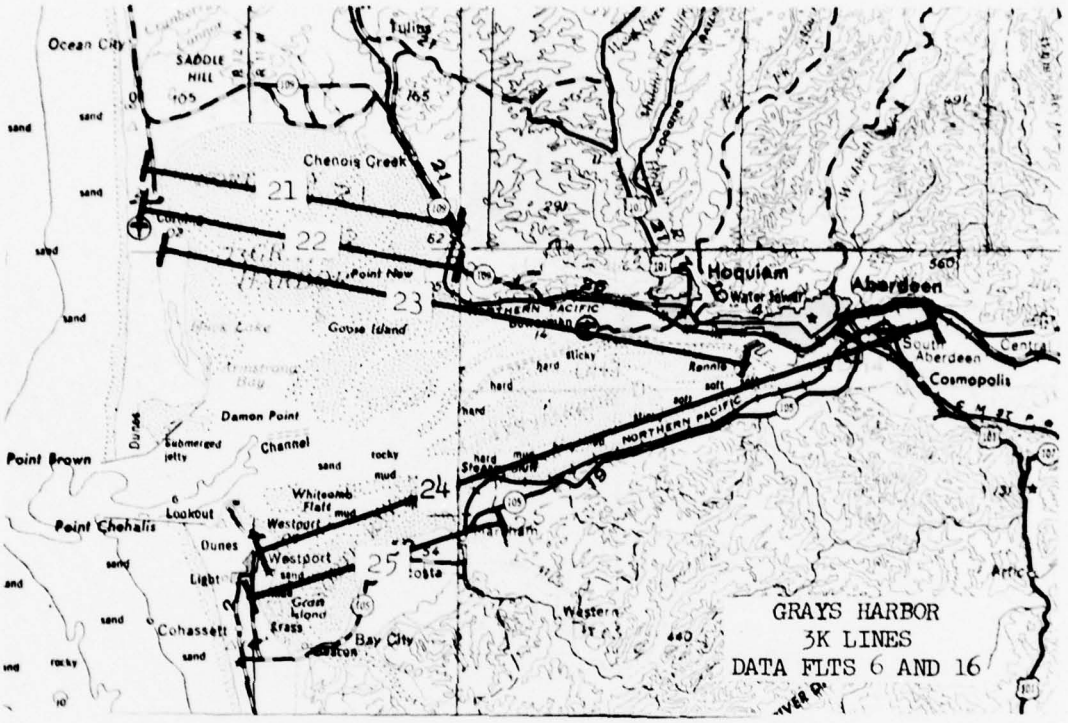

Figure 3. Approximate locations of flight lines for night NASA NP-3A aircraft missions 283 and 305.

on 13 July 1974 (Data Flight 1) and from 1308 to 1346 hr (PDT) on 10 April 1975 (Data Flight 11). Five nighttime flight lines (Fig. 3) totalling 84.9 km (52.7 mi) were flown at an approximate altitude 909 m (3000 ft) from 2347 hr (PDT) on 12 July to 0033 hr (PDT) on 13 July 1974 (Data Flight 6) and from 2144 to 2211 hr (PDT) on 10 April 1975 (Data Flight 16). Daylight coverage from both missions included the entire harbor; night coverage included only nearshore areas to detect sources and dispersion patterns of effluents. The mission 283 daylight photographs were acquired during low water at Aberdeen, and during early flood at Pt. Chehalis (Table II). Mission 283 night imagery was acquired during ebb at Aberdeen and Pt. Chehalis. Mission 305 daylight photographs were acquired during high water at Pt. Chehalis, and late flood at Aberdeen. Mission 305 night imagery was acquired during flood at both locations.

NASA photographs were acquired with two 22.9-cm (9-in.) format metric cameras each with 15.2-cm (6-in.) lenses (Table III). One camera had Ektachrome EF Aerographic film (SO-397) with a 2A filter (occasionally without a filter) and the other, Aerochrome infrared film (Type 2443) with a Wratten 12 filter. The nominal scale of the photographs was 1:24,000 and the quality generally good. Apparent on the photographs were surface circulation patterns; foam and debris lines on the water surface which indicate local wind and/or surface current patterns; sun glint on the sea surface which enhances the view of the direction of wave front movement, of wave refraction and, indirectly, of long shore currents; and nearshore bathymetry, tidal flat morphology, intertidal habitats, and coastal landforms.

The RS-14 Infrared Imaging and Modular Multiband (M^2S) Scanners (Table IV) provided black and white film strips which showed thermal variations in the surface water. The scanner imagery was useful in interpreting surface thermal patterns at selected locations, mixing patterns at the interface between river and harbor water, and sources of warm or cold water entering the harbor. Meyer and Welch (1975) report: "Aerial thermal-infrared sensing can thus be used effectively for specific hydrodynamic investigations as well as for general monitoring."

Passive Microwave Imaging System (PMIS) imagery was also acquired. Originally, it was to be

Table II. Predicted tides at Aberdeen and Pt. Chehalis during NASA aircraft flights (from National Ocean Survey 1973 and 1974).

Location	Time* (PDT)	Height (m)	Height (ft)†
12 July 1974			
Aberdeen	0148	0.58	1.9
	0728	2.10	6.9
	1333	0.64	2.1
	1949	2.80	9.2
Pt. Chehalis	0106	0.54	1.8
	0657	1.76	5.8
	1251	0.60	2.0
	1918	2.47	8.1
13 July 1974			
Aberdeen	0247	0.45	1.5
	0835	2.01	6.6
	1421	0.85	2.8
	2042	2.89	9.5
13 July 1974			
Pt. Chehalis	0205	0.42	1.4
	0804	1.67	5.5
	1339	0.82	2.7
	2011	2.56	8.4
10 April 1975			
Aberdeen	0124	2.95	9.7
	0758	0.18	0.6
	1358	2.74	9.0
	2010	0.45	1.5
Pt. Chehalis	0053	2.62	8.6
	0716	0.15	0.5
	1327	2.40	7.9
	1928	0.42	1.4

*Correction for difference between local meridian and the standard meridian (120° W) has been applied.
†Heights are determined from the mean lower low water datum for a particular location.

Table III. Data for photographs acquired during missions 283 and 305.

Camera	Format/ film type	Lens (cm)	Filter	Shutter speed	f stop	Areal ground coverage/frame (km^2)	Areal ground coverage/frame (mi^2)	Ground coverage/side (km)	Ground coverage/side (mi)	Nominal scale
*Mission 283**										
Wild-Heerbrugg RC8 Metric	22.9-cm pos. trans./ Ektachrome EF Aerographic (SO-397)	15.2**	2A (haze filter)	1/250	5.6	30.6	11.63	5.5	3.4	1:24,000
Wild-Heerbrugg RC8 Metric	22.9-cm pos. trans./ Aerochrome Infrared (2443)	15.2	Wratten 12 (yellow filter)	1/200	5.6	30.6	11.63	5.5	3.4	1:24,000
Mission 305†										
Zeiss RMK A 15/23 Metric	22.9-cm pos. trans./ Ektachrome EF Aerographic (SO-397)	15.2	No filter	1/400	4 to 4.5	30.6	11.63	5.5	3.4	1:24,000
Zeiss RMK A 15/23 Metric	22.9-cm pos. trans./ Aerochrome Infrared (2443)	15.2	Wratten 12 (yellow filter)	1/200	4 to 4.5	30.6	11.63	5.5	3.4	1:24,000

* NP-3A altitude, 3636 m (12,000 ft) (msl); 13 July 1974; avg ground speed, 442 km/hr (239 kt); 60% overlap, 30% sidelap; light cirrus clouds; sun angle, 20°-45°.
† NP-3A altitude, 3636 m (12,000 ft) (msl); 10 April 1975; avg ground speed, 508 km/hr (275 kt); 60% overlap, 30% sidelap; scattered clouds over land; sun angle, 25°-45°.
** 6 in.

used for differentiation of tidal flat characteristics based on moisture content. However, the color-coded PMIS imagery was not used because patterns on the imagery and the imagery signatures could not be correlated with ground or water features.

Airborne environmental sensors (Table V) provided data for determining atmospheric conditions and the Barnes PRT-5 measured gross apparent radiation transmitted from the earth's surface in the 8- to 14-μm range. The Barnes system consists of two units: the power supply,

Table IV. Data for RS-14 Infrared Imaging Scanner and Modular Multiband Scanner (M^2S).

Sensor	Wavelength (μm)	Film format	Ground coverage swath (km)	Ground coverage swath (mi)	Nominal scale (perpendicular to flight line direction)
*Mission 283**					
RS-14	8-14 (thermal)	5.39 cm (2.125 in.) pos. trans. strips	1.42	0.88	1:23,500
Mission 305†					
M^2S	8-14 (thermal)	9.52 cm (3.75 in.) pos. trans. strips	2.87	1.78	1:30,000

* NP-3A altitude, 909 m (3000 ft) (msl); 12-13 July 1974; ground speed, 297 km/hr (160 kt)

† NP-3A altitude, 909 m (3000 ft) (msl); 10 April 1975; ground speed, 334 km/hr (180 kt)

Table V. Airborne environmental sensors (from NASA 1972).

Type	Variable measured	Data format	Range	Accuracy
Barnes PRT-5 Precision Radiation Thermometer*	Apparent radiation in 8 to 14-μm range	Digital printout; graphs	−20° to 40°C (− 4° to 104°F)	±0.5°C (±0.9°F)
Cambridge Dewpoint Hygrometer†	Prevailing dewpoint temperature	Digital printout; graphs	±50°C (122° to −58°F)	±0.5°C above 0°
Johnson — Williams Liquid Water Content Indicator†	Liquid water content	Digital printout; graphs	0-6 g/m³	±15%
Rosemont Total Air Temperature Probe†	Total air temperature	Digital printout; graphs	−70° to 50°C (−137° to 122°F)	±1.0% full scale

* Measures data beyond the aircraft from 0.3 m (0.9 ft) to infinity.

† Measures atmosphere contiguous to aircraft.

Table VI. Time of dye releases on 10 and 11 July 1974.

Location	10 July, near maximum flood (PDT)	11 July, near maximum ebb (PDT)
Disposal site 1	1310; 1353	0845
North jetty	1315	0855
South jetty	1325	0905
Moon Island	1320	0840
Reach (Buoy 41)		

control, and indicator unit mounted on the operator's console and the optical unit mounted in the sensor bay. Incoming radiated energy is continuously compared with a 55°C (131°F) internal reference and converted by the PRT-5 into a voltage which is directly related to the energy difference between the target and the reference. The voltage is displayed on the indicator as equivalent blackbody temperature, to an accuracy of ±0.5°C (±0.9°F), of ground features below the aircraft (NASA 1972). With a 2° conical field of view, the PRT-5 recorded temperatures of successive areas 31.8 m (105 ft) in diameter along the flight lines at 909 m (3000

Table VII. Schedule for acquisition of and data for low altitude photographs.

Location	Roll/photographic pass	Start time (PDT)	Altitude (m)	Altitude (ft)	Ground coverage/ frame side (m)	Ground coverage/ frame side (ft)	Nominal scale
10 July (near maximum flood)							
Disposal site 1	1/1	1312	303	1000	238	788	1:4370
	1/2	1315	303	1000	238	788	1:4370
	1/3	1320	303	1000	238	788	1:4370
	1/4	1323	303	1000	238	738	1:4370
Moon Island	1/1	1329	242	800	191	632	1:3800
(Buoy 41)	1/2	1331	264	870	208	687	1:3500
South jetty	1/1	1334	624	2060	493	1630	1:9030
South jetty	2/1	1337	624	2060	493	1630	1:9030
Moon Island	2/1	1340	247	816	195	645	1:3590
(Buoy 41)	2/2	1342	247	816	195	645	1:3590
South jetty	2/2	1344	187	620	148	490	1:2720
Disposal site 1	2/1	1345	212	700	167	553	1:3060
	2/2	1400	212	700	167	553	1:3060
*11 July (near maximum ebb)**							
Disposal site 1	3/1	0843	196	648	154	511	1:2830
	3/2	0847	196	648	154	511	1:2830
	3/3	0851	196	648	154	511	1:2830
North jetty	4/1	0900	163	540	128	425	1:2360
Disposal site 1	4/1	0910	163	540	128	425	1:2360
	4/2	0913	163	540	128	425	1:2360
South jetty	4/1	0920	163	540	128	425	1:2360

* Only Ektachrome IR photographs taken on 11 July; ceiling too low to fly over Moon Island site; mission terminated due to inclement weather.

ft). The data were used in interpreting thermal patterns observed on the RS-14 and M²S imagery.

Green and Terrell (1978) reported: "The airborne radiometer can be quite useful in studying water motions, especially in support of other measurement techniques. The inferred surface temperature data provide almost instantaneous spatial details not obtainable with more conventional tools. Such a picture can be valuable in devising future sampling strategies and in providing the overview often needed to interpret data taken on a smaller scale."*

Surface circulation patterns

Low altitude aircraft (Cessna 180) photographs were also acquired on 10 and 11 July 1974 to trace movement of uranine dye released from stationary buoys and from drogues at several locations within the harbor (Fig. 4; Table VI). Two Hasselblad cameras [10.2-cm (4-in.) lens, viewing angle, 43°] with Ektachrome MS Aerographic color film (no filter) and Ektachrome IR film (Wratten 12 filter) were used to record the dispersion of the dye. The exposure interval was approximately 2 seconds. The photographs were produced as 55-mm (2.2-in.) positive transparencies. Uranine dye appeared bright green on the color photographs, and bright blue on the color IR. The interface between the dye and the clear water appeared more distinct on the color photographs. Because of low cloud ceilings, the photographs were acquired between altitudes of 163.6 to 624.2 m (540 to 2060 ft) (Table VII). Munday et al (1977) provide a very good description of the use of uranine dye for studies of circulation patterns.

The dye releases were made to analyze surface circulation near the north and south jetties, near the hopper dredge disposal site 1 and near

* Copyright, American Geophysical Union, reprinted by permission.

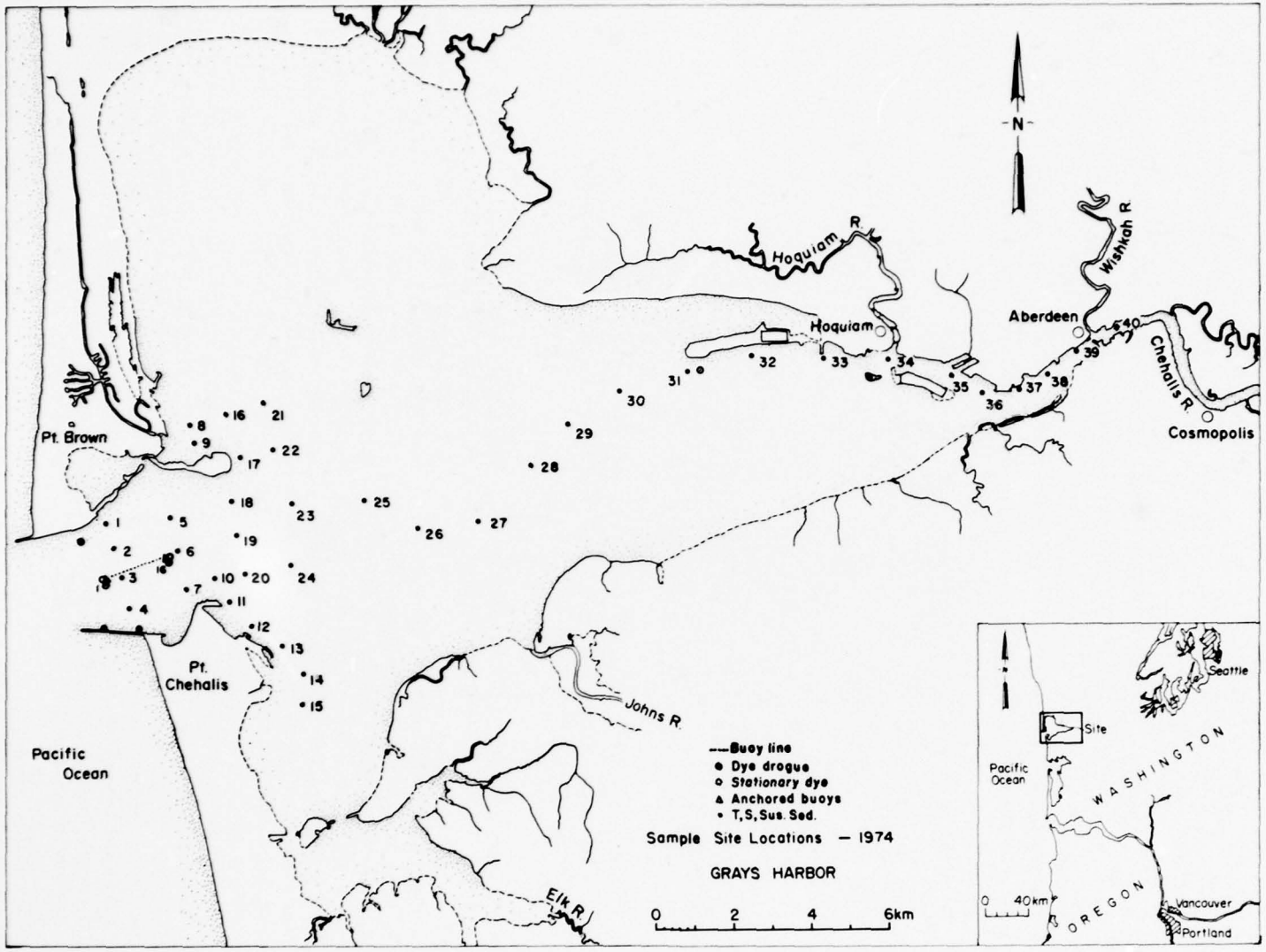

Figure 4. Sample site and dye release locations.

Table VIII. Predicted times of slack water and times/velocities of maximum flood (F) and ebb (E) currents at Grays Harbor entrance (46°55'N, 124°08'W) (from National Ocean Survey 1973).

Slack water time (PDT)	Maximum current		
	Time (PDT)	Velocity (m/sec)	Velocity (ft/sec)
8 July 1974			
0346	0719	1.59	5.24 E
1040	1331	1.13	3.72 F
1704	2006	1.13	3.72 E
2301			
9 July 1974			
0424	0123	0.72	2.36 F
1114	0752	1.43	4.73 E
1739	1400	1.08	3.55 F
2350	2043	1.18	3.88 E
10 July 1974			
	0206	0.67	2.20 F
0507	0829	1.28	4.22 E
1151	1435	1.08	3.55 F
1815	2126	1.23	4.05 E
11 July 1974			
0043	0251	0.62	2.03 F
0559	0914	1.13	3.72 E
1231	1510	1.02	3.38 F
1853	2212	1.23	4.05 E
12 July 1974			
0141	0350	0.56	1.86 F
0704	1003	0.97	3.21 E
1316	1600	0.92	3.04 F
1936	2307	1.33	4.39 E
13 July 1974			
0245	0500	0.51	1.69 F
0822	1106	0.82	2.70 E
1407	1651	0.07	2.87 F
2026	0012 (14 July)	1.43	4.73 E

Data at Aberdeen for slack water time were unreliable; at Aberdeen during period of observations (February), flood was weak, and current was ebbing most of the time with a velocity of about 1.02 m/sec (3.38 ft/sec) at times of maximum ebb which occurred 30 minutes later than at harbor entrance.

the unconfined pipeline dredge disposal site near Moon Island. The dye dispersion and drogue studies were coordinated with personnel from the Seattle District. Marker buoys were required as reference points for the dye dispersion near the hopper dredge disposal site. A line of 16 anchored buoys was positioned and test dyes were released to determine the appropriate amounts of dye to be used. The first dye and drogue releases were made near maximum flood on 10 July 1974 (Table VIII). Buoy locations and dye release sites were recorded by sextant readings. The dye dispersion and drogue movements at all the sites were photographed. Simultaneously, while water samples and water temperature and salinity data were acquired, the sampling sites were photographed to correlate water characteristics with tones on the aerial photographs. Dye and drogue releases, water sampling and aerial photography were also performed near maximum ebb on 11 July.

Intertidal habitats

The areal distribution of the intertidal habitats was mapped utilizing the NASA color infrared photographs and lower altitude CIR photographs. Although the CIR photographs were used for the mapping, eelgrass was also apparent on the color photographs; submerged eelgrass had a rust color, and exposed beds were green. The mapping could not be completed with only the NASA photographs because they were taken during low tide when the water level was 0.9-1.2 m (3-4 ft) above mean lower low water. Most *Z. marina* occurs below the 0.9-m (3-ft) level. To complete the map, CIR photographs were acquired from a Cessna 172 at 1515 m (5000 ft) during lower low water, predicted −0.5 m (−1.8 ft), between 1000 and 1130 hours PDT on 28 June 1975. Complete coverage of the harbor tidal flats was obtained on eleven 20-exposure rolls of Kodak Ektachrome CIR film using a 35-mm (1.4-in.) single lens reflex camera with a Kalcor G15 filter (minus blue) (ASA, 100, f stop, 8, 11 or 16, depending on photo angle to sun).

Slides prepared from these low altitude photographs were projected and areas of eelgrass were transferred to a map of tidal flats [(0.0 to 2.7 m) (0.0 to 8.8 ft) relative to mean lower low water (MLLW)] adapted from U.S. Army Corps of Engineers topographic data. Photointerpretations were verified and augmented by data acquired during extensive field observations in late May and June 1975. Areal determinations were made with a K & E optical, compensating, polar planimeter.

Salt marshes and other wetlands were also mapped from the NASA CIR photographs. Where the photographs did not cover an area of interest, color aerial photographs (nominal scale, 1:24,600) obtained from the Washington Department of Natural Resources (DNR) in 1974 were used. The areal extent of these marshes and wetlands was delineated by tracing each marsh and wetland type, apparent on each photograph, onto a transparent or translucent Mylar plastic overlay. The area of each delineation was then determined using a polar planimeter.

Species composition of the salt marshes, eelgrass beds, and other wetlands was determined by field sampling and observations at various locations in the harbor. Quantitative sampling was done only in salt marsh and eelgrass areas along representative transects. The aerial color and CIR photographs were used to select sampling sites and to measure the canopy cover of bare substrate, or substrate covered with algae, in plots where canopy cover of vascular salt marsh species was not complete.

Salt marshes were typed based on a modification of the classification system presented by Jefferson (1975). All classifications were based on quantitative transect samples, using percentage of canopy cover and percentage of frequency of occurrence. The eelgrass beds were classified as *Zostera noltii* and *Z. marina* beds, which were visually separable entities. *Z. marina* beds were further divided into "dense" and "sparse" beds. Other wetlands were classified according to species composition derived from qualitative surveys.

LANDSAT imagery

The utility of LANDSAT multispectral scanner (MSS) imagery in addressing the project objectives was determined based on a cursory evaluation of imagery acquired in January, February, and October 1973. Each 1:1,000,000 scale image covers 185 km (115 mi) on a side. The MSS records reflected radiation in four bands of the visible and near infrared regions of the electromagnetic spectrum: band 4, 0.5-0.6 μm; band 5, 0.6-0.7 μm; band 6, 0.7-0.8 μm; and, band 7, 0.8-1.1 μm. Coastal landforms, cultural and land use features and turbidity and circulation patterns are most distinct on band 5 (Fig. 5a). The land-water boundary, riverine features, geologic structure and geomorphology are most apparent on the band 7 image (Fig. 5b). In general, only one LANDSAT band is reproduced in this report. However, many of the conclusions formed during the evaluation are fully justified only by inspection of two or more spectral bands.

Ground truth data

Surface circulation patterns

Ground truth data, i.e. temperature (°C), salinity (ppt) and suspended sediment concentrations (mg/l), were acquired from the surface water throughout the harbor and from the water column at the harbor mouth. Temperature and salinity data were acquired with an in-situ probe. Suspended sediment concentrations were determined in the laboratory by weighing the amount of particulates filtered from water samples collected at each station. The surface water data were acquired at 40 sampling sites (Fig. 4), 26 near the harbor entrance, and 14 along the main navigation channels. There were 6 water column sites near the harbor entrance (stations 2, 3, 5, 6, 18, 19 on Fig. 4). Data were collected by personnel from Grays Harbor College during flood and ebb tides on 9, 10 and 11 July 1974 (Tables IX and X).

These temperature, salinity and suspended sediment data were used to produce maps of isotherms, isohalines and sediment concentrations, from which, in turn, were inferred surface circulation patterns during the different tidal stages. The water column data were used to prepare water profile diagrams to determine water characteristics at depth, subsurface processes, and degree of harbor stratification.

Huebner (1975) reports: "Some of the main physical aspects of interest in estuaries and bays include water movement, mixing processes, and salinity distribution. The movement of sediments (in suspension or by saltation) is related to these conditions. Basic physical parameters affecting prediction of flow and circulation are the physical dimension of an estuary, river flow, and tidal conditions. Measurement of these parameters, in addition to the in situ collection and analysis of horizontal and vertical salinity, and temperature and turbidity data, provide information for analysis. Certain inferences can be drawn from cross sections of the data; however, direct observation of currents is essential for quantitative understanding. Flow and drift methods are used to obtain direct observation, e.g., current meters, drogues, buoys, and dye releases."*

* Copyright, American Society of Photogrammetry, reprinted by permission.

east of the mouth of the Wishkah River vary from 0.0 parts per thousand (ppt) (total salt) at

tions). Annual maintenance dredging is required to ensure navigability in the channels leading to

a. Band 5.

Figure 5. Grays Harbor and northwestern Washington, portion of LANDSAT-1 image 1169-18375 acquired on 8 January 1973.

b. Band 7.

Figure 5 (cont'd). Grays Harbor and northwestern Washington, portion of LANDSAT-1 image 1169-18375 acquired on 8 January 1973.

Table IX. Predicted tides at Aberdeen and Pt. Chehalis during dye dispersal studies and acquisition of ground truth data [from National Ocean Survey (1973 and 1974)].

Location	Time (PDT)	Height (m)	Height (ft)
8 July 1974			
Aberdeen	0409	2.67	8.8
	1102	-0.09	-0.3
	1712	2.55	8.4
	0324	0.76	2.5
Pt. Chehalis	0338	2.33	7.7
	1020	-0.06	-0.2
	1641	2.21	7.3
	2242	0.73	2.4
9 July 1974			
Aberdeen	0451	2.52	8.3
	1138	0.06	0.2
	1747	2.61	8.6
Pt. Chehalis	0420	2.18	7.2
	1056	0.03	0.1
	1716	2.27	7.5
	2325	0.70	2.3
10 July 1974			
Aberdeen	0007	0.73	2.4
	0534	2.39	7.9
	1214	0.24	0.8
	1823	2.67	8.8
Pt. Chehalis	1503	2.06	6.8
	1132	0.21	0.7
	1752	2.33	7.7
11 July 1974			
Aberdeen	0056	0.67	2.2
	0627	2.24	7.4
	1251	0.45	1.5
	1903	2.73	9.0
Pt. Chehalis	0014	0.64	2.1
	0556	1.91	6.3
	1209	0.42	1.4
	1832	2.39	7.9

Table X. Schedule for ground truth data acquisition, 9-11 July 1974.

Date	Time (PDT)	Tidal stage
Water surface		
9 July	0955-1132	Late ebb
	1428-1701	Late flood
10 July	0523-0745	Late flood – Early ebb
	1025-1240	Late ebb – Early flood
11 July	0519-0725	Late flood – Early ebb
	1052-1358	Late ebb – Early flood
Water column		
10 July	0540-0635	Early ebb
	1055-1144	Late ebb – Early flood
11 July	0600-0640	Early ebb
	1215-1255	Early flood

Aircraft and satellite imagery interpretations of circulation patterns were subsequently compared with interpretations made from the above data obtained from shipboard surveys and from the Grays Harbor hydraulic model studies to determine the accuracy, reliability, and cost effectiveness of remote sensing versus more conventional data acquisition procedures.

The Grays Harbor model studies were conducted by the Hydraulics Division of the U.S. Army Engineer Waterways Experiment Station (Brogdon 1972a). The model, a fixed-bed model with provisions for future conversion to a movable-bed model, was designed and constructed (February 1968-June 1969) to scales of 1:500 horizontally and 1:100 vertically. It reproduced all of Grays Harbor, the Chehalis River to the head of tidal influence (South Montesano), and a portion of the Pacific Ocean adjacent to the harbor entrance. The primary purposes of the overall model study were to evaluate the possible effects of rehabilitation of both the north and south jetties and of enlarging and realigning the navigation channel, to investigate the stability of Point Chehalis, and to locate suitable dredge disposal areas. The flushing rate and dispersion characteristics of waste materials discharged into the system were also to be investigated.

Hydraulic and salinity verifications were conducted from June to December 1969. Fixed-bed shoaling verification was accomplished from August to September 1970. Hydraulic, salinity and dye dispersion base tests were performed from January to July 1970 (Brogdon and Fisackerly 1973). Model verification tests indicated that the model hydraulic and salinity regimes were in satisfactory agreement with those of the prototype for comparable conditions. It was assumed that the model would provide quantitative data concerning the effects of the proposed improvement plans on the hydraulic and salinity regimes of the estuary. After completion of all fixed-bed model verifications and base tests, the general model investigation program was initiated.

To date, model studies have been performed for the north jetty (Brogdon 1972b), Westport small boat basin (Brogdon 1972c and 1975b), the south jetty (Brogdon 1972d), the existing 9.1-m (30-ft) (MLLW) deep navigation channel (Brogdon 1975a), and a 12.1-m (40-ft) deep navigation channel (Brogdon 1976).

a.

Figure 6. Color (a) and color infrared (b) photographs, taken 13 July 1974. (Note: not all CIR photographs show the minor amount of water surface detail as shown here. Different camera settings and solar conditions could produce a more useful CIR photograph.)

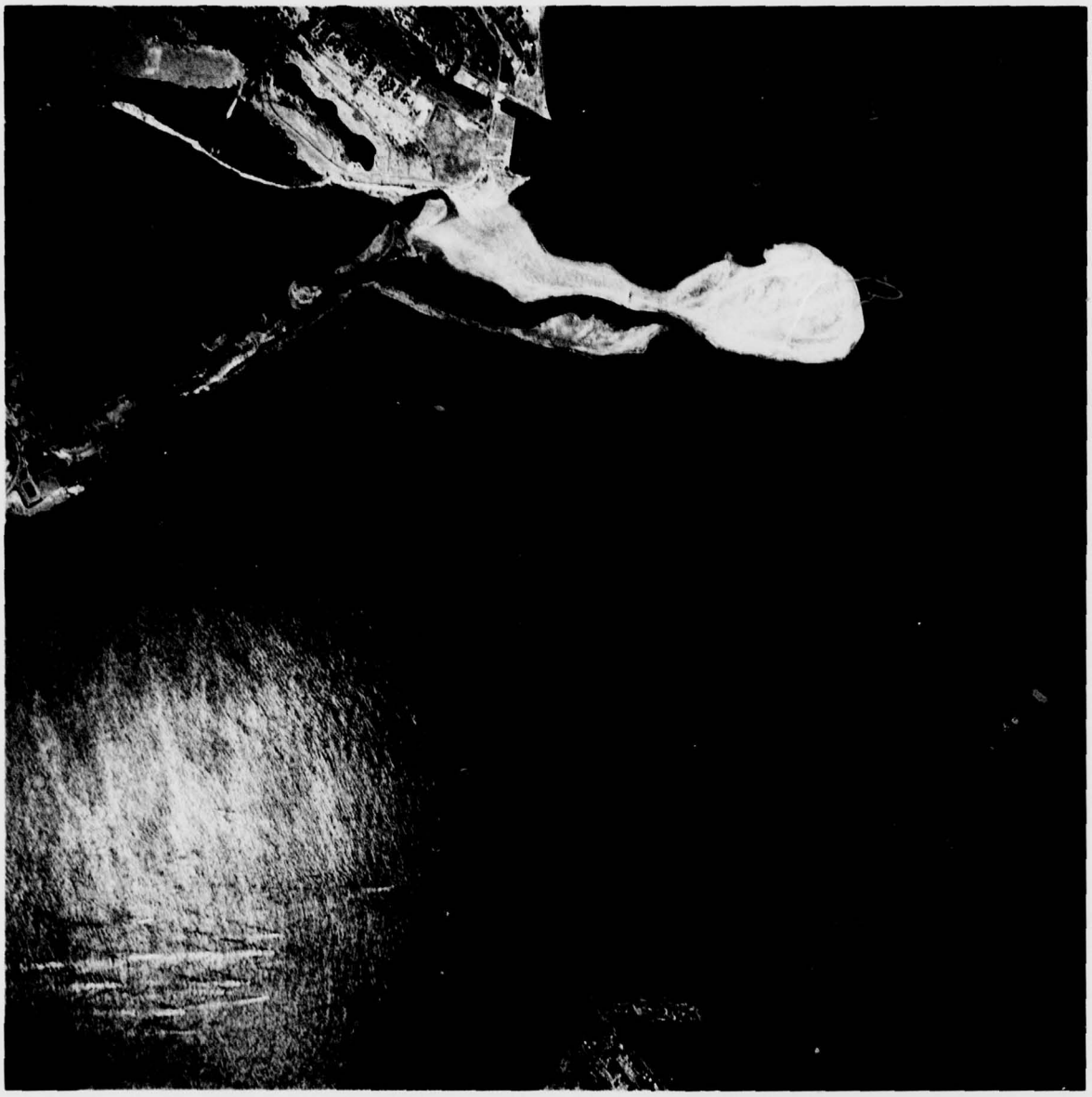

b

Figure 6 (cont'd)

Intertidal habitats

Species composition of the wetlands was determined by identification of specimens collected along transects using standard sampling techniques and by field observations during related investigations. Quantitative sampling of vegetation was done only in salt marsh and eelgrass areas. Other surveys were qualitative and were done to determine plant communities based on abundant species.

RESULTS AND DISCUSSION

Remote sensing techniques

Surface circulation patterns

NASA NP-3A imagery. Circulation patterns were determined from the NASA NP-3A color and CIR photographs based on foam (debris) lines formed at mixing zones on the water surface, changes in water color (turbidity) in the open areas of the harbor and suspended sediment patterns near shore. Meyer and Welch (1975) point out that water color is influenced by its optical properties, type and amount of suspended organic and inorganic particles, and water surface roughness, and by the nature of the bottom in shallow water.

The color photographs were more useful than the color infrared photographs for analyzing the circulation patterns because there was less contrast and sun glint (Fig. 6). Generally, variations in suspended sediment concentrations in the surface water were not significant enough to be observed on the photographs. However, thermal differences of the water surface were readily apparent on the RS-14 and M²S imagery and circulation patterns based on these differences were easily delineated. There was more subsurface information on the color photographs, although wave patterns were more apparent on the CIR photographs (possibly because of the greater sun glint which enhanced the appearance of individual waves).

The 13 July 1974 (Mission 283) photographs were acquired during early flood just after low water slack. Consequently, water movement was minimal and, except at a few locations, circulation patterns were not readily discernible (Fig. 7). Most of the patterns observed on the color and CIR photographs were near the harbor entrance because flood tide had begun. A turbid zone along the north jetty to Damon Point was more pronounced on the color photographs because the suspended solids in a greater portion of the water column were visible. Water penetration on the color photographs was greater, from the surface to 0.9 to 2.42 m (3 to 8 ft). Because the exposure setting is critical when CIR photographs are being taken and because it was difficult to see the water surface with uniform solar illumination, the water surface frequently appeared dark (underexposed). The setting with color photographs was not as critical and better exposed photographs were acquired. The water surface was not too dark and surface detail was generally very good on the color photographs.

A zone with high turbidity was observed on the south side of the south jetty (Fig. 8). It appeared that currents were moving west along the jetty and transporting suspended sediment from the surf zone. From the conjunction of the south jetty and the shoreline to approximately 4.5 km (2.79 mi) south along the Pacific coast, high concentrations of suspended sediment were apparent in the surf zone. Also, linear patterns that may have been internal waves were observed in this area.

The surface wave patterns were more discernible on the CIR than on the color photographs, especially where sun glint was high. The detection of wave refraction near submerged shoals could be very useful in locating unmapped shoals or in analyzing changes in shoaling patterns and shoal topography. The land/water interface between exposed tidal flats and water in North Bay was more apparent on the CIR photographs than on the color photographs. Foam lines which delineate water type boundaries or form parallel to wind directions because of surface Langmuir circulation were apparent in the color and CIR photographs.

Surface thermal patterns (Fig. 9) apparent on RS-14 scanner imagery acquired on 12-13 July 1974 from the time of mid-ebb through maximum ebb currents were very useful in delineating surface circulation (Fig. 10) and in showing the relative water temperatures of the main tributaries to the harbor (Table XI). Huebner (1975) reports: "In addition to the study of the temperature patterns in the mixing zones, there is interest in mapping the distribution of the water masses that are moved about by nearshore currents"; and "Several investigations have concluded that thermal infrared imagery in the 8 to 14-μm band can provide useful information on estuarine circulation."

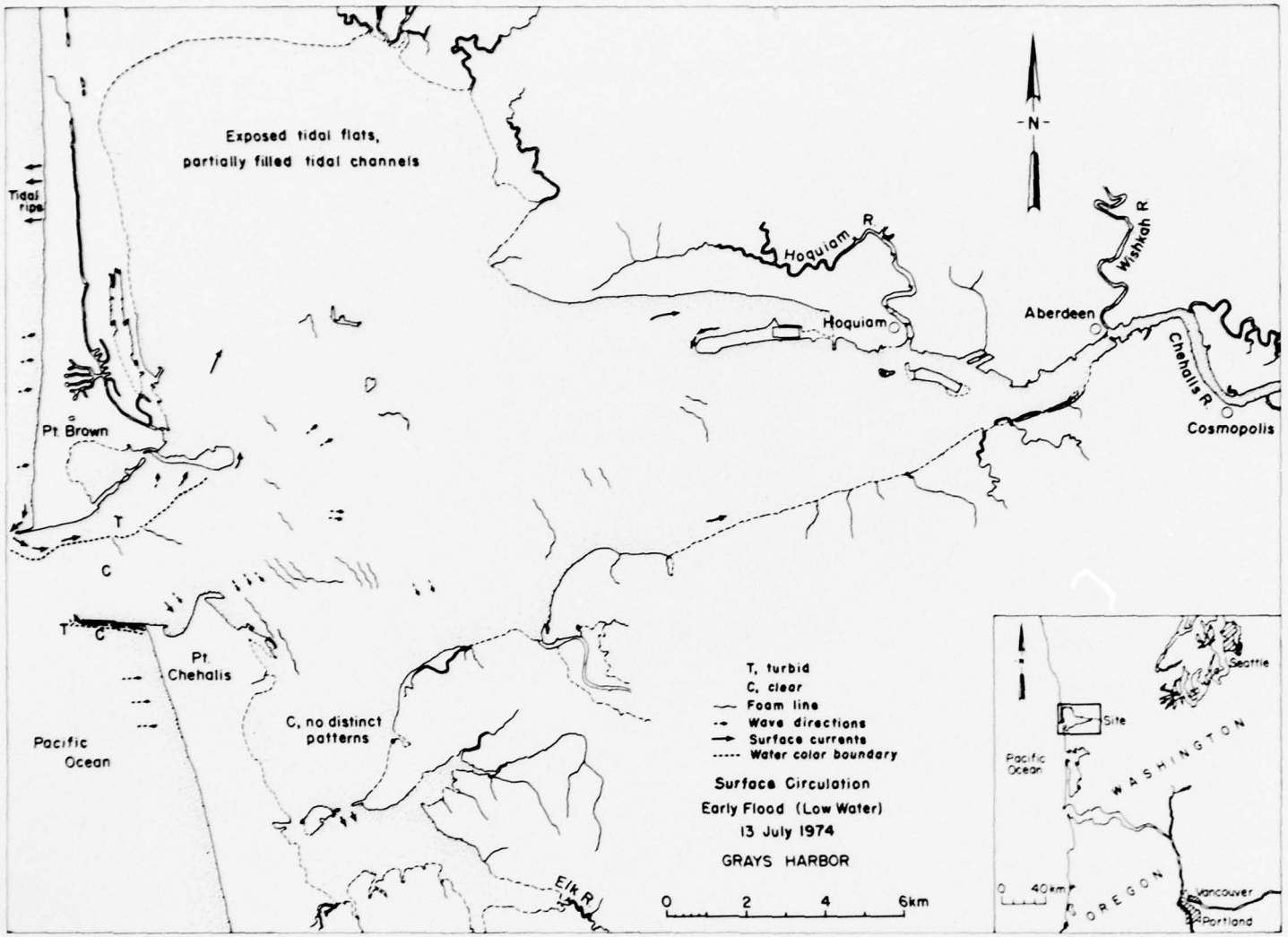

Figure 7. Surface circulation patterns inferred from NASA NP-3A color and CIR photographs acquired on 13 July 1974.

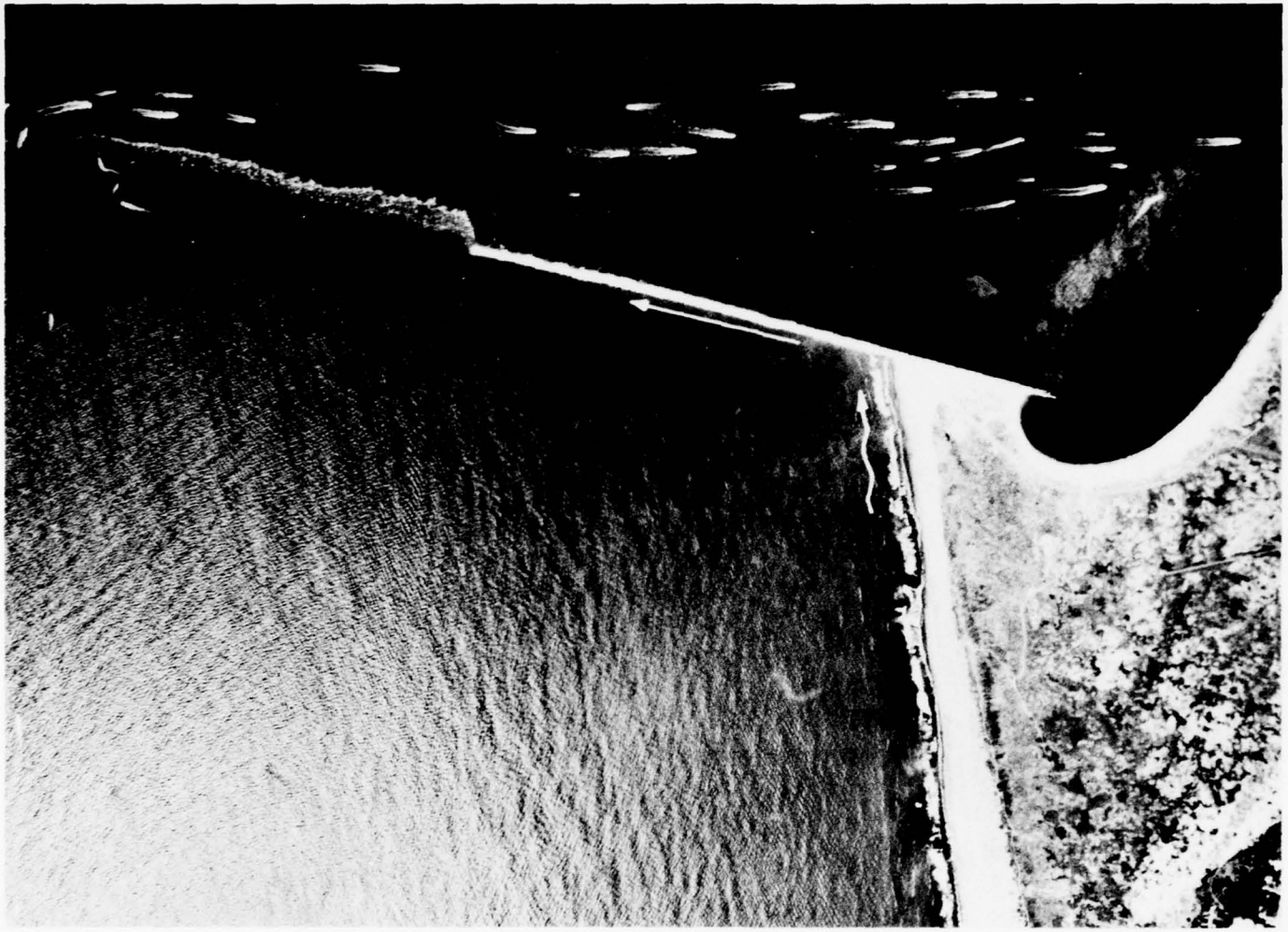

Figure 8. South jetty, 13 July 1974.

a. Line 21

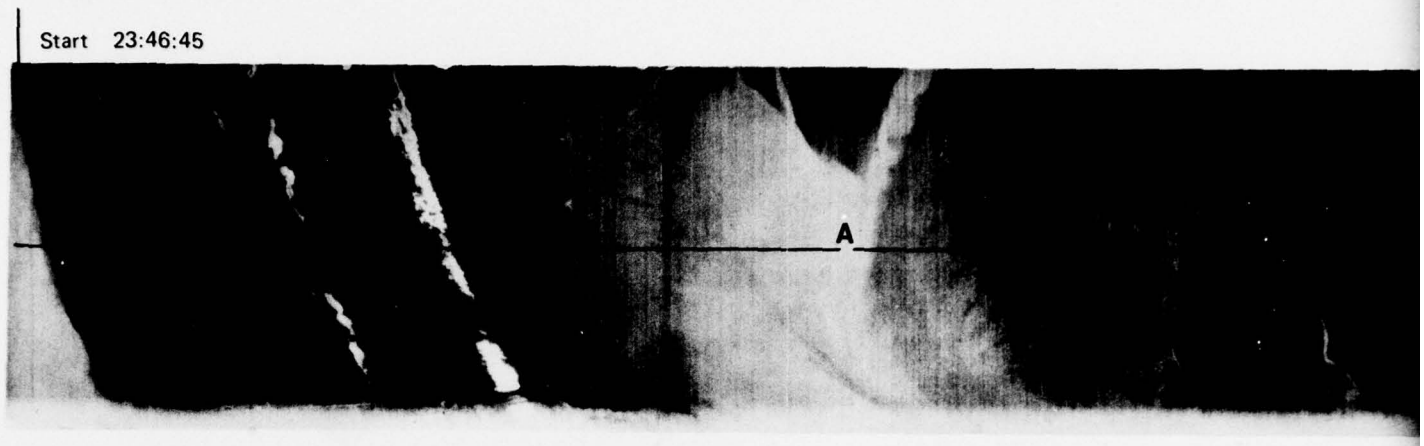

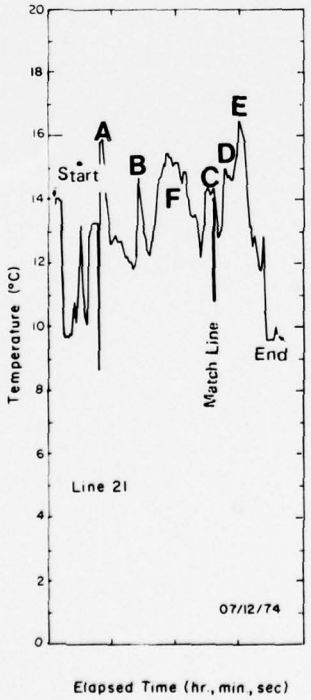

Approximate Scale
(1:23500)

0.4 0 0.4 0.8mi

0.64 0 0.64 1.3km

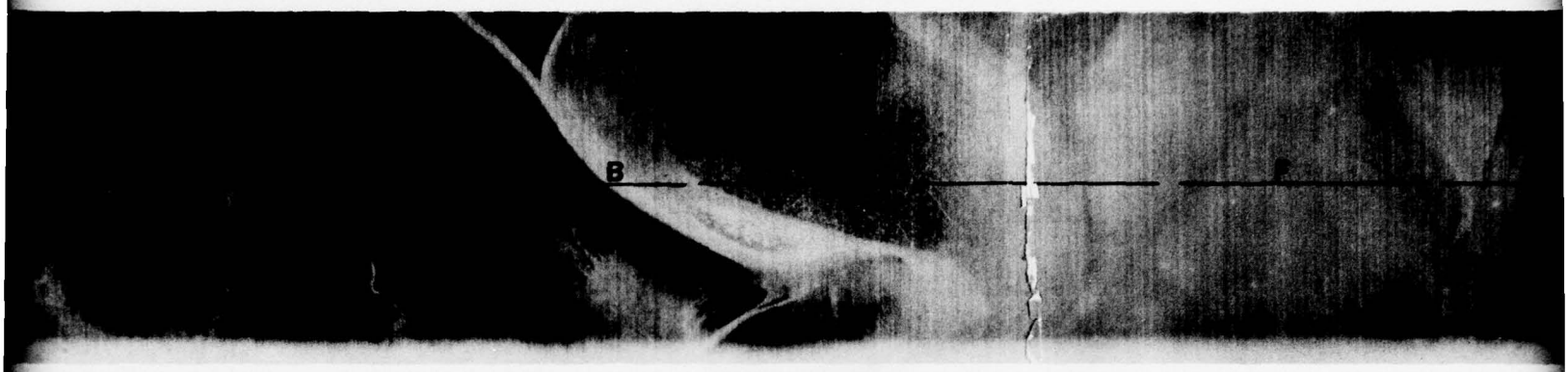

Match Line

Direction of Flight

ximate Scale
23500)

0.4 0.8 mi
0.64 1.3 km

Figure 9. RS-14 thermal IR imagery with graph of PRT-5 radiation ther
agery. Note the occasional high temperature spike on the PRT-5 graph.
surge.

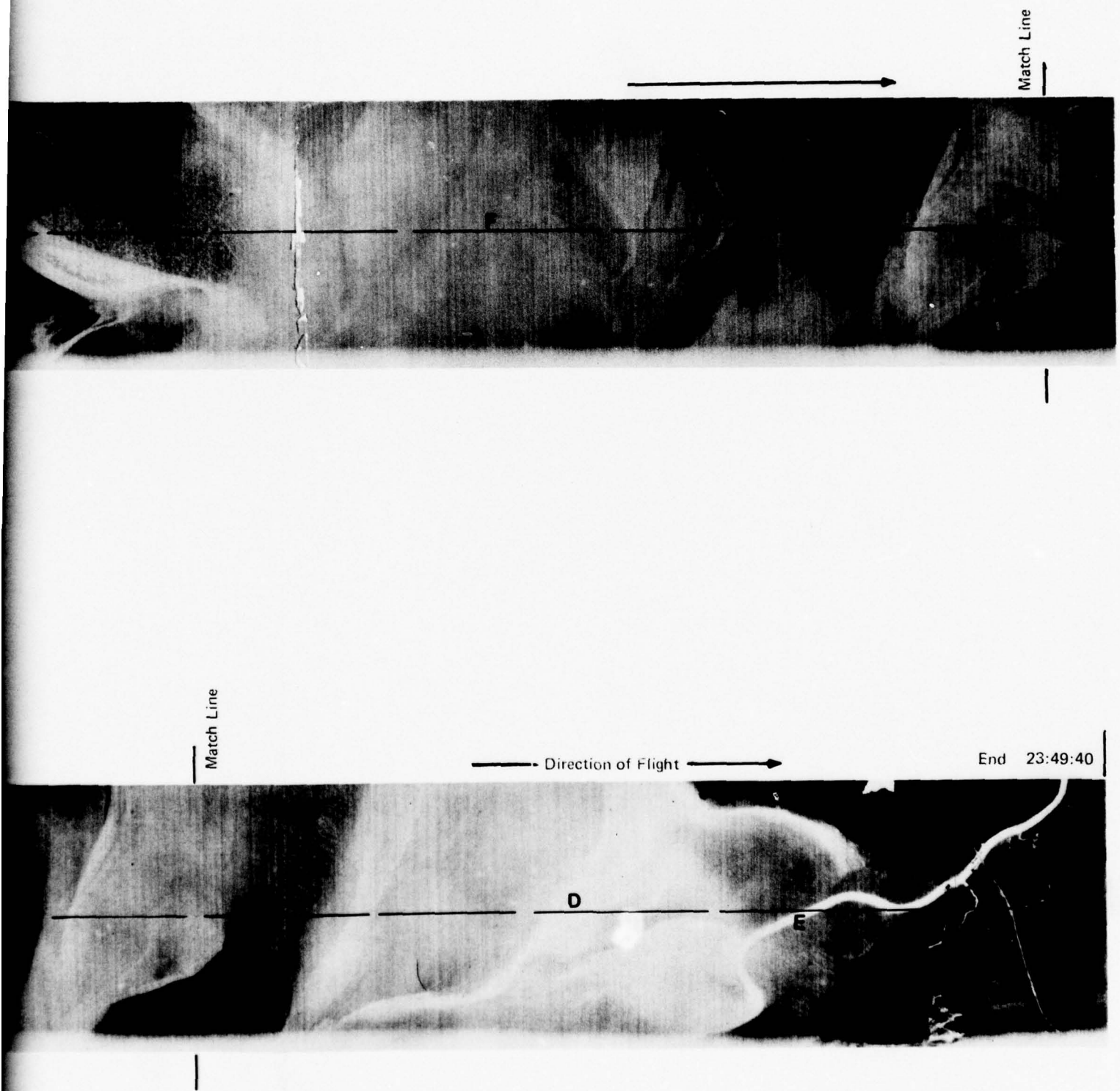

Figure 9. RS-14 thermal IR imagery with graph of PRT-5 radiation thermometer data. Warm features are lighter on the imagery. Note the occasional high temperature spike on the PRT-5 graph. This spike is probably caused by an electronic signal surge.

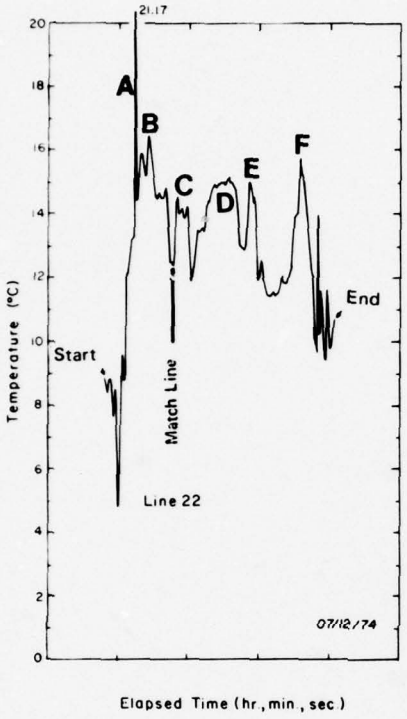

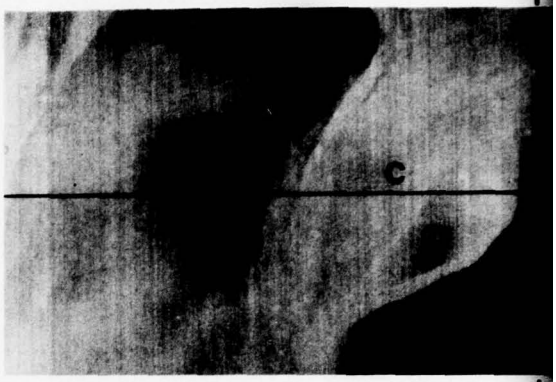

Approximate Scale
(1:23500)

0.4 0 0.4 0.
0.64 0 0.64 1.3

End 23:58:25

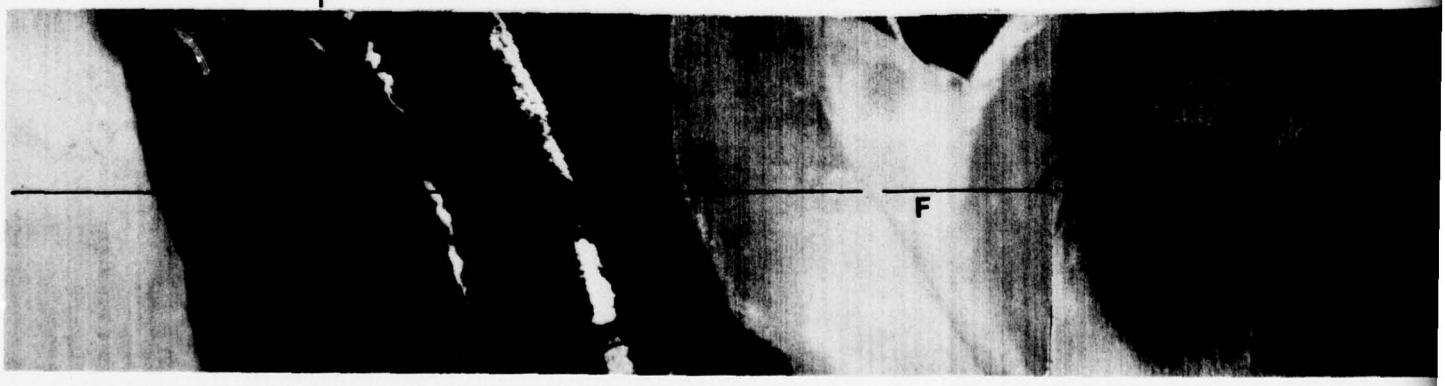

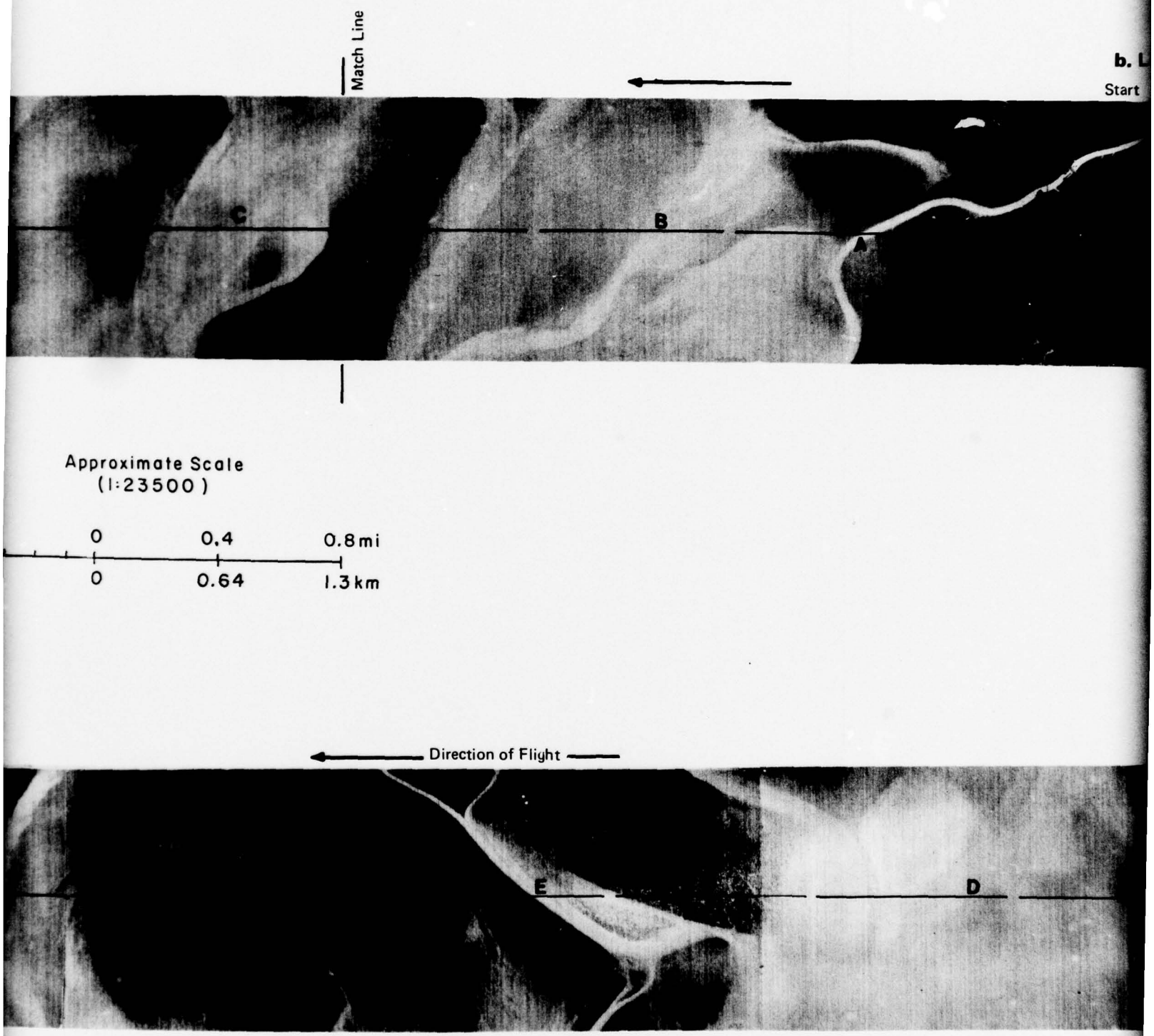

Figure 9 (cont'd). RS-14 thermal imagery with graph of P imagery. Note the occasional high temperature spike o signal surge.

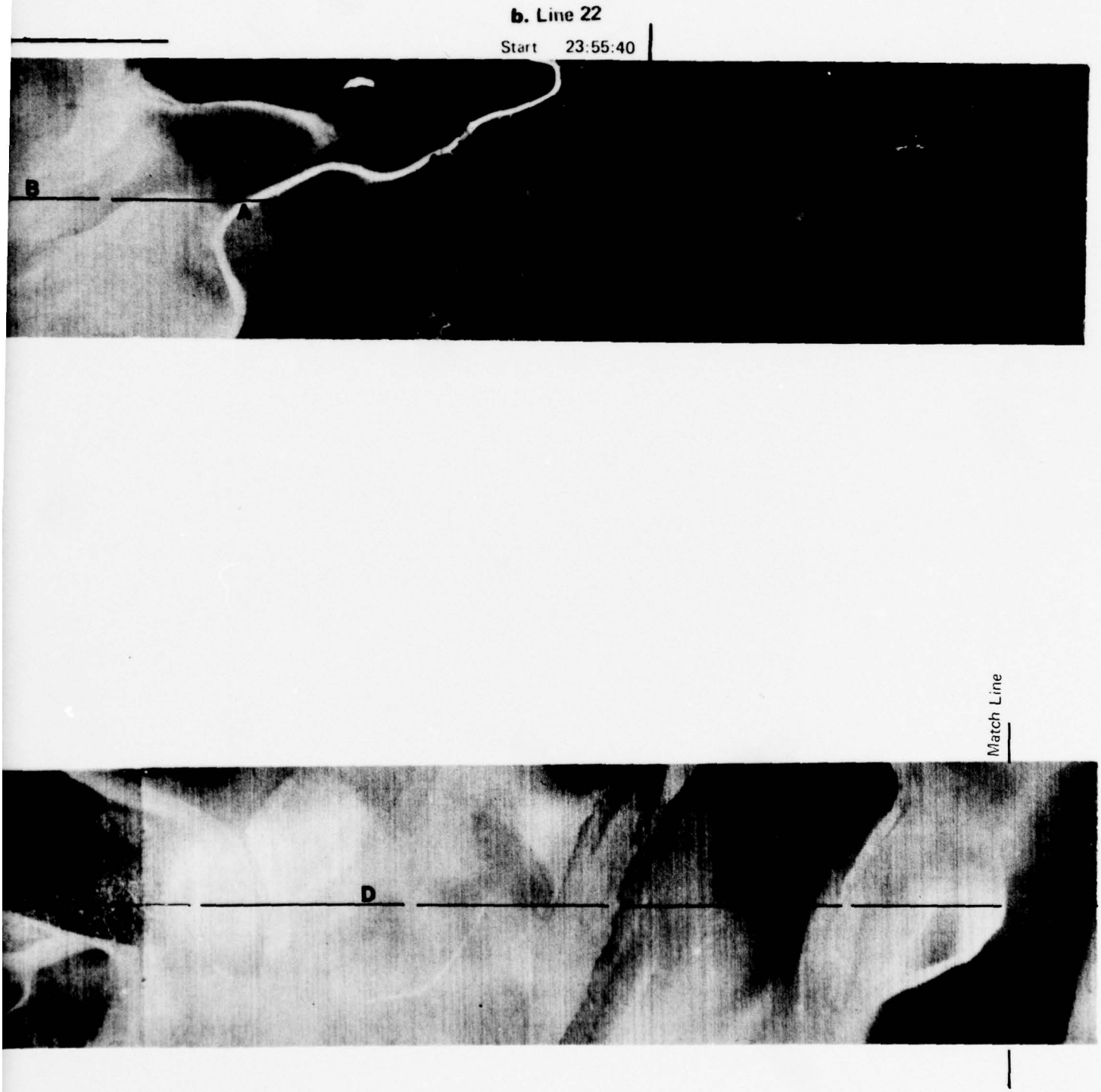

Figure 9 (cont'd). RS-14 thermal imagery with graph of PRT-5 radiation thermometer data. Warm features are lighter on the imagery. Note the occasional high temperature spike on the PRT-5 graph. This spike is probably caused by an electronic signal surge.

c. Line 23

Start 00:04:55

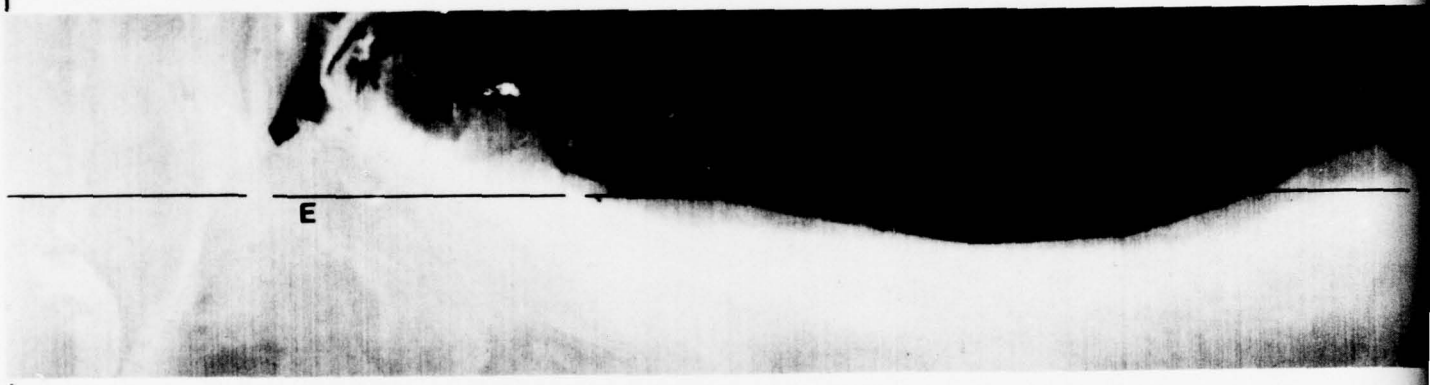

Match Line 1

Approximate Scale
(1:23500)

0.4 0 0.4 0.8 mi

0.64 0 0.64 1.3 km

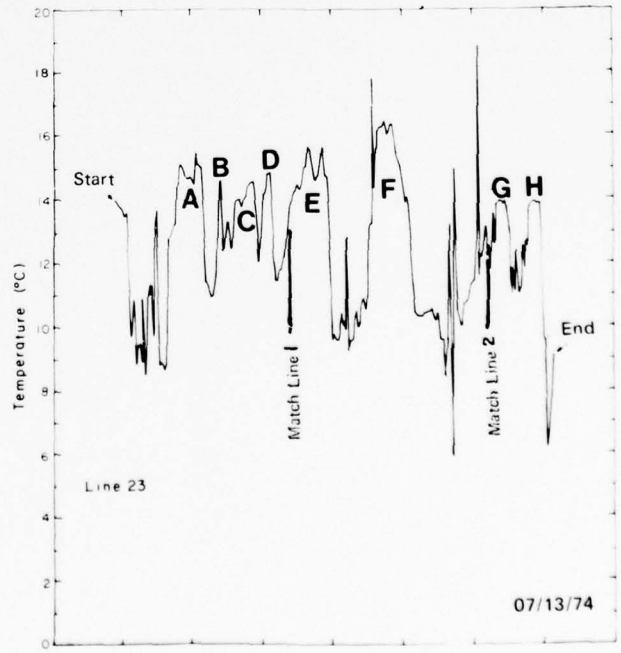

Elapsed Time (hr, min, sec)

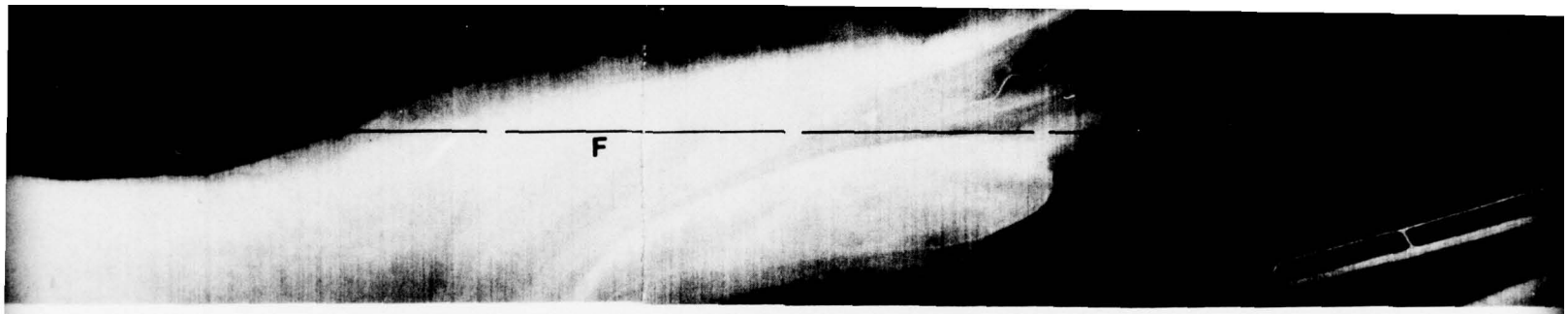

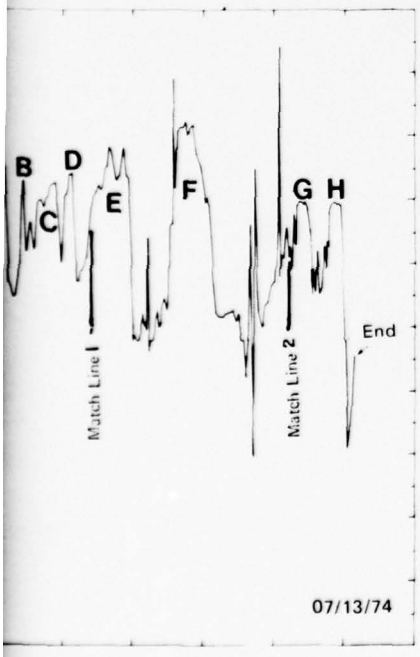

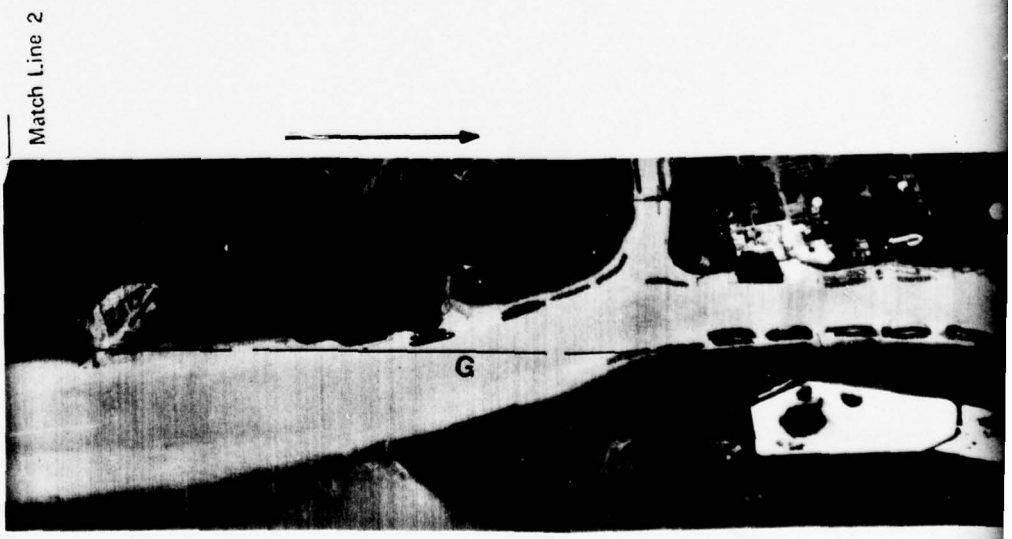

Figure 9 (cont'd). RS-14 thermal imagery with graph of PI imagery. Note the occasional high temperature spike on signal surge.

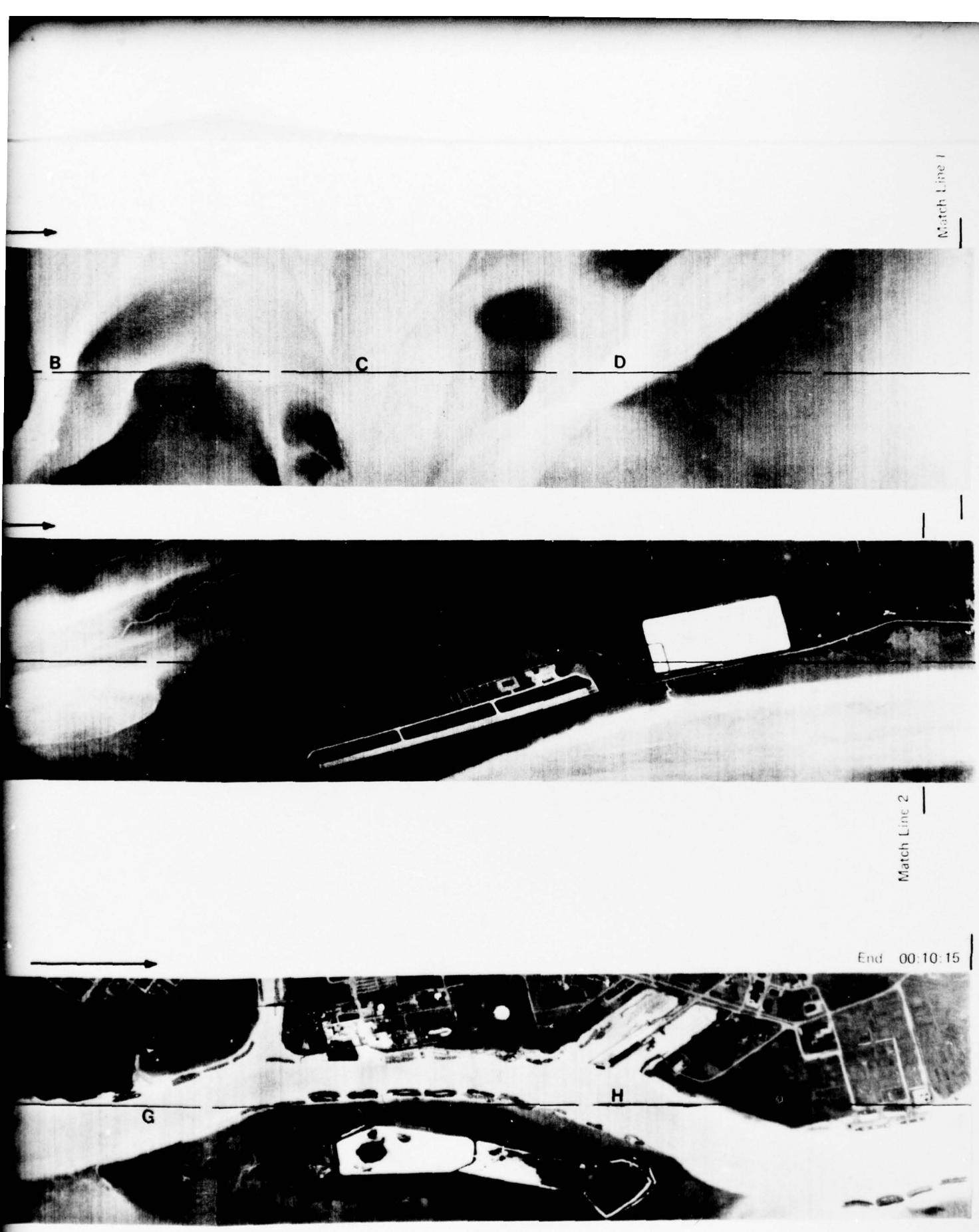

Figure 9 (cont'd). RS-14 thermal imagery with graph of PRT-5 radiation thermometer data. Warm features are lighter on the imagery. Note the occasional high temperature spike on the PRT-5 graph. This spike is probably caused by an electronic signal surge.

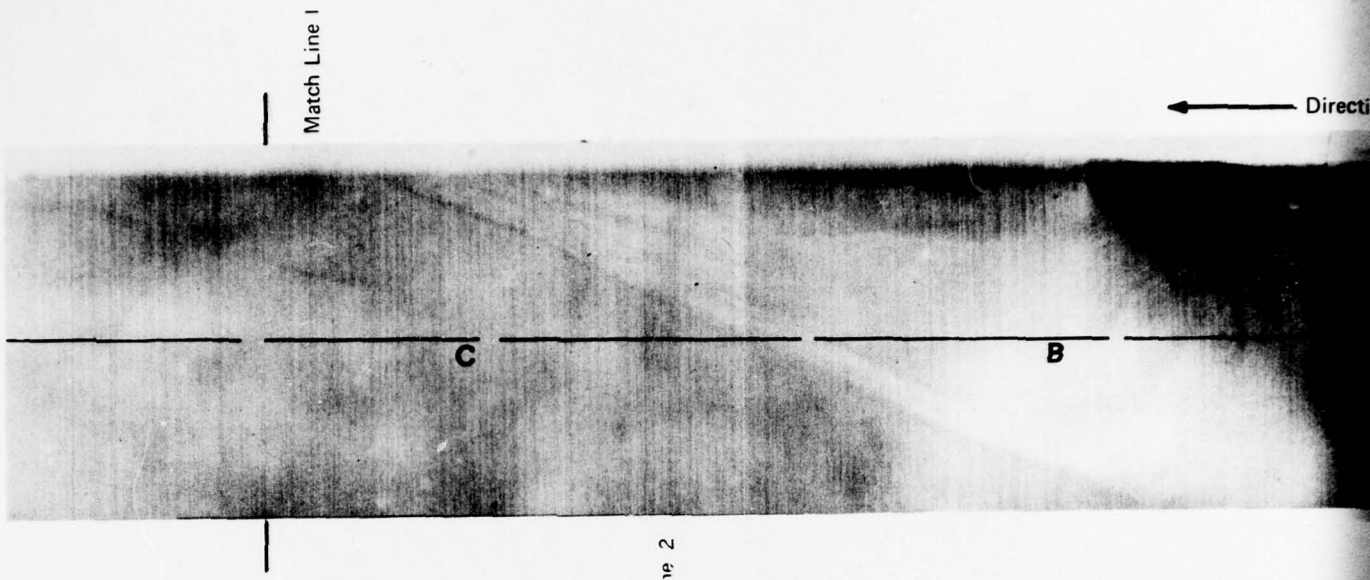

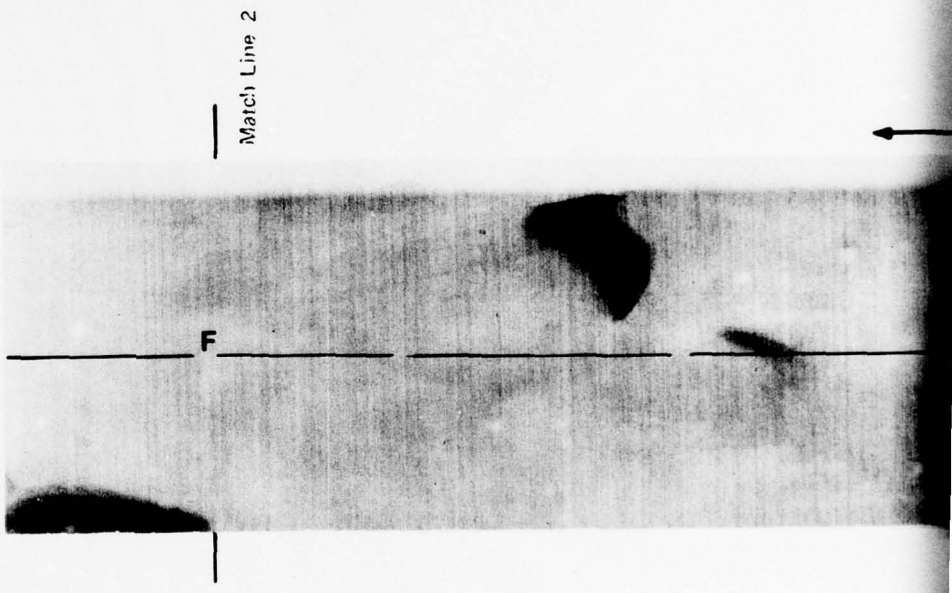

Approximate Scale
(1:23500)

0.4 0 0.4 0.8 mi
0.64 0 0.64 1.3 km

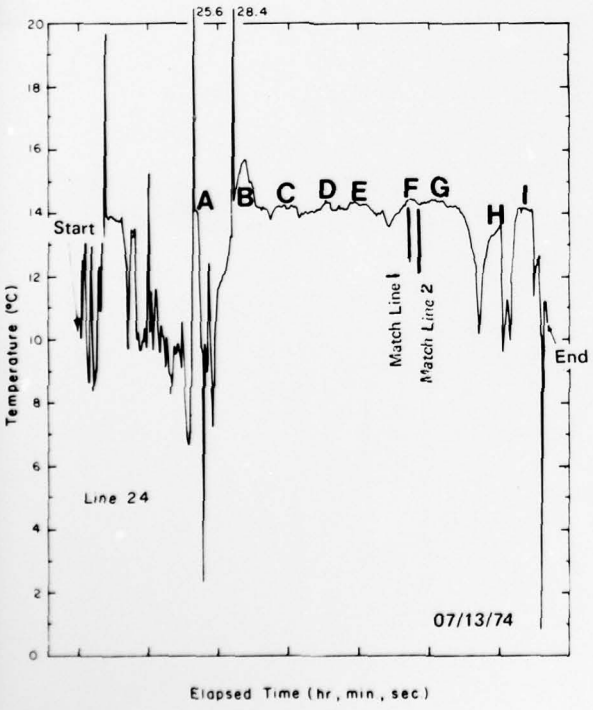

End 00:22:15

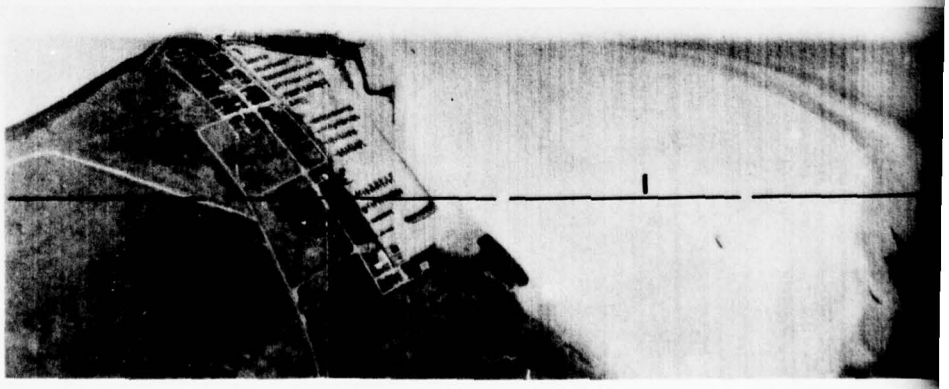

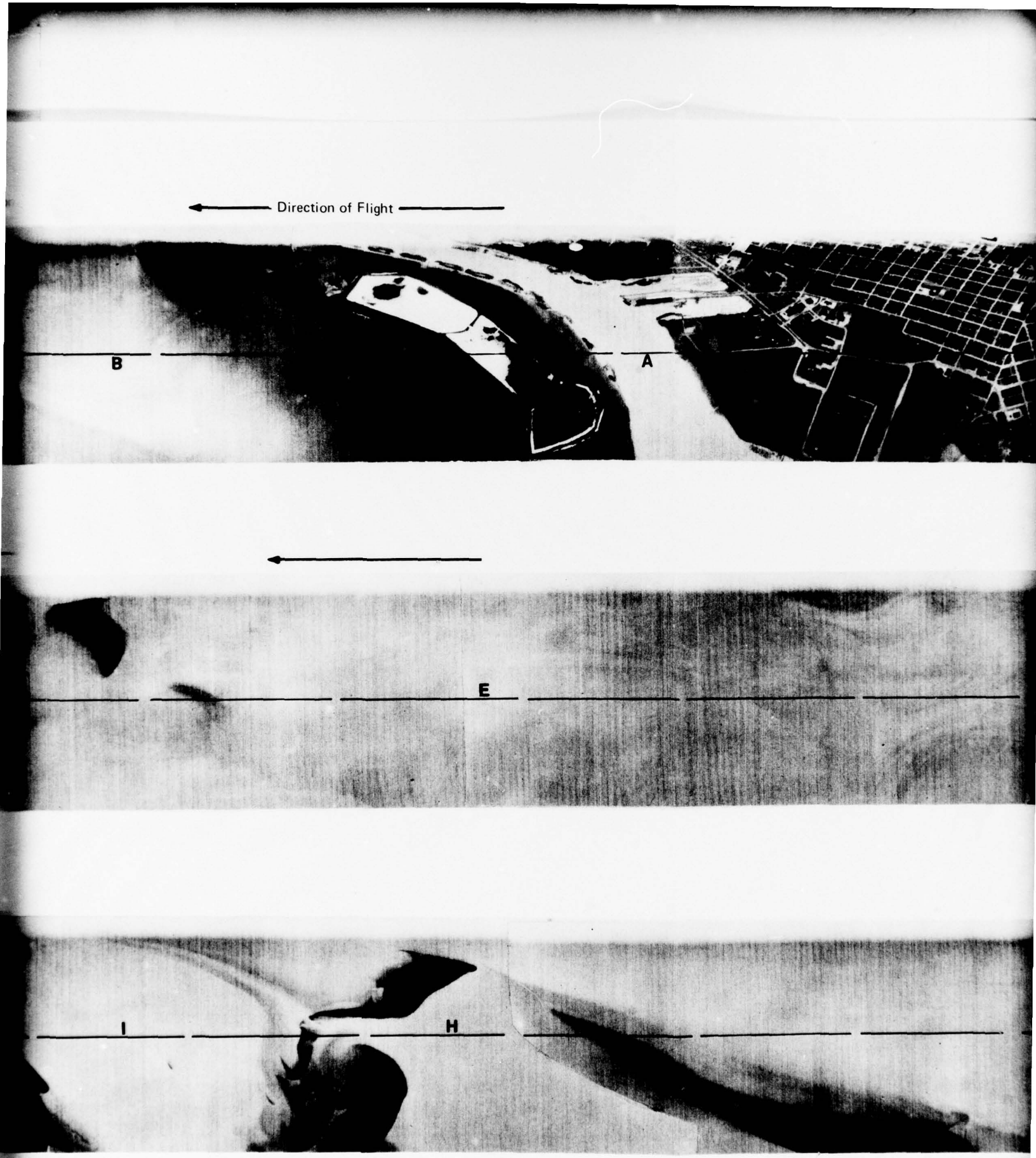

Figure 9 (cont'd). RS-14 thermal imagery with graph of PRT-5 radiation therm
imagery. Note the occasional high temperature spike on the PRT-5 graph.
signal surge.

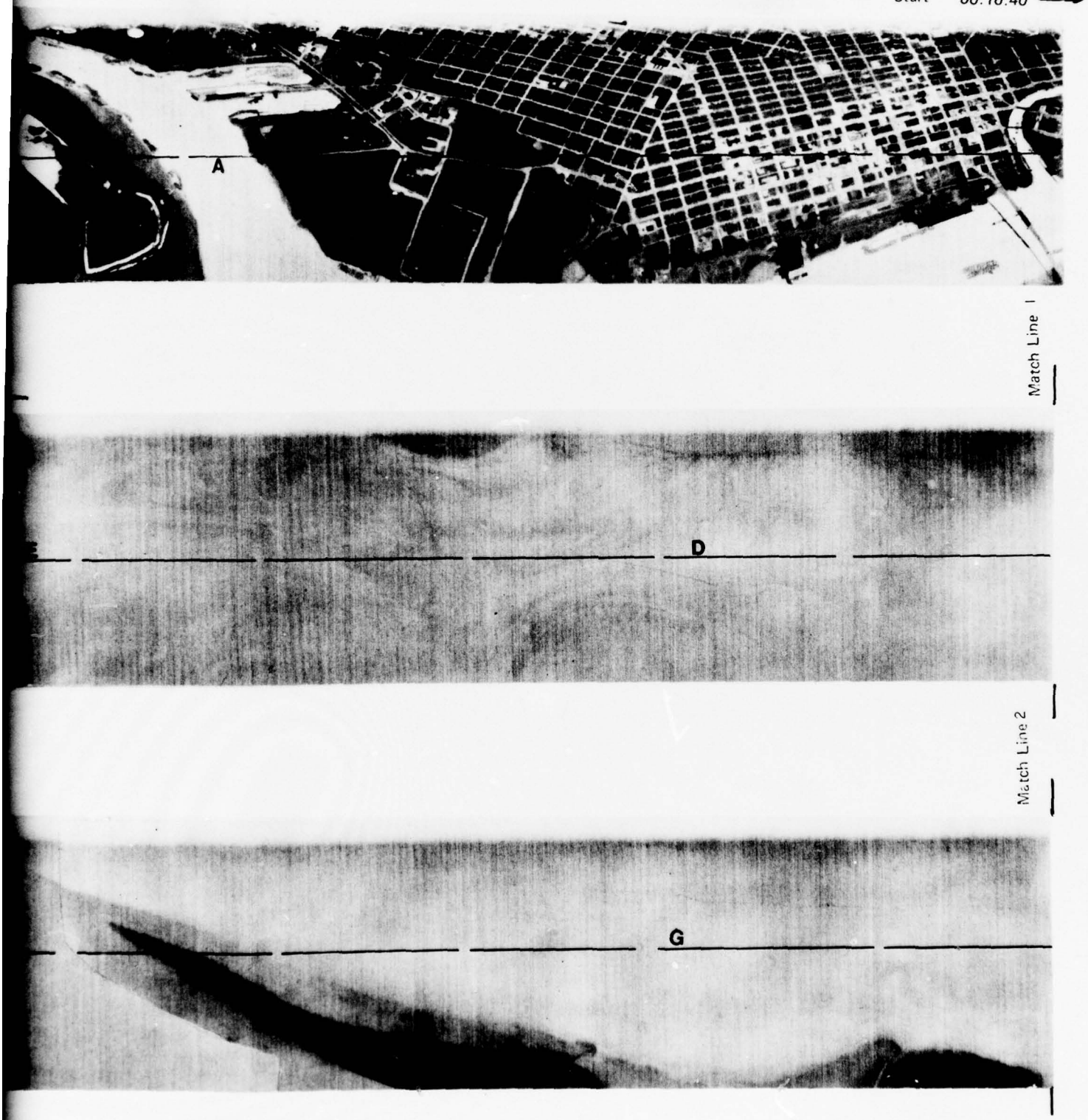

Figure 9 (cont'd). RS-14 thermal imagery with graph of PRT-5 radiation thermometer data. Warm features are lighter on the imagery. Note the occasional high temperature spike on the PRT-5 graph. This spike is probably caused by an electronic signal surge.

Approximate Scale
(1:23500)

0.4 0 0.4 0.8mi
0.64 0 0.64 1.3km

e. Line 25

Start 00:27:50

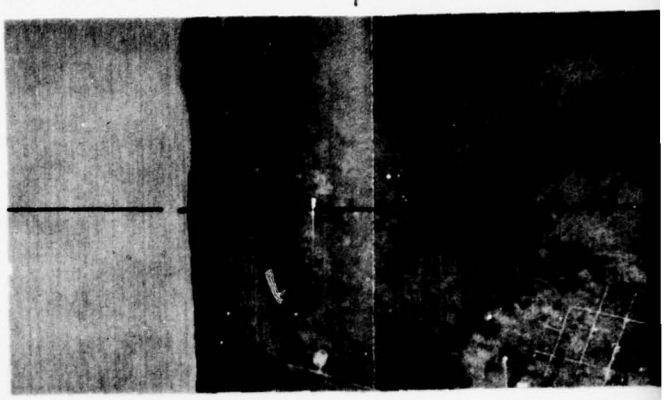

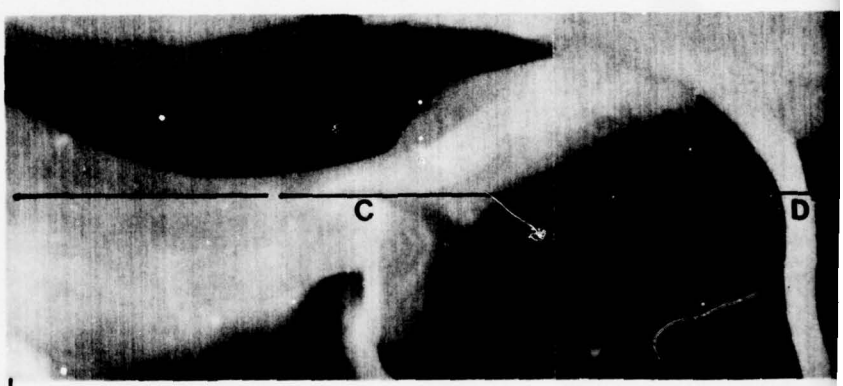

Match Line 2

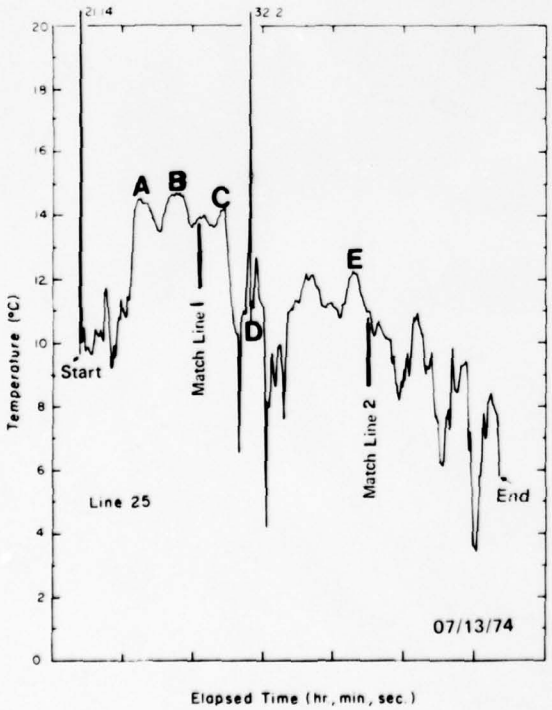

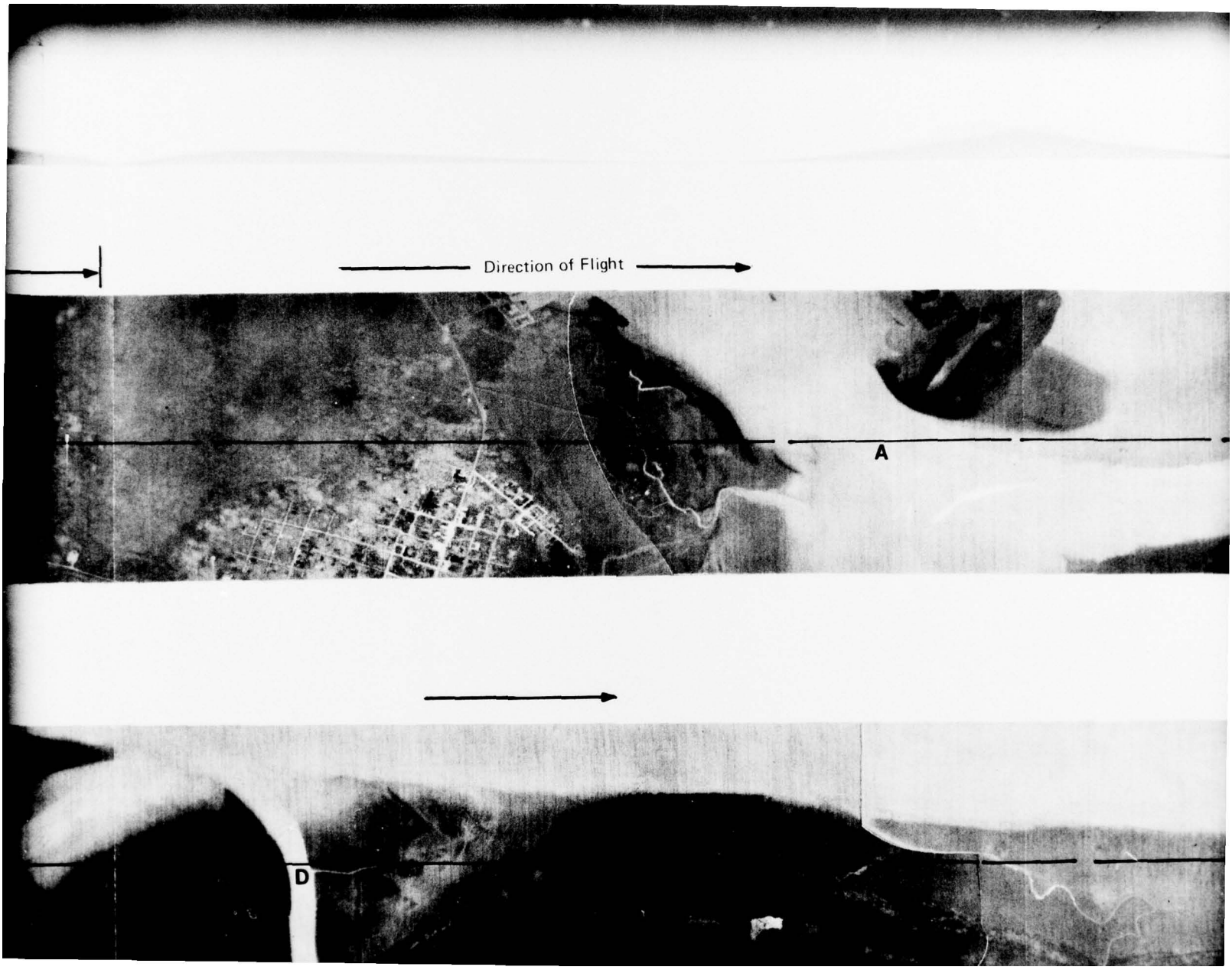
Direction of Flight
A
D

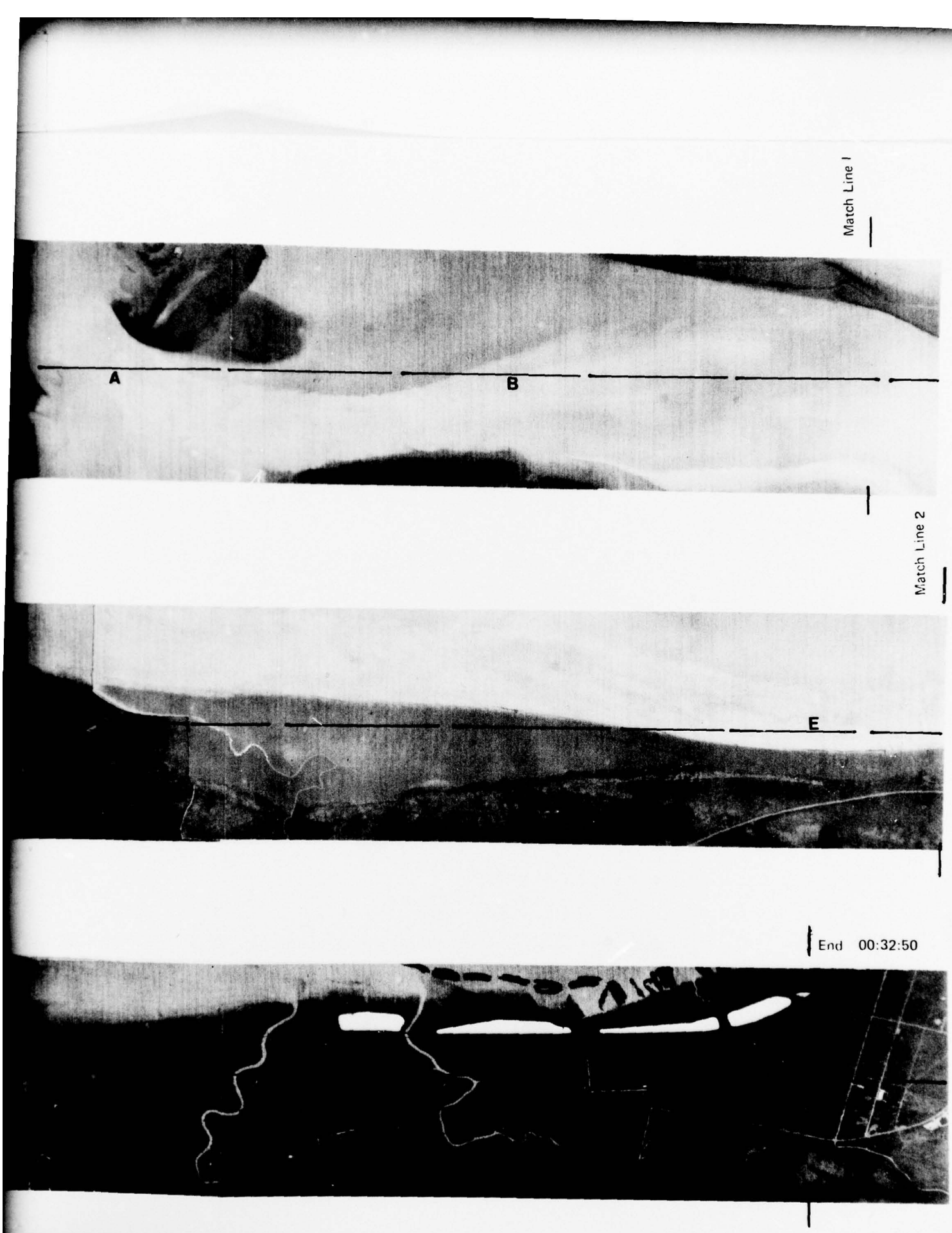

re 9 *(cont'd). RS-14 thermal imagery with graph of PRT-5 radiation thermometer data. Warm features are lighter on the* **gery.** *Note the occasional high temperature spike on the PRT-5 graph. This spike is probably caused by an electronic* **al** *surge.*

Table XI. Relative temperatures of tributary water and harbor water as observed on RS-14 imagery, 12-13 July 1974, and M^2S imagery, 10 April 1975.

	12-13 July 1974	*10 April 1975*
Elk River	*	*
Johns River	Warmer	Warmer
Newskah Creek •	~ Same	Warmer
Charley Creek	~ Same	Warmer
Chehalis River	Colder	Colder
Wishkah River	Colder	Colder
Hoquiam River	Warmer	Colder
Grass Creek	Warmer	Warmer
Chenois Creek	Warmer	Warmer
Humptulips River	Warmer	Warmer

* Not visible on imagery.

Complex circulation patterns were visible in three areas where mixing appeared extensive: North Bay, near Pt. New (lines 21 and 22), and between Moon Island and the coast east of Stearn's Bluff (line 23). Generally, observed ebb flow patterns were restricted to the tidal channels; e.g., water in the vicinity of the settling ponds south of Aberdeen moved primarily out South Channel (line 25).

PRT-5 data showed detailed thermal variations along the flight lines. The location of the PRT-5 viewing line is approximate. In fact, it probably meandered gradually from the centerline. These data (Fig. 9) were correlated with the RS-14 imagery interpretations (warm features are lighter) and provided information on relative temperature distributions and, indirectly, on surface circulation. Meyer and Welch (1975) report: "A thermal scanner records relative temperature difference and, therefore, must be used in conjunction with a temperature reference source and with actual surface temperature records obtained during scanner overpasses."

To calibrate the PRT-5 data, temperatures recorded by the PRT-5 must be compared with temperatures taken at selected ground features to adjust the recorded PRT-5 temperature for atmospheric effects. This was not done during this study; therefore, temperatures shown are not adjusted and are relative values, not absolute temperatures of the ground or water. Since temperature differences were of primary importance, relative accuracy is more important than absolute accuracy.

Temperatures (not absolute) along line 21 (Fig. 9) on 12-13 July 1974 varied from 16.4°C (61.5°F) near the mouth of Grass Creek (E)* to 14.6°C (58.3°F) in the northern part of Oyhut Channel (A, B). Temperatures of the tidal flats were approximately 12°-13°C (53.6°-55.4°F). Water temperatures in Campbell Slough and Humptulips River Channels (F, C, D) were approximately 15°C (59°F). Temperatures along line 22 varied from 11.4°C (52.5°F) in the middle of a tidal flat to 16.4°C (61.5°F) near the mouth of Grass Creek (A). Note the occasional high temperature spike on the PRT-5 graph. This spike is probably caused by a voltage surge in the instrument. It cannot be correlated with a feature on the imagery.

Temperature fluctuations along line 23 were more frequent than those along lines 21 and 22 because the land/water boundary was traversed many times (Fig. 9). Temperatures of the harbor and tributary waters were as follows: on the west side of the channel at the confluence of the Oyhut and Campbell Slough Channels (A), 14.7°C (58.5°F) and 15.5°C (59.9°F); on the east side, at the confluence of the Humptulips River and Chenois Creek Channels (C, D), there was a well defined mixing zone and temperatures varied from 12.4°C (54.3°) on the west to 14.8°C (58.6°F) on the east; south of Pt. New and Brackenridge Bluff (E) was a mixing zone with temperatures variable from 14.4°C (57.9°F) to 15.6°C (60.1°F); the warmest observed water, 17.8°C (64°F), along line 23 was found along the shore from Pt. New to Grays Harbor City (E, F); water in Hoquiam Reach (G) varied from 12° to 13°C (53.6° to 55.4°F).

Water temperatures along line 24 from west of Rennie Island to Whitcomb Flats varied minimally from 14.3°C (57.7°F) to 13.5°C (56.3°F). Well defined mixing zones occurred in the area around Crossover Channel (D) and south of Moon Island Reach (C, B). In the channel west of Whitcomb Flats and east of Westhaven Cove (I), temperatures were approximately 14°C (57.2°F). Temperatures in Westhaven Cove were approximately 12°C (53.6°F).

In the northern portion of South Bay (A, B on line 25), warm water from Redman Slough (C) and the Johns River (D) mixed with cooler water further north. Temperatures in the mixing zone varied from 13.5°C (56.3°F) to 14.7°C (58.4°F). Temperatures along South Channel (C, D) varied from 10.8°C (51.4°F) to 12.2°C (54°F).

* Letters refer to locations on film strips.

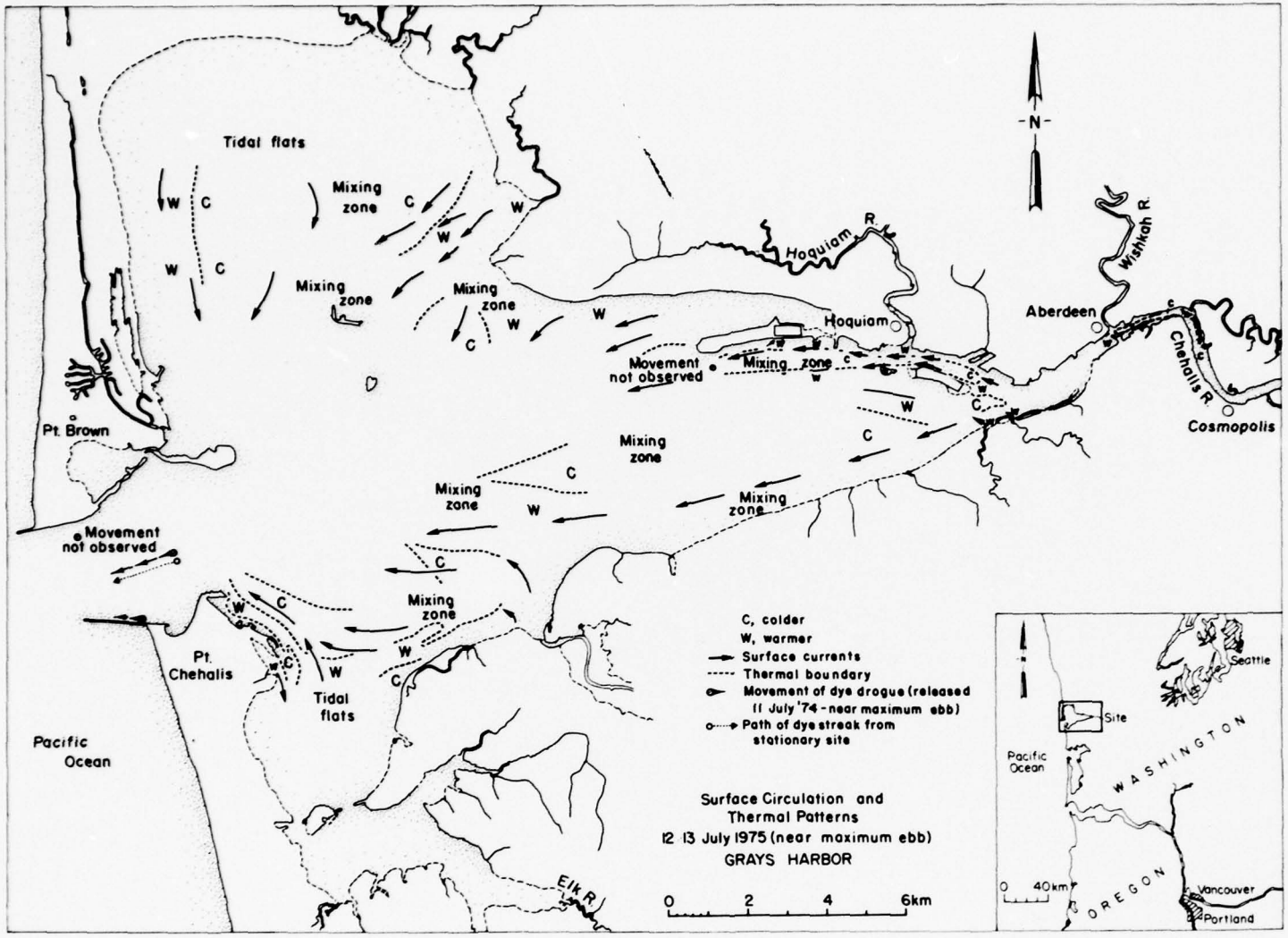

Figure 10. Surface circulation patterns inferred from NASA RS-14 thermal scanner imagery acquired 12-13 July 1974 shown in Figure 9.

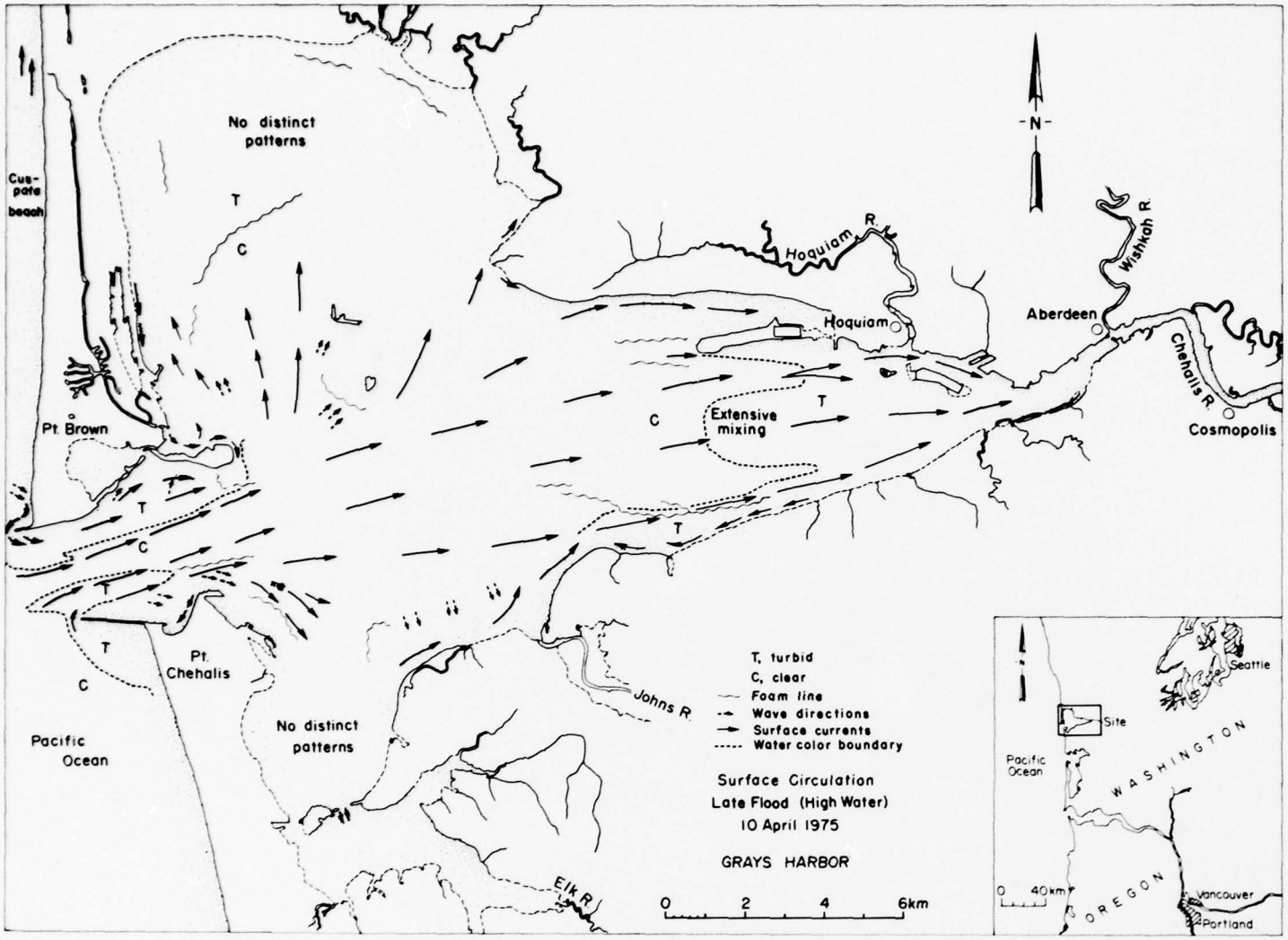

Figure 11. Surface circulation patterns inferred from NASA NP-3A color and CIR photographs acquired on 10 April 1975.

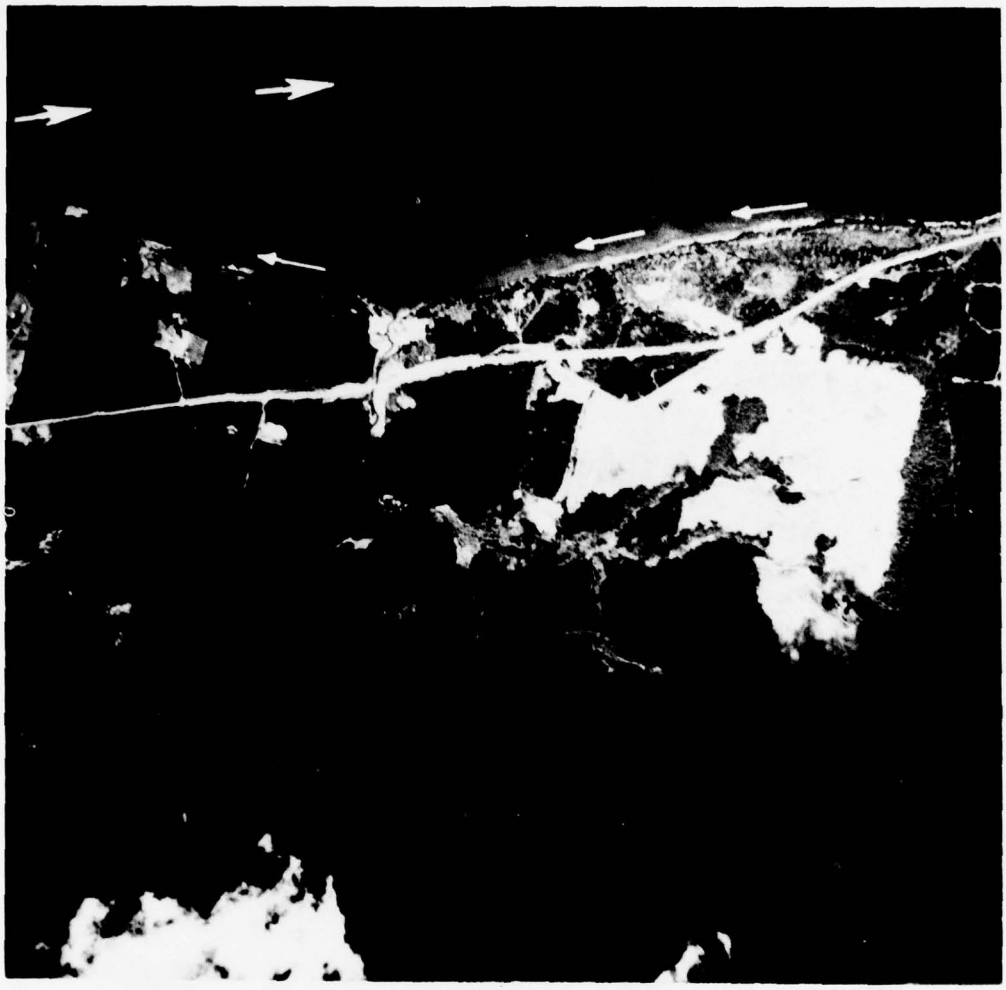

Figure 12. South shore, east of Stearns Bluff near O'Leary Creek, 10 April 1975

The 10 April 1975 (Mission 305) photographs were acquired during late flood nearly at high water slack and during the generally moderate to low freshwater discharge season (U.S. Army Corps of Engineers, Seattle District 1975). Flows on 10 April 1975 were normal.

Grand Mound	41.6 m^3/sec	(1470 ft^3/sec)
Satsop	35.9 m^3/sec	(1270 ft^3/sec)
Wynoochee (Montesano)	15.8 m^3/sec	(560 ft^3/sec)
Total Chehalis Basin	93.4 m^3/sec	(3300 ft^3/sec)

Circulation patterns were more apparent on the color photographs than on the CIR photographs. Many of the suspended sediment patterns observed along the shoreline were probably due to tidal flat sediment resuspension. The topography of submerged tidal flats was apparent on the color photographs.

The general surface circulation during late flood on 10 April 1975 is shown in Figure 11. Nearshore counter currents were apparent in several locations along the west shore of North Bay, the north and east shores of Damon Pt., east of the south jetty, and east and west of the mouth of O'Leary Creek (see also Fig. 1 and Fig. 12).

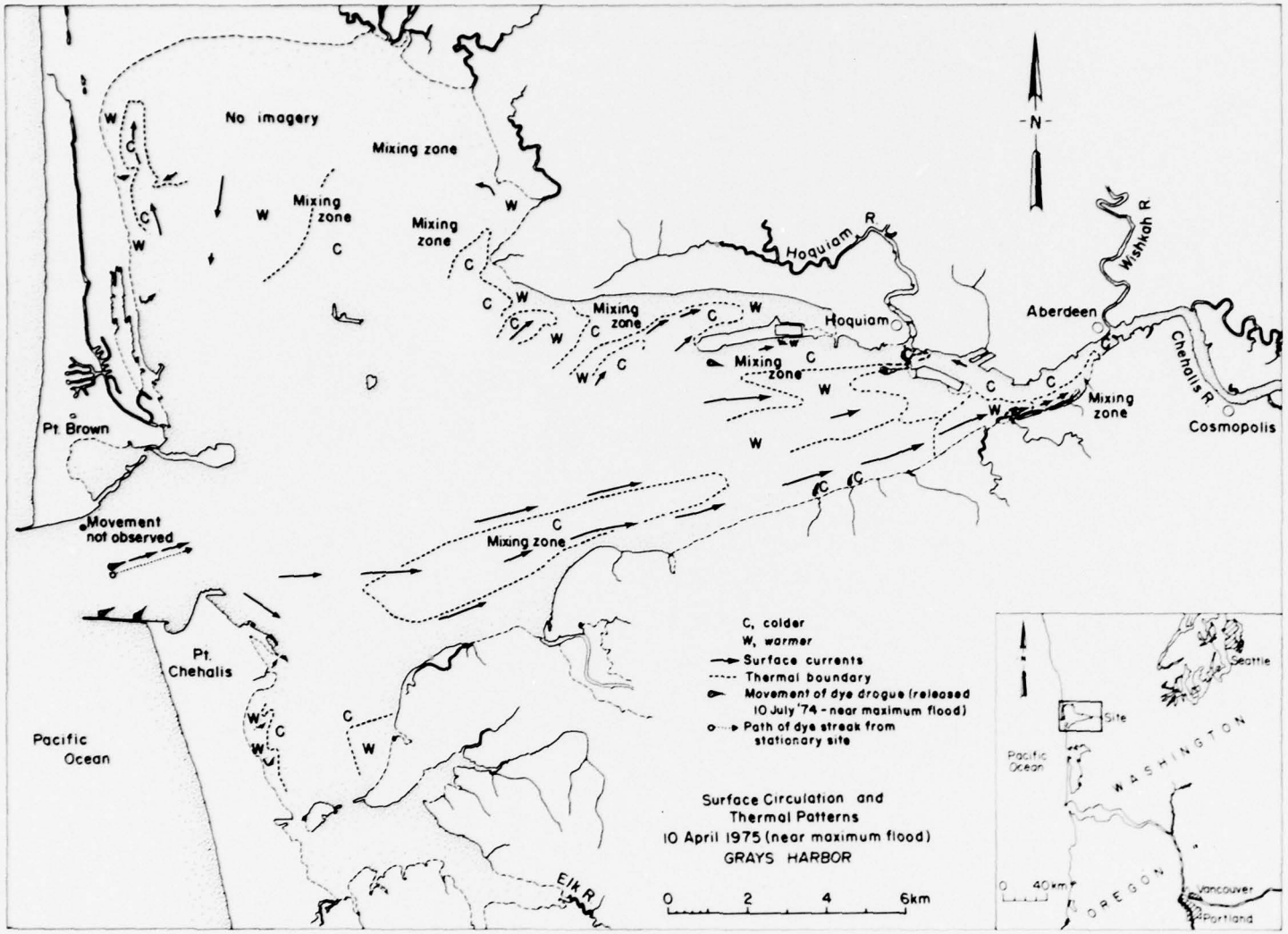

Figure 13. Surface circulation patterns inferred from NASA M²S imagery acquired 10 April 1975 shown in Figure 14.

Surface circulation patterns during mid-flood just before the time of maximum flood currents are shown in Figure 13. Water temperatures (not absolute) in the northern portion of Oyhut Channel (A) varied from 12°C (53.6°F) to 13.5°C (56.3°F) (Fig. 14). The tidal flats northwest of Campbell Slough Channel were approximately 9°C (48.2°F). Water in the Campbell Slough (B and C, Fig. 14), Humptulips River (D), and Chenois Creek (E) Channels varied from 10.5°C (50.9°F) to 12.5°C (54.5°F). Thermal data acquired along line 22 were also variable as the land/water interface was frequently crossed. Water temperatures were comparable to those observed along line 21: on the west side of North Bay (E, D, C), 10.1°C (50.2°F) to 13.2°C (55.8°F); in the central portion (B), 10.5°C (50.9°F) to 12.3°C (54.1°F); and, on the east (A) near the mouth of Grass Creek, 10.2°C (50.4°F) to 12.6°C (54.7°F).

Mixing was prominent in several locations as observed on thermal data from line 23: south of Cow Pt. where Chehalis River water and harbor water converge; in Cow Pt., Hoquiam and Moon Island Reaches; and, south of Brackenridge Bluff near Pt. New. Surface water temperatures varied as follows: in South Channel (A) southeast of Rennie Island, 10.0°C (50.0°F) to 11.4°C (52.5°F); southwest (B) of Rennie Island, as high as 12.5°C (54.5°F); south (C) of Bowerman Airport, 10.8°C (51.4°F); from west of the pipeline dredge disposal site E to the west shore of lower North Bay (D-G), 12.5°C (54.5°F) to 11.8°C (53.2°F).

Surface water temperatures along line 24 were warmest in the western half of the line. From the northern portion of South Bay along South Channel to the area near Middle Channel (A-G), 3.7 km (2.7 mi) west of Rennie Island, temperatures varied from 10.8°C (51.4°F) to 11.6°C (52.9°F). Water (H) in Middle Channel was 12.5°C (54.5°F) to 13.3°C (55.9°F). Water in the North Channel (I) between Hoquiam and Cow Pt. Reaches was 10.2°C (50.4°F). A well defined mixing zone was apparent in the South Channel near the mouth of Johns River. Temperatures in South Bay along line 25 showed very minor variability, 11.4°C (52.5°F) (B and C) to 12°C (53.6°F) (A). The small streams north (C) and south of Grass Island in South Bay were discharging water considerably warmer than the bay water.

Low altitude photographs with dye releases. Surface current directions and velocities near the north and south jetties, near the hopper dredge disposal site 1 and south of Moon Island were estimated using low altitude photographs to record dispersion of uranine dye (the tracer). However, several difficulties were encountered during these dye studies.

First, because of the low cloud ceiling during the aircraft flights, it was not always possible to gain enough altitude to photograph the floating drogues and adjacent land reference features simultaneously. It was not possible to estimate velocities or observe the direction of movement when this occurred.

Second, the line of buoys near disposal site 1 (Fig. 4) consisted of anchored white and fluorescent orange plastic gallon containers. The white buoys were more visible on the low altitude CIR photographs, and the organge more visible on the color photographs. Occasionally these anchored buoys were difficult to see on the photographs because they were periodically covered by waves, and because they were easily confused with the bright spots on the waves formed by sun glint on the water. In addition, the strong currents at this location moved the buoys from their original straight line positions. Larger, more stable buoys would be required for similar studies in the future.

Third, because the camera exposure setting is critical with CIR photography (½ stop latitude), and because the weather conditions were marginal, with lighting continuously changing, the CIR photographs were frequently underexposed and not useful.

In spite of these difficulties, the dye dispersion technique proved to be very useful in determining the current directions and in estimating velocities at several locations. The dye streams visible from the dye packet attached to the stationary buoys on the west side of the buoy line during flood, and on the east during ebb, were very narrow and paralleled the buoy line during all the photographic passes, suggesting strong northeasterly and southwesterly surface currents, respectively (Fig. 15). But hydraulic model studies for this area show surface currents to be more east-west. There appeared to be very little lateral mixing or movement of the dye. By measuring the distance travelled by the dye drogue between aircraft passes, the current velocities were estimated. Velocities during flood near disposal site 1 (measured from photographs on roll 1) varied from 1.4 m/sec (4.6 ft/sec) to 2.2 m/sec (7.1 ft/sec). In contrast, the model velocities were approximately 1.2 m/sec (4.0 ft/sec). During ebb, measurements from roll

Approximate Scale
(1:30000)

0.5 0 0.5 1.0 mi
0.8 0 0.8 1.6 km

a. Line 21

Start 22:03:15

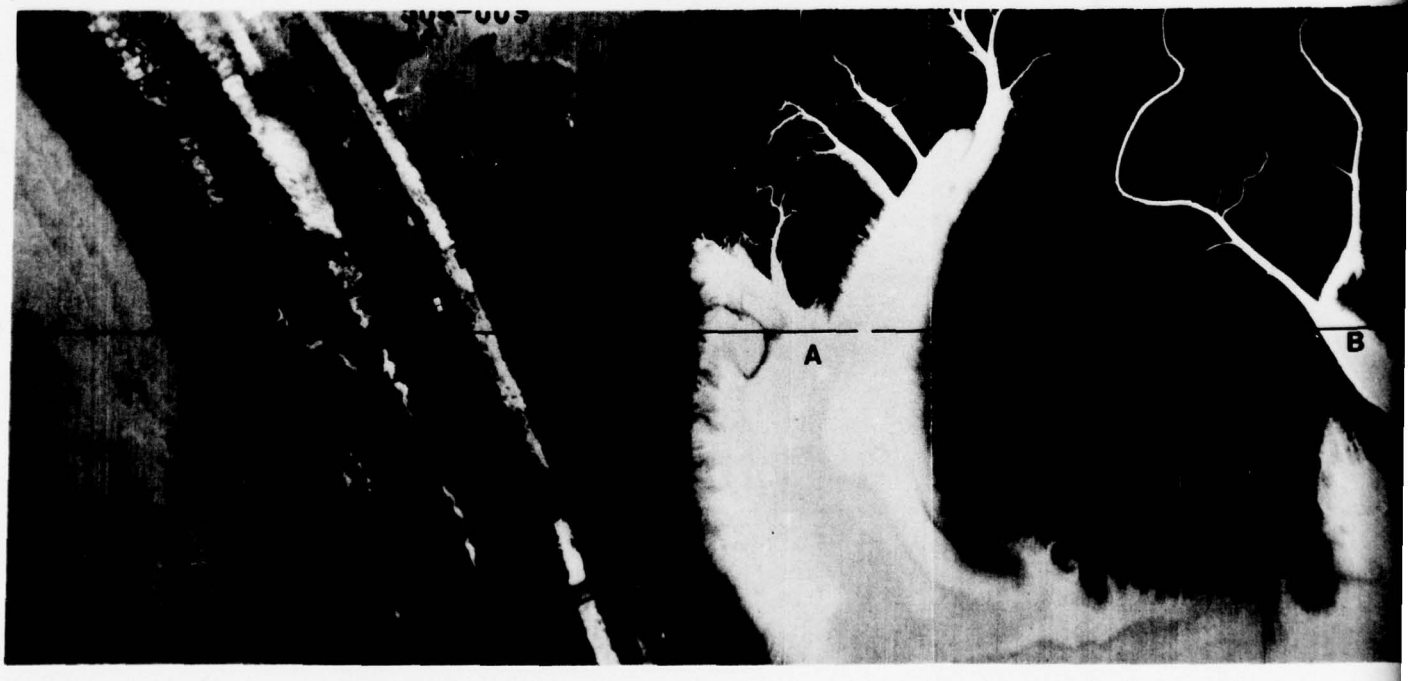

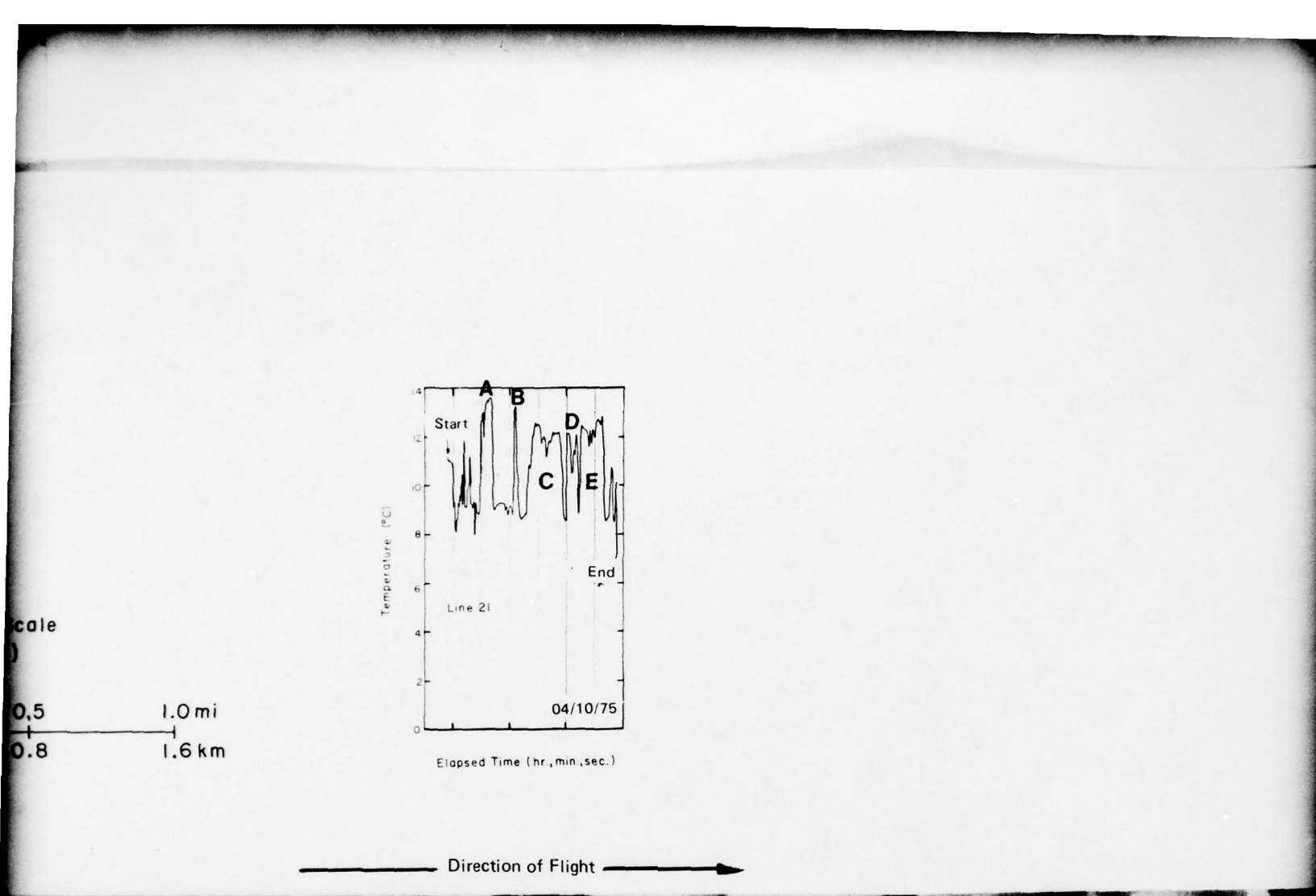

Figure 14. M²S thermal

Figure 14. M²S thermal IR imagery with graph of PRT-5 radiation thermometer data.

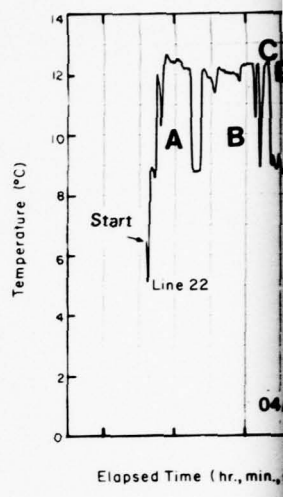

Approximate Scale
(1:30000)

0.5 0 0.5 1.0 mi
0.8 0 0.8 1.6 km

b. Line 22

End 22:11:00

Direction of Flight

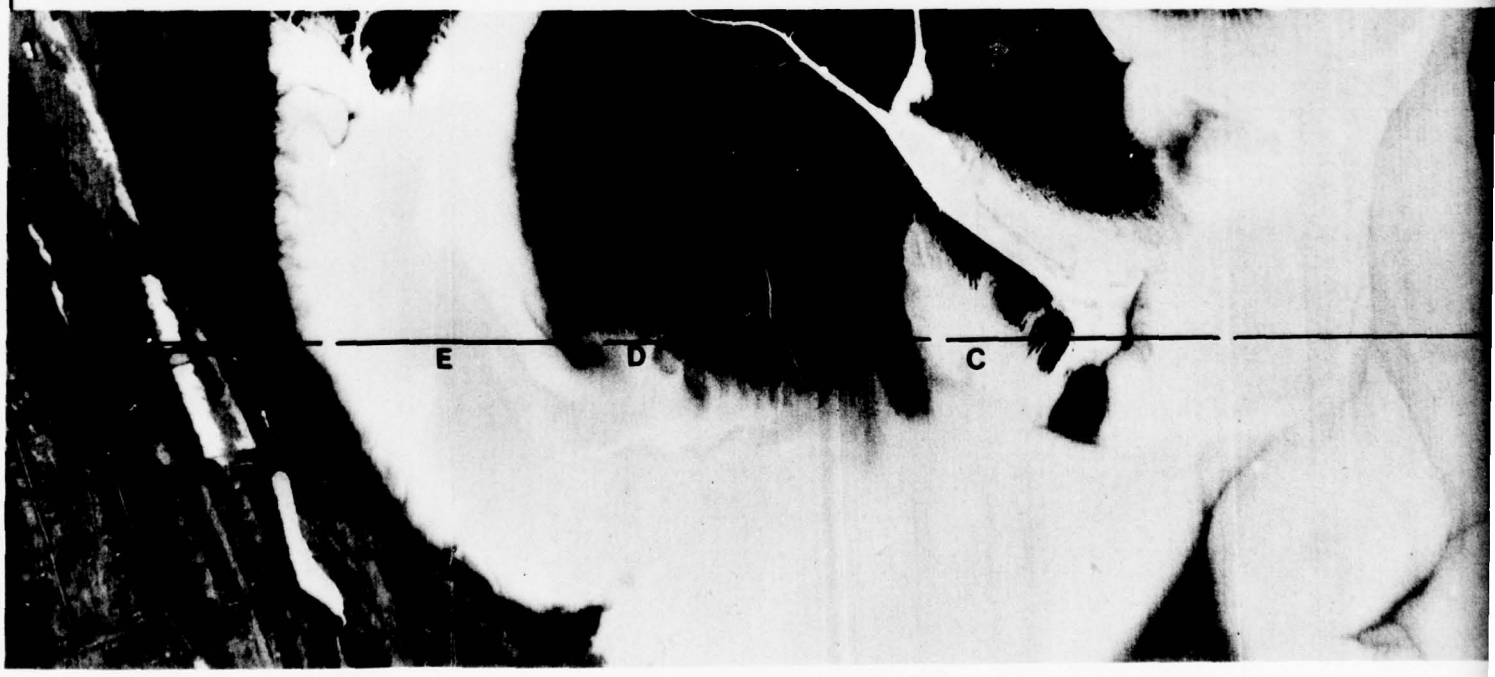

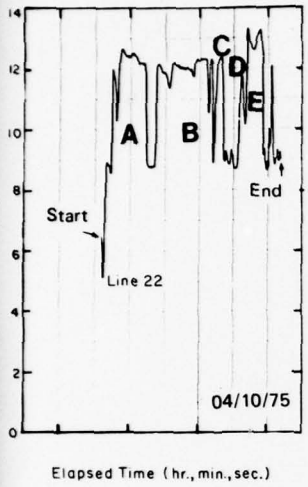

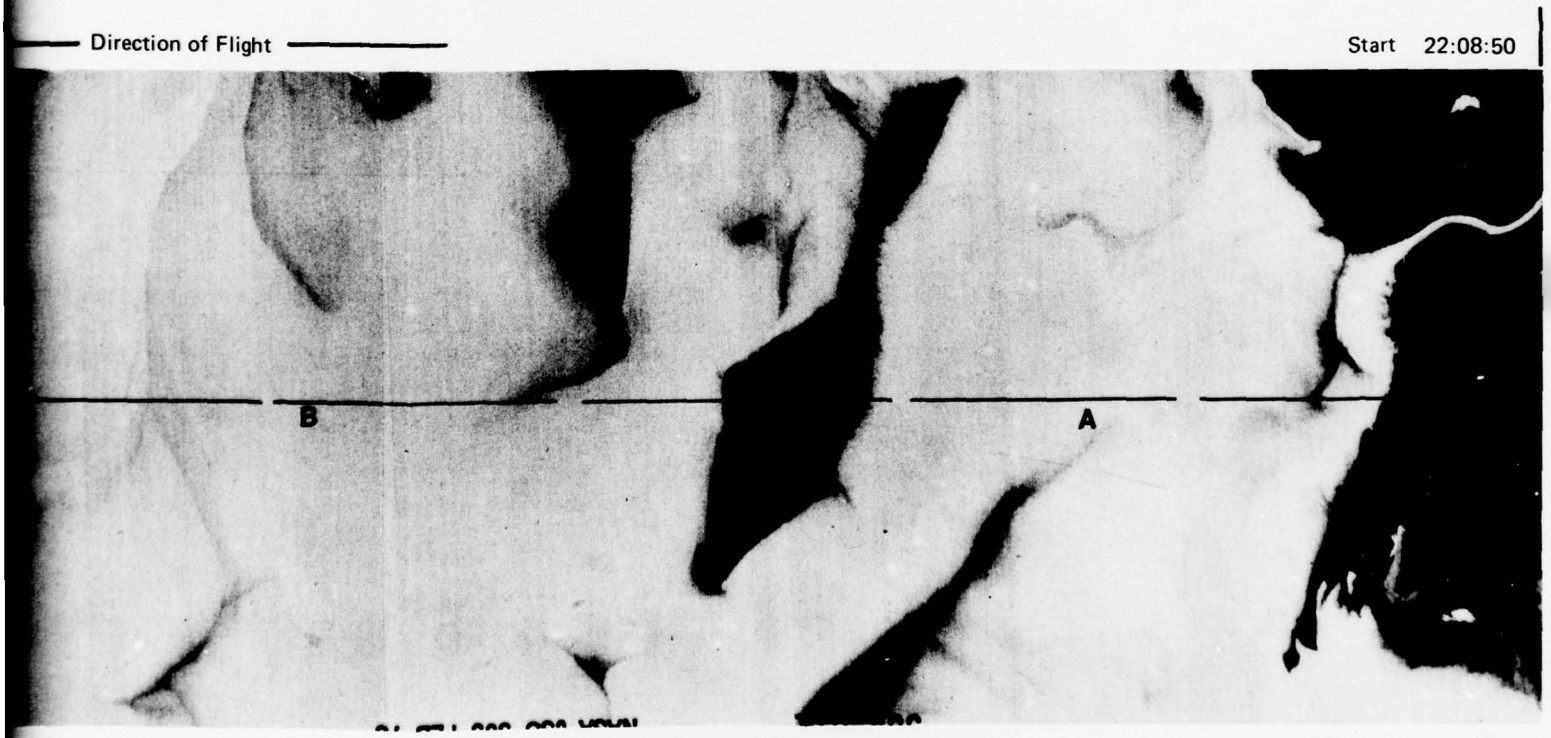

Figure 14 (cont'd). M²S thermal IR imagery with graph of PRT-5 radiation thermometer data.

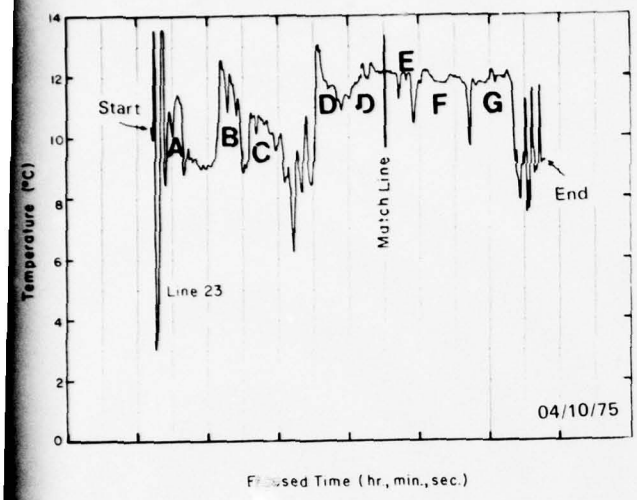

Approximate Scale
(1:30000)

0.5 0 0,5 1.0 mi
0.8 0 0.8 1.6 km

End 22:00:40

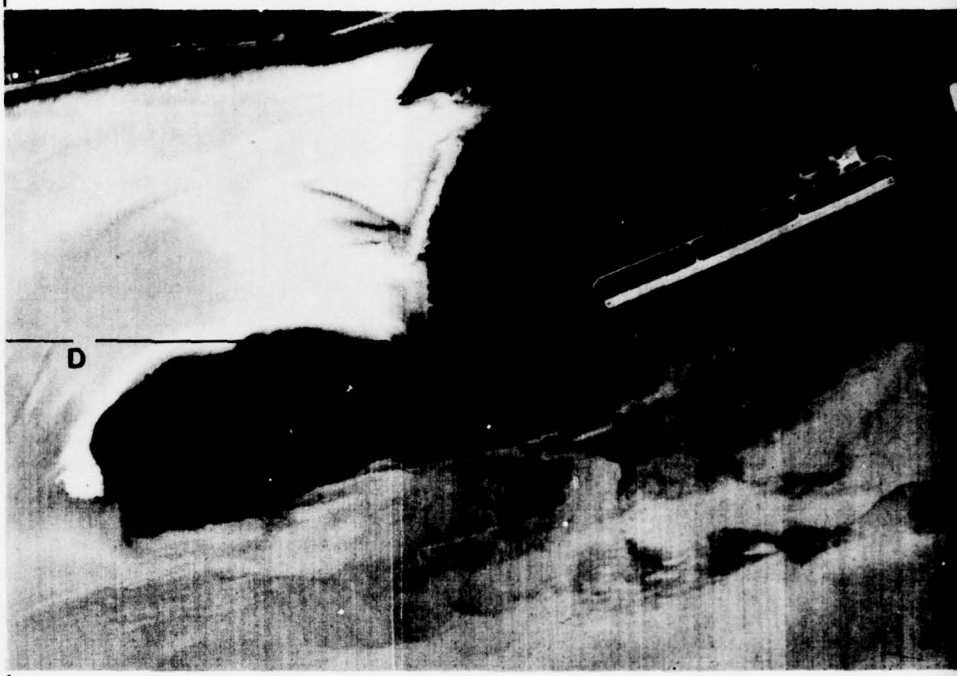

Match Line

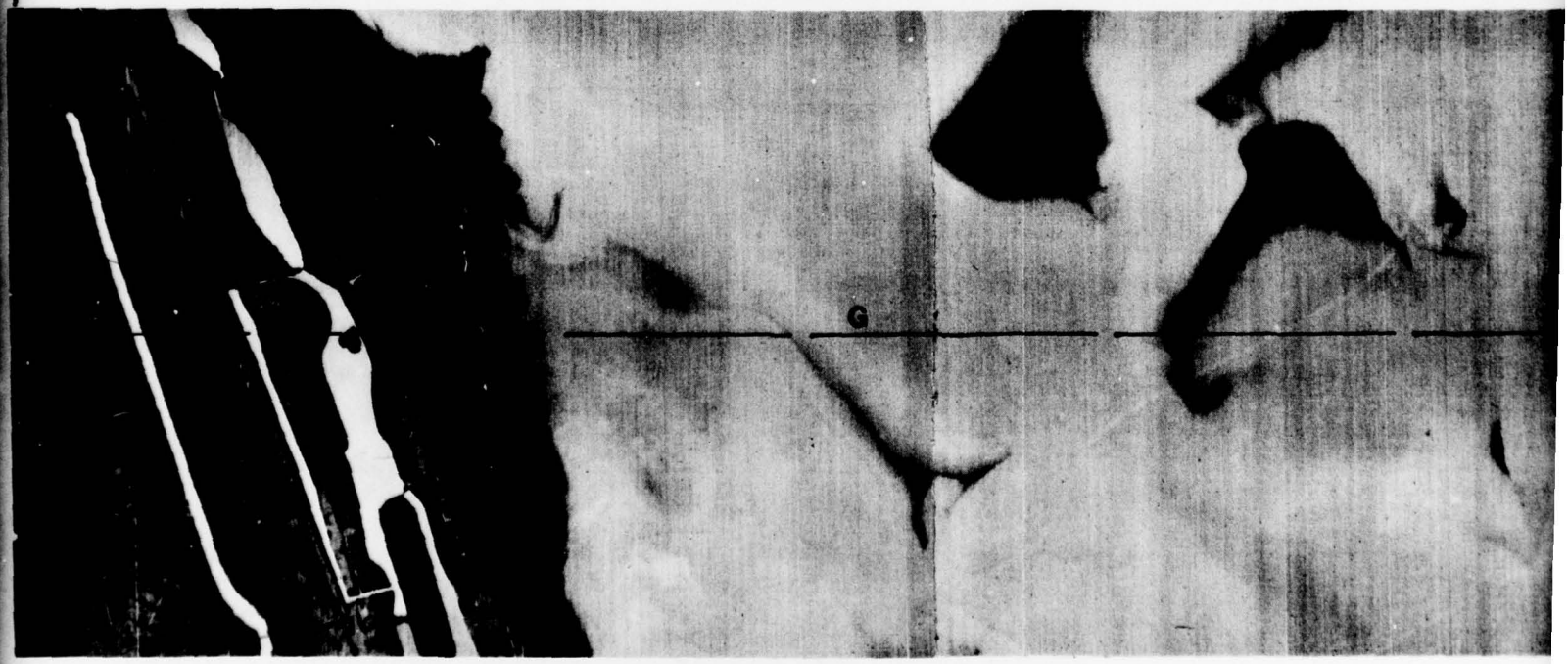

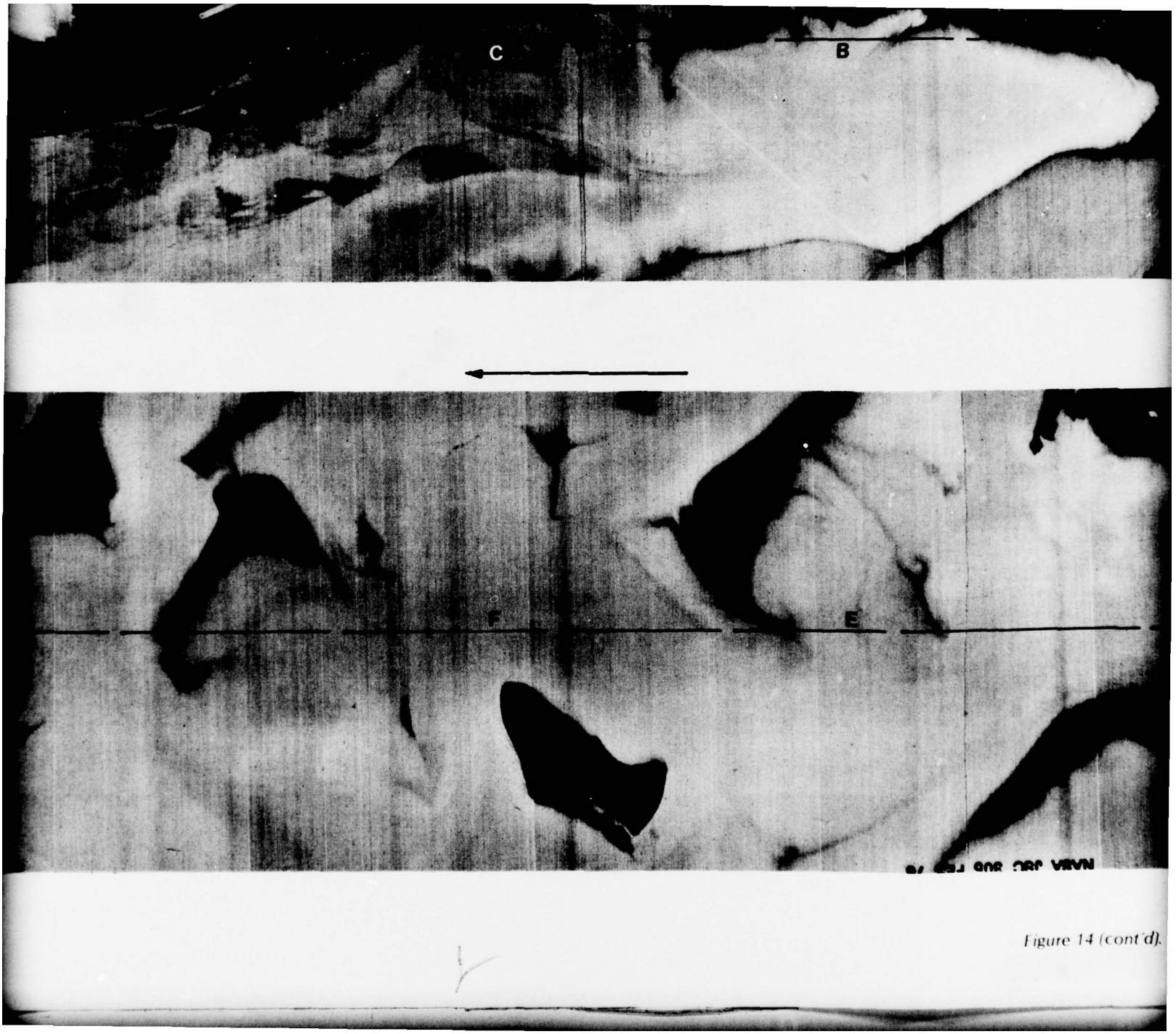

Figure 14 (cont'd).

Figure 14 (cont'd). M²S thermal IR imagery with graph of PRT-5 radiation thermometer data.

d. Line 24

Start 21:48:05

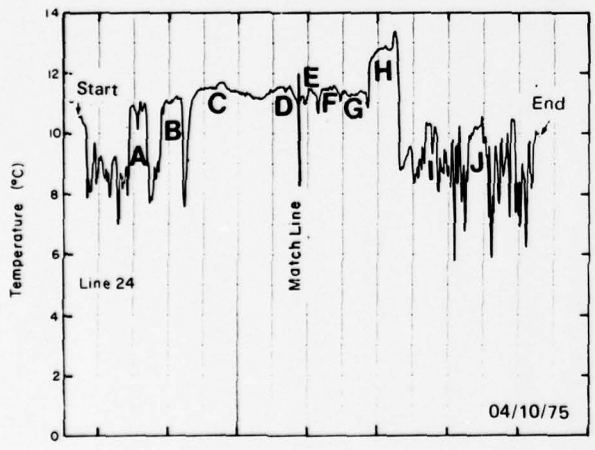

Approximate Scale
(1:30000)

0.5 0 0.5 1.0 mi
0.8 0 0.8 1.6 km

Match Line

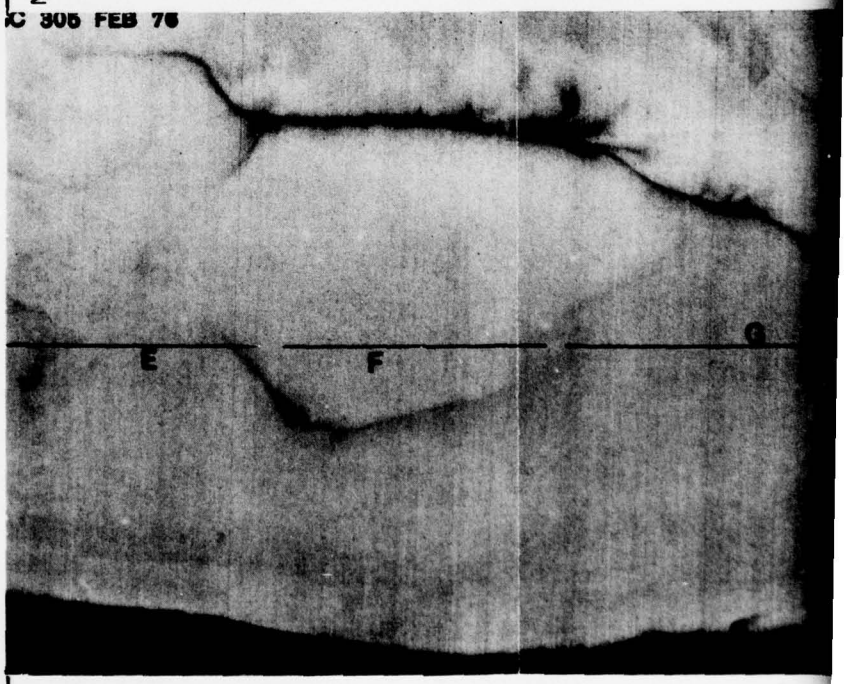


Direction of Flight
B
C
G
H

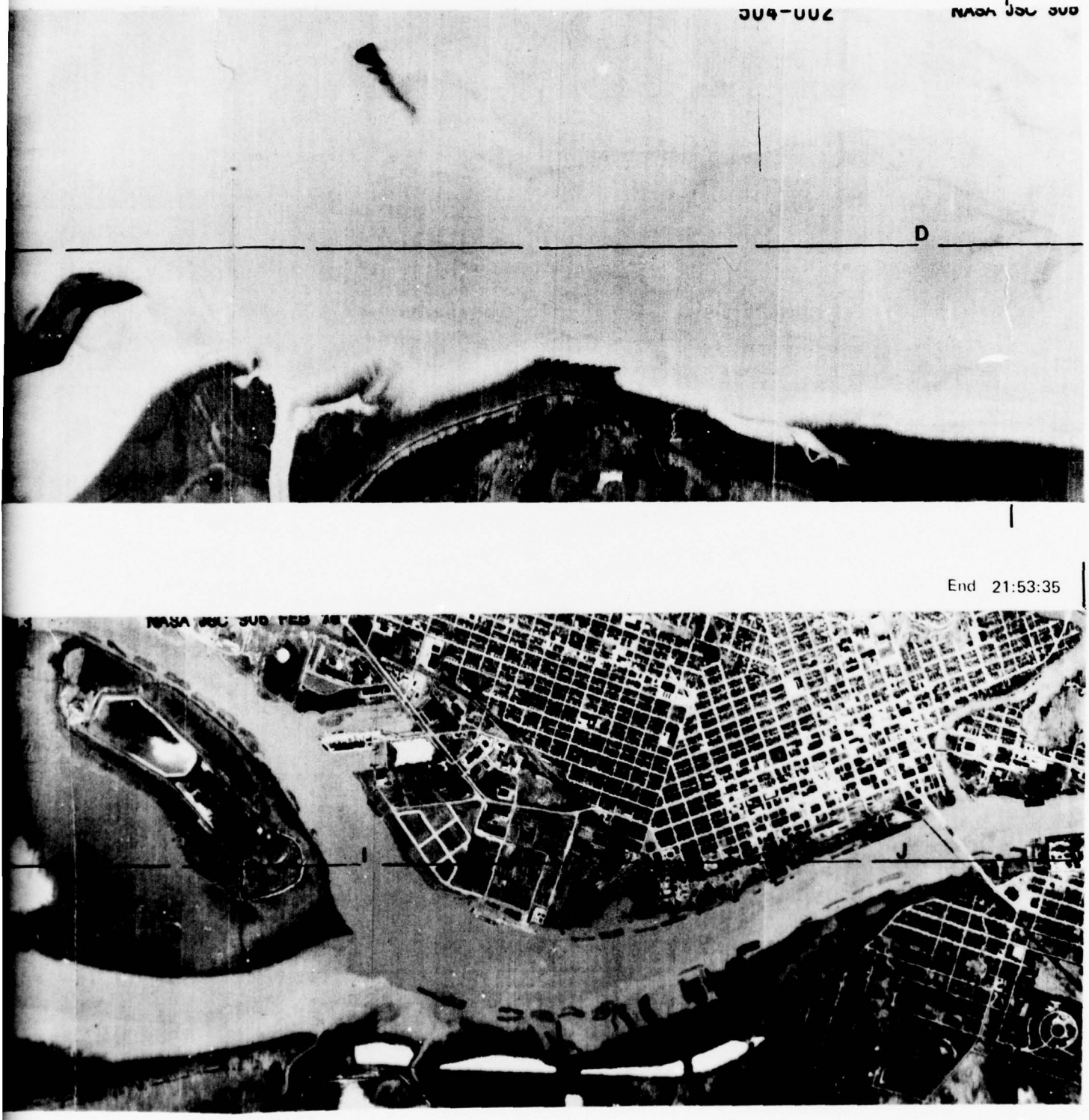

Figure 14 (cont'd). M²S thermal IR imagery with graph of PRT-5 radiation thermometer data.

Total Chehalis Basin	95.4 m³ sec (3300 ft³ sec)	

Circulation patterns were more apparent on the color photographs than on the CIR photographs

mouth of O'Leary Creek (see also Fig. 1 and Fig. 12)

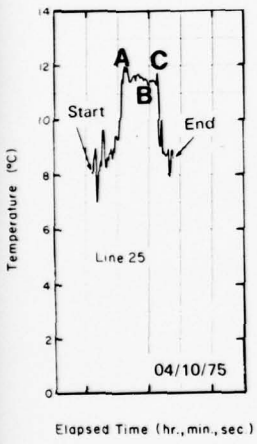

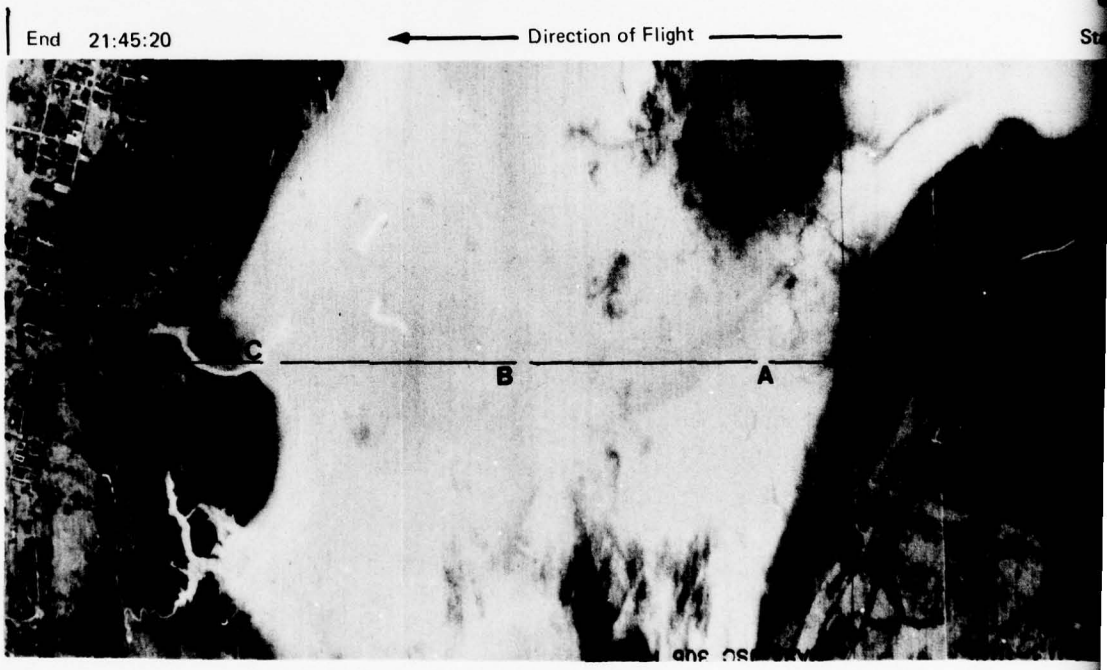

Approximate Scale
(1:30000)

0.5 0 0.5 1.0 mi
0.8 0 0.8 1.6 km

e. Line 25

Direction of Flight

Start 21:44:15

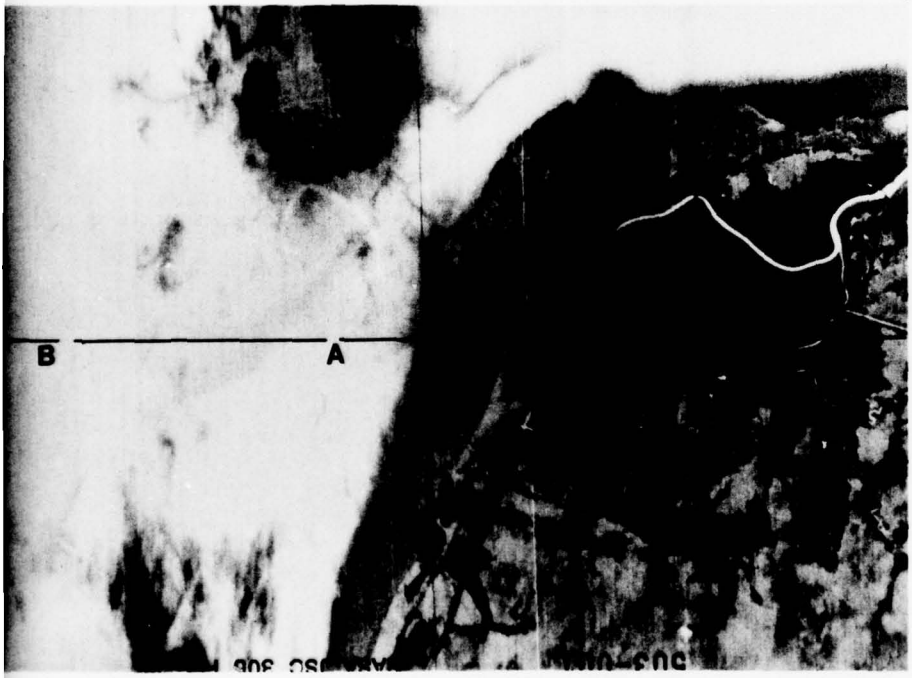

Approximate Scale
(1:30000)

0 0,5 1.0 mi
0 0.8 1.6 km

Figure 14 (cont'd). M²S thermal IR

Figure 14 (cont'd). M²S thermal IR imagery with graph of PRT-5 radiation thermometer data.

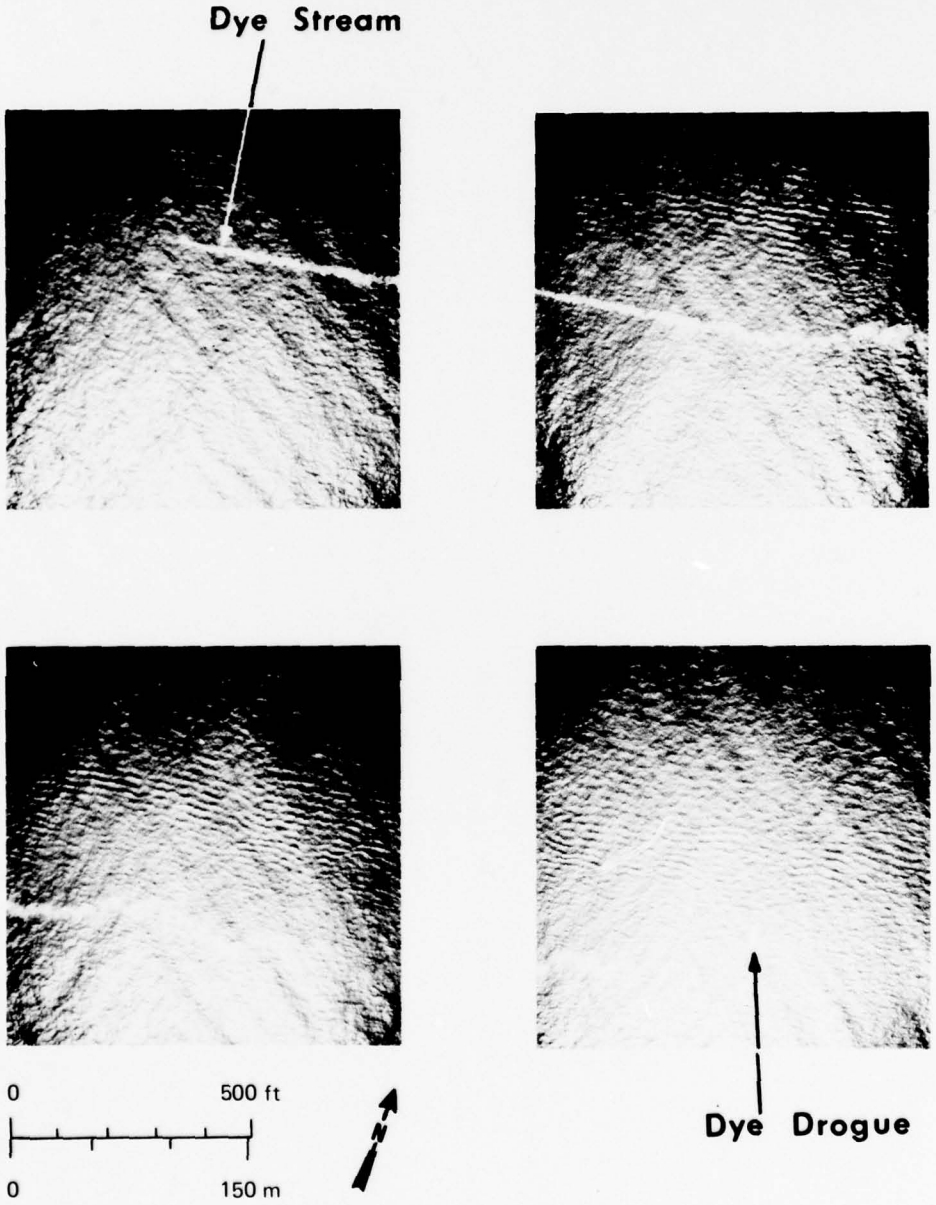

Figure 15. Dye stream at disposal site 1 during flood on 10 July 1974; black and white reproduction of Ektachrome MS Aerographic color film from roll 1, pass 1.

3 varied from 1.7 m/sec (5.7 ft/sec) to 1.9 m/sec (6.3 ft/sec). Modelled maximum velocity was 1.61 m/sec (5.3 ft/sec). White and Knowles (1976) discuss the underwater currents at this disposal site as observed during scuba dives.

Two dye drogues were released at channel buoy 41 during flood on 10 July in the Moon Island Reach south of Bowerman Airport (Fig. 16). The drogues gradually moved southeasterly away from the tidal flats and up the reach. Measured velocities were variable. While still near the tidal flats shortly after release, the velocity (from roll 1) was approximately 0.9 m/sec (2.9 ft/sec). After the drogues had moved farther out into and up the reach (roll 1/pass 1 to roll 2/pass 2) velocity was approximately 1.5

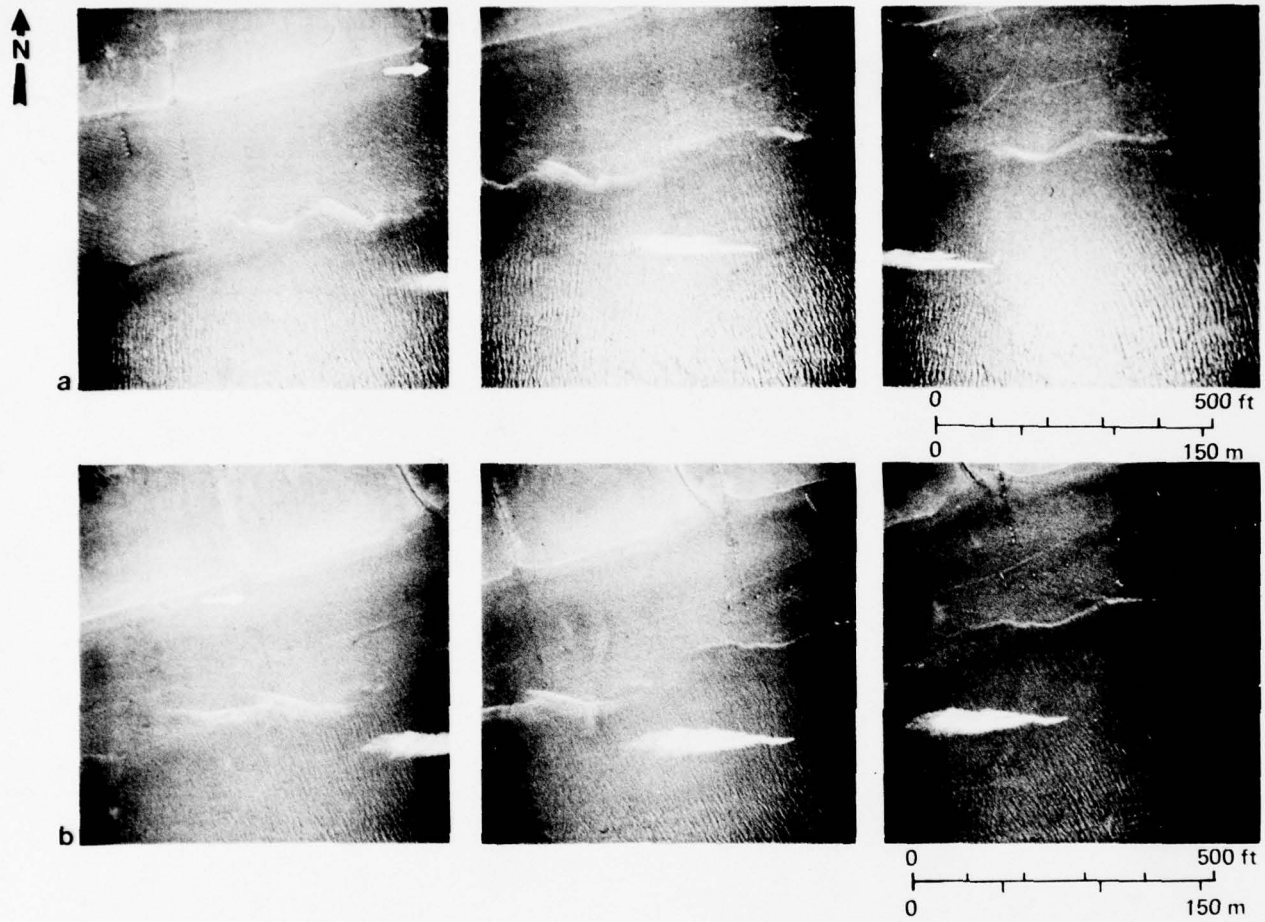

Figure 16. Black and white reproductions of Ektachrome MS Aerographic 70-mm color photographs of dye drogues near Moon Island; a. roll 1/pass 1, b. roll 1/pass 2; arrow marks a line of piles.

m/sec (4.8 ft/sec). Model tests gave maximum velocities of 0.6 m/sec (2.0 ft/sec) and 1.2 m/sec (4.0 ft/sec) during flood and ebb tides, respectively, at this location. The dye patterns produced from these drogues also suggested that lateral movement and mixing of the water was greater in this reach than at the harbor mouth, probably due to lower current velocities and greater bottom effect.

Dye drogues were also released near the north and south jetties. However, continued observation of the drogue near the north jetty was not possible from the air. During flood tide on 10 July, it drifted into the jetty shortly after release. During ebb on 11 July, it disappeared shortly after release and the aerial photographer and pilot could not follow its movement. Movement of the dye drogue near the south jetty was observed during flood and ebb. Flood velocities measured (from roll 1) soon after release were approximately 0.7 m/sec (2.2 ft/sec) (Fig. 17). The approximate location of the drogue 9 minutes after release (roll 1/pass 1) is shown on photographs taken on roll 2/pass 1 (Fig. 17a). Velocity measured for the 3 minutes between roll 1/pass 1 and roll 2/pass 1 was 1.1 m/sec (3.8 ft/sec). After it had moved northeast from the jetty, the velocity increased (roll 2/pass 1 to roll 2/pass 2) to 1.2 m/sec (4.1 ft/sec). Ebb velocity measured from shipboard observations on 11 July was 1.3 m/sec (4.3 ft/sec). Because of poor flying conditions, the dye drogue was not photographed during the pass on 11 July.

The use of the dye and the low altitude photographs for measuring its dispersion and movement was very useful for determining current directions and velocities. With more favorable weather conditions, dye tracing could

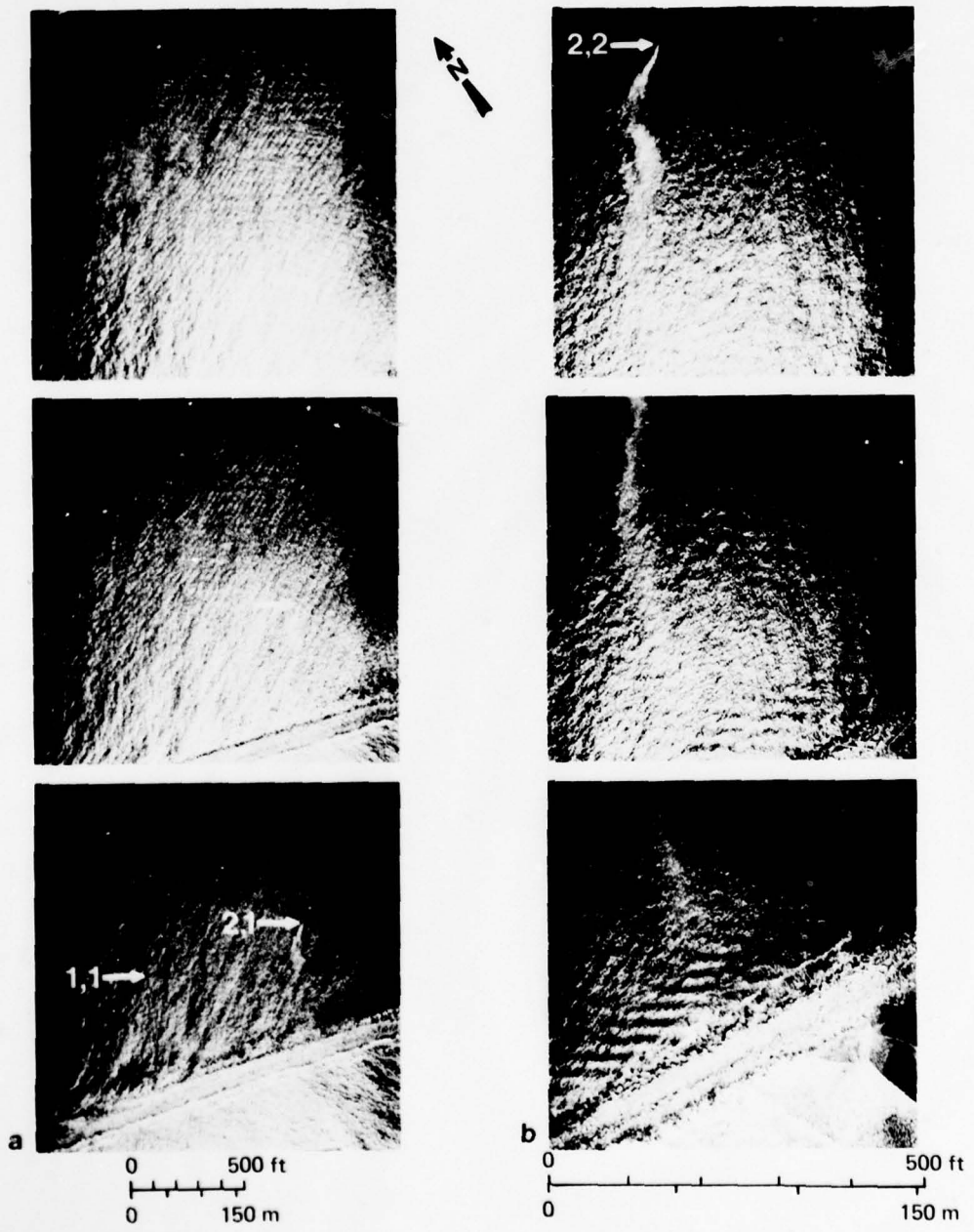

Figure 17. Black and white reproductions of Ektachrome MS Aerographic 70-mm color photographs of dye drogues near the South jetty; a. roll 2/pass 1; b. roll 2/pass 2; photographs from roll 1/pass 1 not shown.

be accomplished at selected sites throughout the harbor and provide circulatory data for many tidal conditions.

LANDSAT-1 imagery. A cursory evaluation was made of the utility of LANDSAT-1 imagery in providing data that would be useful for dredging effects or related studies in Grays Harbor. The following images were used: image 1169-18375, acquired 8 January 1973; image 1187-18380, acquired 26 January 1973; image 1205-18382, acquired 13 February 1973; and, image 1439-18361, acquired 5 October 1973. Predicted tidal stages at Aberdeen during the time of image acquisition were: for 1169-18375, early flood (≅ 1.5 hours after low water); 1187-18380, late ebb (≅ 2 hours before lower low water); 1205-18382, early ebb (≅ 2 hours after higher high water); and, 1439-18361, mid-ebb (2.5 hours before low water) (National Ocean Survey 1972b). Approximate tidal currents at these times were: 1169-18375, 1 hour after low water slack, 0.6 m/sec (1.9 ft/sec) flooding; 1187-18380, 0.5 hours after maximum ebb, 1.3 m/sec (4.25 ft/sec) ebbing; 1205-18382, 1.3 hours after high water slack, 0.5 m/sec (3.1 ft/sec) ebbing; and, 1439-18361, 40 minutes before maximum ebb, 0.6 m/sec (2 ft/sec) ebbing (National Ocean Survey 1972a).

Original 70-mm (2.75-in.) LANDSAT negative transparencies (approximate scale, 1:3,300,000) were received from the Corps of Engineers LANDSAT depository* and enlarged in house to the following nominal scales: 1:1,000,000, 1:500,000, 1:250,000 and 1:120,000. Generally, the 1:1,000,000 rendition appeared clearer and showed greater contrast than the larger scaled products. In addition, the latter versions were physically larger, but showed less ground coverage per print. However, the 1:500,000 or 1:250,000 products were considered the most convenient for handling.

Surface water patterns (1) were visible near and north of the mouth of Grays Harbor (2) during early flood on 8 January 1973 (Fig. 18). There appeared to be a northerly current along the Washington coast and these patterns indicate the path taken by suspended particulates or dissolved solids discharged from the harbor during the previous ebb. Similar patterns were discernible west of Willapa Bay (3). The positions of tidal flats (4) in North Bay and islands (5) were especially evident. The darker flats were probably submerged during the previous high water, but the lighter flats were not. Tonal differences of the harbor water may have been due to turbidity but, more likely, they resulted from light reflected off the harbor bottom. Generally, the darker water is indicative of deeper water.

Turbidity patterns along the Washington coast apparent on the 1:1,000,000 scale rendition (Fig. 19) of image 1187-18380, acquired 26 January 1973, clearly showed northerly coastal currents (Davidson current) that predominate, especially in the winter. Scheidegger and Phipps (1976) reported the sands from the Columbia River (to the south) are transported northward via these littoral currents, deposited along the beaches and in the near-shore zone adjacent to the entrance of the harbor, and eventually move into the harbor by tidal currents. The image was acquired during late ebb and the water discharging from the harbor was very evident. As in Figure 18, the 1:500,000 scale enlargement (Fig. 20) shows the configuration and location of the tidal flats and of the deep (1) and shallow water (2).

Haze appeared to obscure much of the detail of the surface water in Grays Harbor on 13 February 1973 (Fig. 21). Nearshore coastal currents appeared to be northerly and at several locations (1) rip currents were prominent. The enlargement (Fig. 22) of Figure 21 showed less surface water detail than observed in Figures 18 and 19. Surface currents near the harbor entrance were ebbing at approximately 0.9 m/sec (3 ft/sec) about 1.3 hours after high water slack, and tidal stage was early ebb. Most of the tidal flats were still submerged and the tonal variations in the water were probably due to variable water depths. Instrument noise (1) and clouds (2) dominate image 1439-18361 acquired 5 October 1973 (Fig. 23). Tidal flats (3) and islands (4) in North Bay are visible, but cloud shadows (5) cause confusing patterns.

Although LANDSAT-1 imagery was useful in observing large scale currents along the Washington coast, circulation patterns within Grays Harbor were not apparent. However, the locations of tidal flats, navigation channels and islands were evident. Generally, it is felt that the imagery would not provide information of any direct application to monitoring currents and/or sediment patterns in the harbor.

Intertidal habitats

Based on a comparison of Jefferson's (1975)

* Now maintained at U.S. Army Engineer Topographic Laboratory, Ft. Belvoir, Virginia.

Figure 18. Grays Harbor, portion of LANDSAT-1 band 5 image 1169-18375 acquired 8 January 1973, approximate scale, 1:500,000.

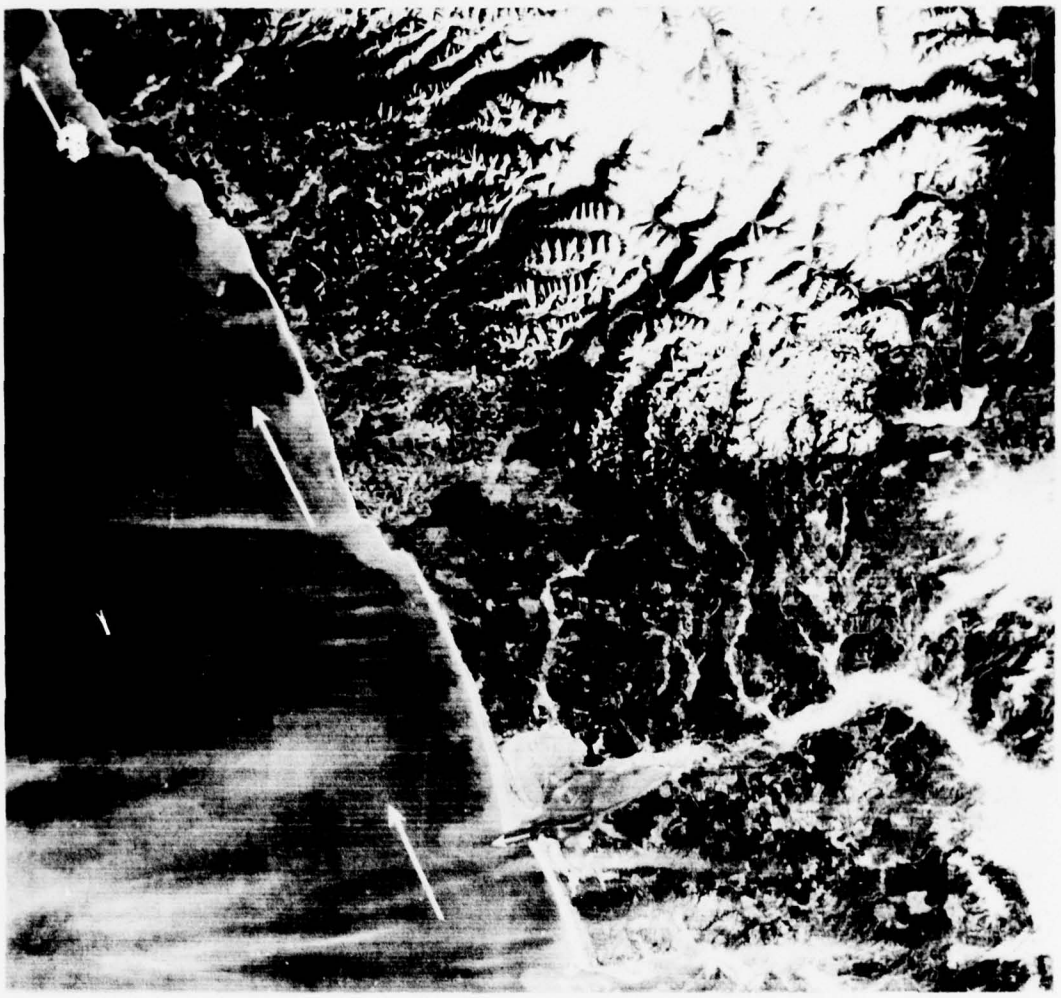

Figure 19. Grays Harbor and the northwestern Washington coast, LANDSAT-1 band 5 image 1187-18380 acquired 26 January 1973; approximate scale, 1:1,000,000.

classification of Oregon salt marshes which he reported to be similar to those in Washington, and previous studies of Grays Harbor marshes, the following marshland vegetation types were mapped: low silty, low sandy, sedge, high immature, high mature, diked salt marsh, diked pasture, freshwater marsh, and wooded swamp (Fig. 24, Table XII). Low sandy marshes usually occur on bay-mouth sand spits and are typified by a low, scattered to continuous vegetation cover. Coalescing circular clones of colonizing plants at low intertidal elevations characterize low silty marshes that are dominated by one and two-species communities. Sedge marshes occupy intermediate elevations on sand and silt. Pure stands, or nearly pure stands of *Carex lyngbyei*, distinguish the sedge marsh. High marshes were identified by an abrupt elevation rise of 0.3-1.5 m (1-5 ft) above the tide flat. Vegetation cover was continuous, with two to three species dominating communities of immature high marsh, and more complex communities dominating mature high marsh. Jefferson (1975) found high marshes to be more common along the upper reaches of the estuaries; this is the case for Grays Harbor in South Bay and the Elk River estuary. However, high marshes are extremely limited in higher portions of the Chehalis River estuary because of urban encroachment and other land development activities.

Figure 20. Grays Harbor, enlarged portion of Figure 19; approximate scale 1:500,000

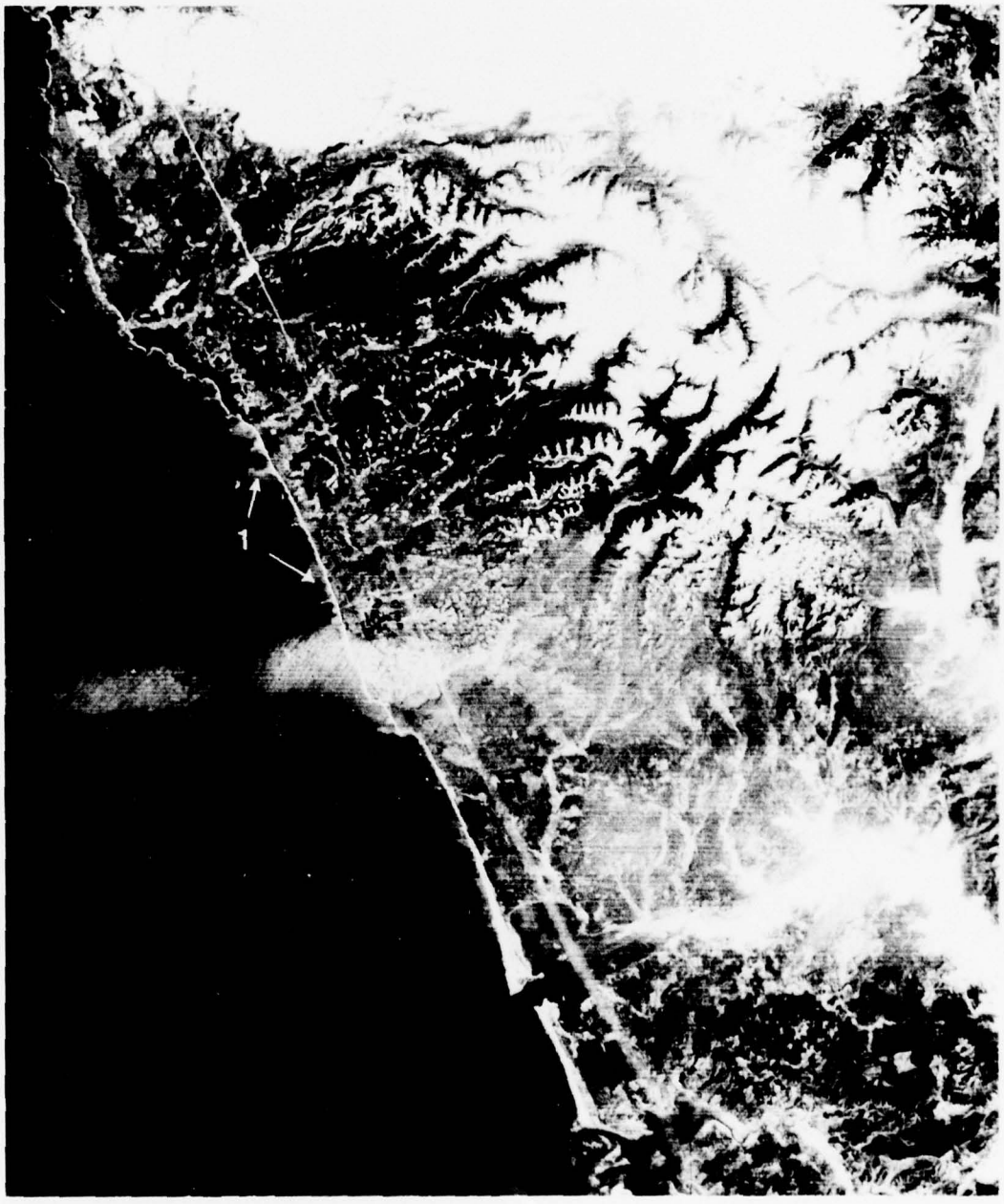

Figure 21. Grays Harbor and the northwestern Washington coast, LANDSAT-1 band 5 image 1205-18382 acquired 13 February 1973; approximate scale, 1:1,000,000.

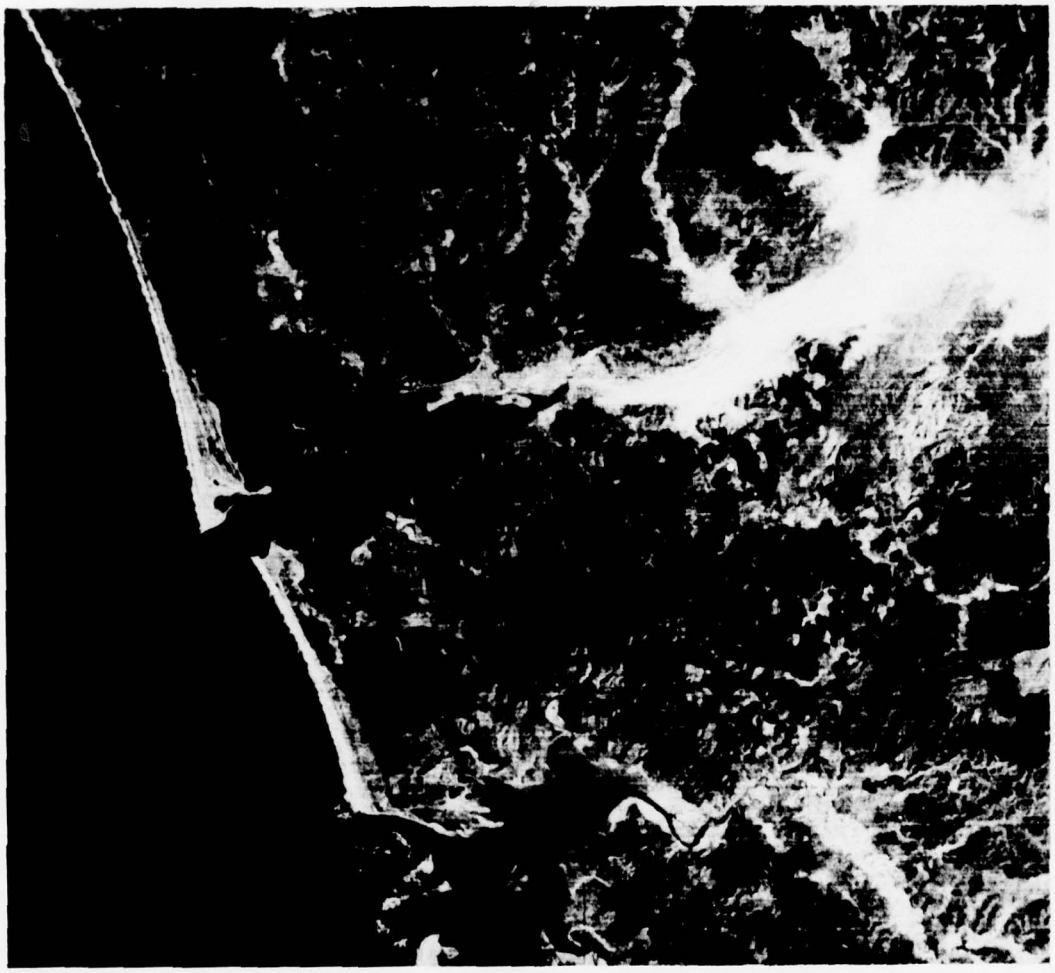

Figure 22. Grays Harbor, enlarged portion of Figure 21; approximate scale, 1:500,000.

Diked salt marsh generally occurred at the highest extremes of high marshes. This type was characterized by being diked, dominated by *Juncus* sp., *Agrostis* sp., and *Potentilla pacifica*, with scattered *Pyrus fusca* and invading *Picea sitchensis*. These areas were ungrazed, and influenced mainly by freshwater. Vegetation was generally 0.5 to 1.5 m (1.6 to 5 ft) tall.

Diked pasture was heavily grazed by livestock, diked and removed from tidal influence, and was generally adjacent to a tidal stream or slough. Vegetation was dominated by pasture grasses 0.01 to 0.1 m (0.03 to 0.3 ft) tall. Freshwater marsh was inundated by standing water for much of the year. The vegetation was dominated by *Carex obnupta*, *Eleocharis palustris*, and *Phalaris grundinaceae* up to 0.5 to 2.5 m (1.6 to 8.2 ft) tall in summer. Wooded swamp was similar to freshwater marsh but was characterized by a tree overstory. Vegetation was dominated by communities of *Alnus rubra*, *Thuja plicata*, *Carex obnupta* and *Lysichitum americanum*.

Sixteen percent of the area between mean lower low water (MLLW) and extreme high water (EHW) was salt marsh. Five defined types of undiked salt marsh compose 15.33 km^2 (3740 acres) of Grays Harbor wetlands. Another 6.88 km^2 (1680 acres) have been diked, drained, or otherwise altered by man for agricultural use. This diked acreage, in most cases, was probably taken from higher salt marshes, most likely from the high immature or high mature salt marsh types. Diked areas are subject to tidal flooding

Figure 23. Grays Harbor and the northwestern Washington coast. LANDSAT-1 band 5 image 1439-18361 acquired 5 October 1973; approximate scale, 1:1,000,000.

in some areas because of tidal sloughs such as Redman Slough at Ocosta.

Approximately 1.02 km² (250 acres) of freshwater marsh are contiguous to Grays Harbor. Many of these areas were apparently formed by sandspits blocking small streams draining into Grays Harbor. Wooded swamp consisting of 3.85 km² (940 acres) was identified contiguous to Grays Harbor. The beaver (*Castor canadensis*) was usually associated with this type of swamp. The 3.88 km² (940 acres) is a very conservative estimate. Large areas of this type (or a similar habitat) occur in the Humptulips River delta area and were not included in this estimate. Diked and undiked salt marsh types encompass 22.22 km² (5420 acres).

The sedge marsh type has been most affected by dredged material deposition in conjunction

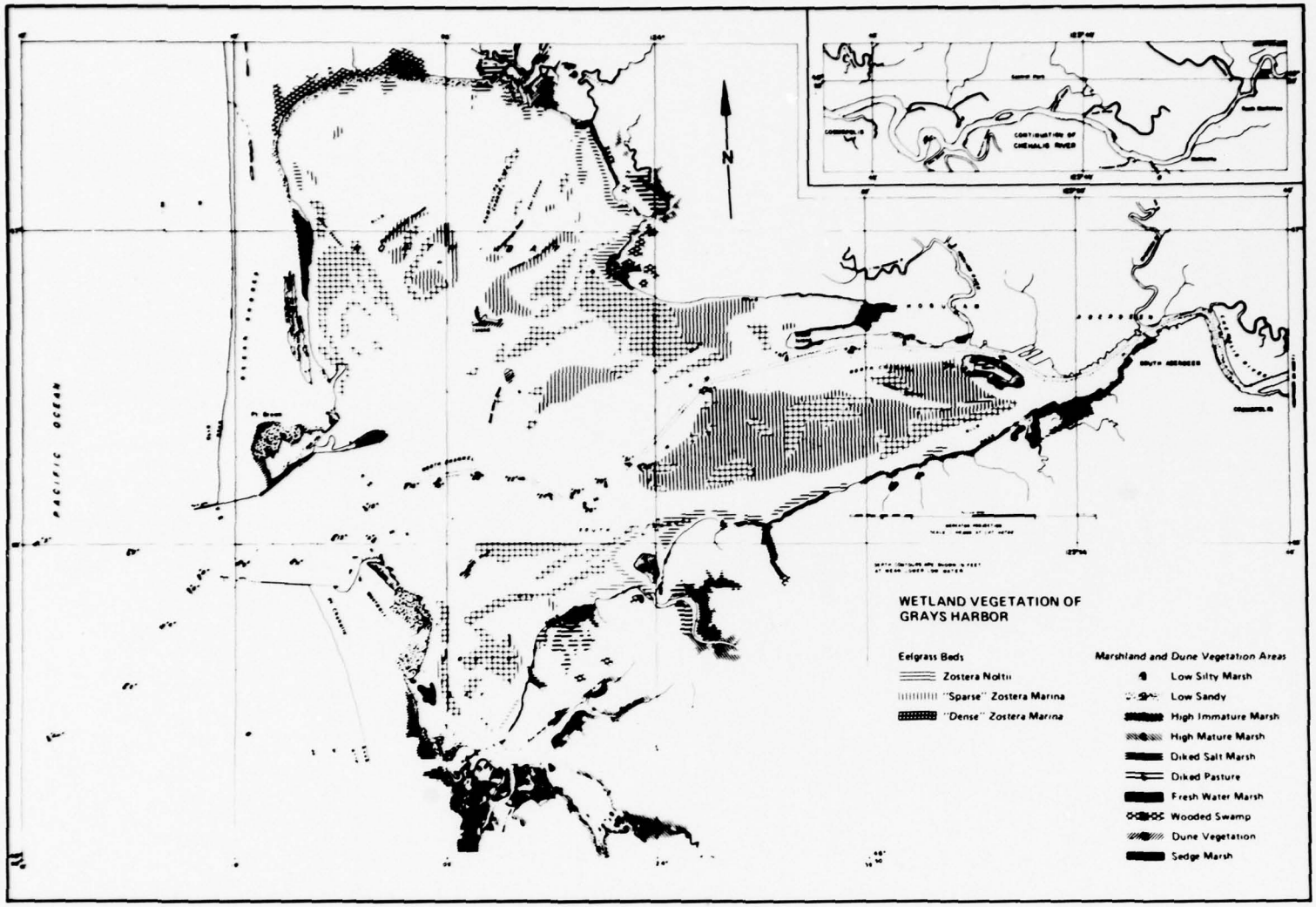

Figure 24. Distribution of wetland vegetation in Grays Harbor, 1975 [from Smith et al. (1976)].

Table XII. Areal extent of Grays Harbor marshland types, 1975. (Adapted from Smith et al. 1976.)

Wetland type	Areal extent (km^2)	(acres)
Undiked salt marsh		
Low silty marsh	6.64	1620
Low sandy marsh	2.66	650
Low marsh subtotal	9.30	2270
High immature marsh	0.98	240
High mature marsh	4.22	1030
High marsh subtotal	5.20	1270
Sedge marsh	0.82	200
Undiked salt marsh subtotal	15.33	3740
Diked salt marsh	4.46	1090
Diked pasture	2.41	590
Diked area subtotal	6.88	1680
Salt marsh subtotal	22.22	5420
Freshwater marsh	1.02	250
Wooded swamp	3.85	940
Freshwater subtotal	4.87	1190
Total marshlands	27.10	6610*

* Due to rounding, numbers may not add up to total.

Table XIII. Total acres used as dredged material disposal areas in Grays Harbor, 1950-1975 (from Smith et al. 1976).

Location	Area (km^2)	(acres)	(mi^2)
West of Hoquiam River and NE of Bowerman Field	2.6	650	1.0
East of Hoquiam River to Highway 101 bridge over Chehalis River	1.9	400	0.6
Bowerman Field and Site E	4.2	1000	1.6
Rennie Island, South Channel, Middle Channel	5.2	1300	2.0
North Mid-harbor Flats	2.1	500	0.8
Total	16.0	3850	6.0

with expansion of the urban area. However, estimation of the extent of sedge and other marsh destruction without previous baseline data is extremely difficult and subject to a high degree of error.

Based on aerial photographs taken in April 1950, approximately 2.66 km^2 (650 acres) of tidal flat and salt marsh has been removed from the estuary west of the Hoquiam River and northeast of Bowerman Field (Table XIII). These photographs show Rennie Island to be less than a third of its present extent. These changes are due to dredged material deposition. It also appears that another 1.64 km^2 (400 acres)of tidal flat and marsh east of the Hoquiam River to the present Highway 101 bridge over the Chehalis River have been filled since about 1950. Other areas affected by dredged material disposal in Grays Harbor are summarized in Table XIII. Approximately 15.7 km^2 (3850 acres) have been premanently removed from tidal influence since 1950.

The areal distribution and extent of three classes of eelgrass were mapped: *Zostera noltii*, "dense" *Z. marina* and "sparse" *Z. marina* (Table XIV). The "sparse" *Z. marina* beds were not sampled quantitatively because of large inherent variability in the occurrence of the plant. Ground checks at several locations, however, indicate that "sparse" beds are an order of magnitude less dense than dense beds. Figure 24 shows the locations of dense and sparse beds of *Z. marina* and beds of *Z. noltii*.

Elevation data acquired along transects visited during ground surveys were used to determine the intertidal range of the eelgrass beds. Most of the denser *Z. marina* in Grays Harbor occurred at or above the +0.3 m (1.0 ft) MLLW. Keller (1963) concluded that desiccation during exposure at low tide undoubtedly affects vegetation vigor and reproduction. However, water remaining in shallow depressions in mudflats apparently permits clumps of *Z. marina* to survive, reproduce, and grow. This seemed to be the prevalent condition in Grays Harbor.

Other factors, including water temperature, weather conditions, chemical pollution, turbidity from dredging, oyster culture, and siltation rate can be causal factors in changing eelgrass distribution and density (Parker 1975, McRoy 1966). Any activity that alters tidal action can also cause changes in *Z. marina* occurrence and distribution (Keller 1963). In Grays Harbor, during 1975, *Z. marina* seemed to do well at elevations up to +0.9 (3 ft). It is also certain that elevational increases beyond this point will reduce or eliminate the density of *Z. marina* below present levels.

Z. noltii was found only in the higher portions of the transects, usually on small mounds. The estimated lower limit of occurrence for *Z. noltii* in Grays Harbor was approximately +0.9 m (3 ft). It was only abundant at +1.5-1.8 m (5-6 ft) or higher on tideflats. *Z. noltii* also occurred in many creek channels, forming exceptionally dense clusters. It is obvious from Figure 24 that

Table XIV. Areal extent of *Zostera marina* and *Zostera noltii* in Grays Harbor, June 1975). (Adapted from Smith et al. 1976.)

	Z. marina						*Z. noltii*	
	Dense		*Sparse*		*Total*			
Location	*(acres)*	*(km²)*	*(acres)*	*(km²)*	*(acres)*	*(km²)*	*(acres)*	*(km²)*
North side*	3020	12.4	1780	7.3	4,800	19.7		
South side†	1280	5.3	170	0.7	1,450	5.9		
Mid-harbor flats	1240	5.0	3510	14.4	4,750	19.5		
Total harbor	5540	22.7	5450	22.4	11,000	45.2	680	2.7
Total *Z. marina* and *Z. noltii* = 47.88 km² (11,680 acres)								

* North of major shipping channel.

† South of major shipping channel and South Channel.

Table XV. Areal relations in Grays Harbor, 1975. (Adapted from Smith et al. 1976.)

		Area	
Area description	*Data used*	*(km²)*	*(acres)*
1) Entire harbor to EHW	C and GS chart 6195	221.4	54,720
2) Entire harbor to +2.7 m (+9 ft)	USACE 1968 topographic data	217.3	53,696
3) MLLW to EHW	C and GS chart 6195	136.0	33,600
4) MLLW to +2.7 m (+9 ft)	USACE 1968 topographic data	115.5	28,544
5) Salt marsh	This study, Table XII	22.0	5,420
6) Tideflats	MLLW to EHW minus salt marsh	114.0	28,160
7) Total eelgrass	This study, Table XIV	47.4	11,680
8) Total "dense"* *Z. marina*	This study, Table XIV	22.5	5,540
9) -0.9 to +0.9 m (-3 ft to +3 ft) estimated growth range of eelgrass	USACE 1968 topographic data	46.6	11,520
10) Inner harbor area used as dredged material disposal sites, to 1975	C and GS chart 6195; USACE aerial photographs, 1950	16	3,850

* Dense eelgrass ranged from 36.8 turions/m² to 137.6 turions/m², with a mean of 79.8 turions/m².

Z. noltii occurs at higher elevations (adjacent to shoreline) than *Z. marina*. In most cases, aggregations of each type of plant were readily separable from one another because of growth at characteristic elevations. "Dense" *Z. marina* is found in protected waters at elevations below +0.9 m (3 ft) in most areas of the harbor. *Z. marina* and *Z. noltii* are absent from the west end of Whitcomb Flats and the Sand Island shoals where wave action is intense. Figure 24 also shows that eelgrass is absent from the immediate site E area; this is directly attributable to elevation increases due to dredged material disposal at site E. Conservatively, 0.71 km² (175 acres) of "dense" eelgrass has been destroyed in the site E disposal area.

The areal extent of *Z. noltii* and *Z. marina* in Grays Harbor is summarized in Table XV. *Z. marina* occupies 45.1 km² (11,000 acres) of the total 47.88 km² (11,680 acres) covered by eelgrass in 1975. "Dense" *Z. marina* makes up slightly over half of the total area occupied by *Z. marina*.

The relationship of *Zostera* acreages to other acreages in Grays Harbor is summarized in Table XV. Both *Zostera* species occupy 41.6% of all tidal flats, while dense *Z. marina* covers 19.7% of all tidal flats.

Table XV also shows the estimated growth range, −0.9 to +0.9 m (−3 to +3 ft), of *Z. marina* in Grays Harbor. Plus 0.9 m (+3 ft) was the highest elevation at which "dense" *Z. marina* occurred in Grays Harbor. Minus 0.9 m (−3 ft) was chosen as the lower growth limit based on

ground surveys which indicate that eelgrass did not occur below −0.6 or −0.9 m (−2 or − 3 ft). Scoured channels with steep banks, caused by strong currents, and low light penetration due to turbid conditions inhibit eelgrass growth below −0.9 m (−3 ft).

This study has shown that Grays Harbor *Z. marina* occurred in "dense" stands at elevations higher than those reported from other areas. It is interpreted that the aggregated pattern of *Z. marina* occurrence suggests an adaptation to survival at intertidal elevations generally higher than considered optimum for this plant. It was also determined that "dense" *Z. marina* does not occur above +0.9 m (+3 ft) in Grays Harbor.

These data indicate that a threat to *Z. marina* occurrence and productivity in Grays Harbor is presented by dredged material disposal; namely, that of raising tidal flat areas above the growth range for *Z. marina*. In view of the productive nature of *Z. marina* and its importance to the estuarine and adjacent coastal systems, dredged material disposal should not take place where *Z. marina* occurs. Disposal at site E has already eliminated at least 0.71 km² (175 acres) of "dense" eelgrass beds and may have lowered the productivity of adjacent *Z. marina* by raising intertidal elevations above those optimum for eelgrass growth.

The data presented on distribution and extent of Grays Harbor eelgrass are valid for 1975 only. Waddell (1964) pointed out that yearly changes of more than 100% in extent of eelgrass coverage have occurred in Arcata Bay and Humbolt Bay, California. Similar changes are likely in Grays Harbor, depending on growing conditions and other factors. It is not possible to judge whether 1975 was an average or a typical year for eelgrass in Grays Harbor.

Conventional techniques

Shipboard surveys

Temperature, salinity and suspended sediment concentration data were acquired during flood and ebb from 9 to 11 July 1974 using conventional shipboard sampling methods. The data were subsequently used to prepare surface temperature, salinity and sediment distribution maps. These maps were then used to infer surface circulation patterns. Phipps (1977) also used these data to prepare distribution maps.

Surface temperature distribution during late ebb tide (after predicted maximum ebb currents at harbor entrance) and low water slack on 9 July 1974 (refer to Tables VIII-X) is shown in Figure 25a. Warmer harbor water has migrated toward the harbor mouth and has appeared to move nearer the mouth on the north side possibly because of the Coriolis effect. Cooler oceanic water was generally restricted to the area between Damon Pt. and Westhaven Cove (Fig. 1), although there appeared to be a minor intrusion of oceanic water into the harbor on the south. Oceanic surface water intrusion occurred in the channel just north of Whitcomb Flats. Temperatures increased upstream in the navigation channels to the area near the confluence of the Chehalis and Wishkah Rivers.

Surface temperature distribution and inferred circulation patterns during late flood (Fig. 25b), after predicted maximum flood currents and just before high water slack, were more complex than those observed during late ebb (Fig. 25a). Oceanic water flooding into the harbor appeared to occupy most of the harbor mouth. The small cove east of the east end of the south jetty and the area east of Westhaven Cove contained warmer water, and circulation out of these areas may have been reduced because these areas are protected from the main harbor currents. The cooler oceanic water had also migrated past Damon Pt. and mixed with the water just north of Damon Pt., although it appears that ebb flow may have started along the north side of the entrance. Temperatures in Crossover and Moon Island Channels were lower than those at the harbor mouth, suggesting that colder water below the surface may have come to the surface in this area during flood tide. Warmer water observed near the harbor mouth during ebb (Fig. 25a) was pushed up the harbor during flood and was restricted to the harbor east of Rennie Island.

Surface salinity data acquired concurrently with the temperature data showed the same general patterns as previously observed. During late ebb (Fig. 26a) the less saline water from the eastern harbor migrated toward the mouth. The major portion of the ebb stream appeared to move through the harbor mouth along the northern side. The highest salinities were found in South Bay, east of Westhaven Cove, in the harbor mouth and in the southern portion of North Bay. The saline water in North and South Bays may have been oceanic water that was not flushed from the harbor during ebb because it was in areas protected from the main ebb stream. Mixing of oceanic and brackish water appeared to intensify at two locations: west of Rennie Island

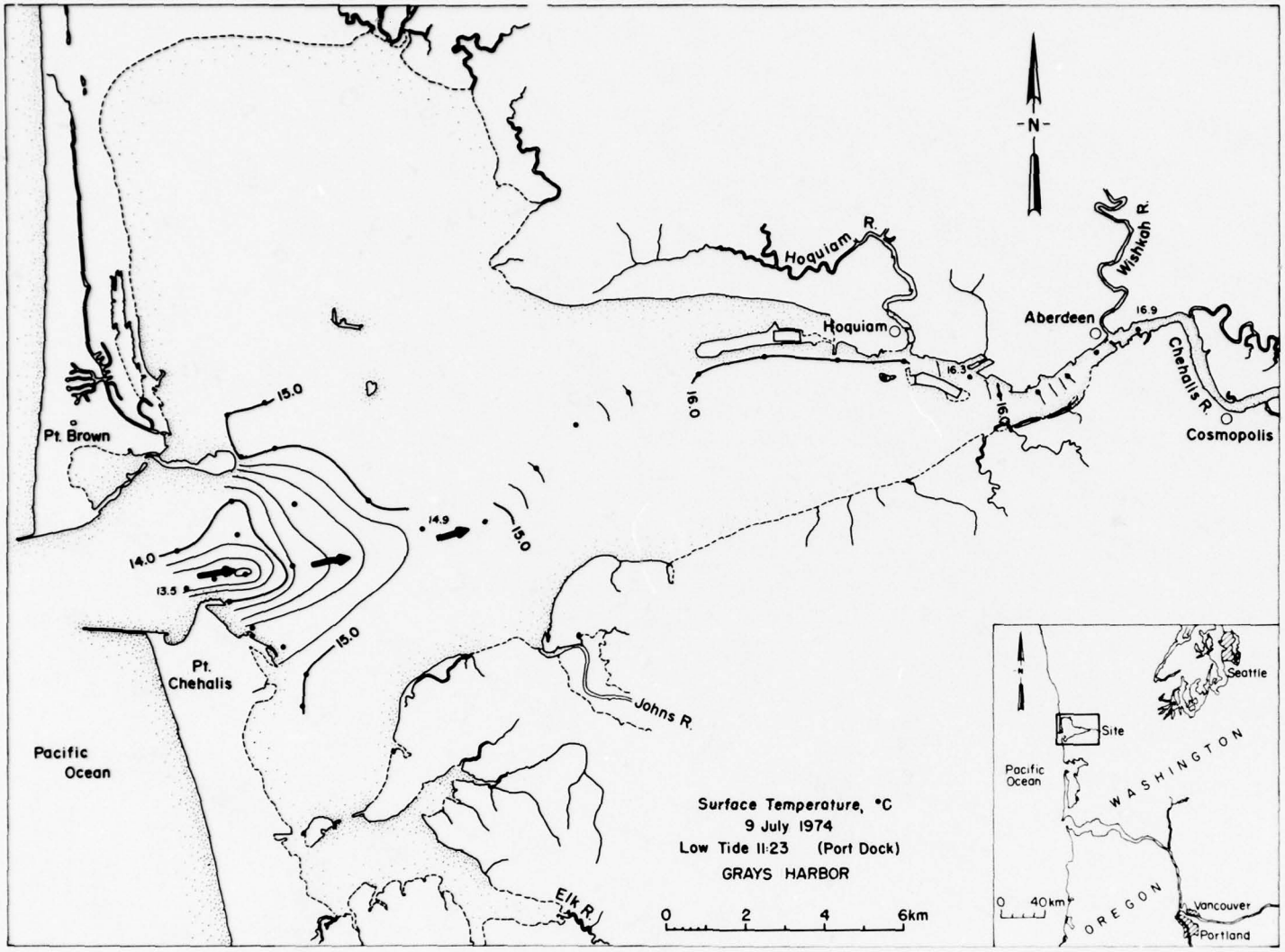

a. Late ebb.

Figure 25. Surface temperature distribution, 9 July 1974.

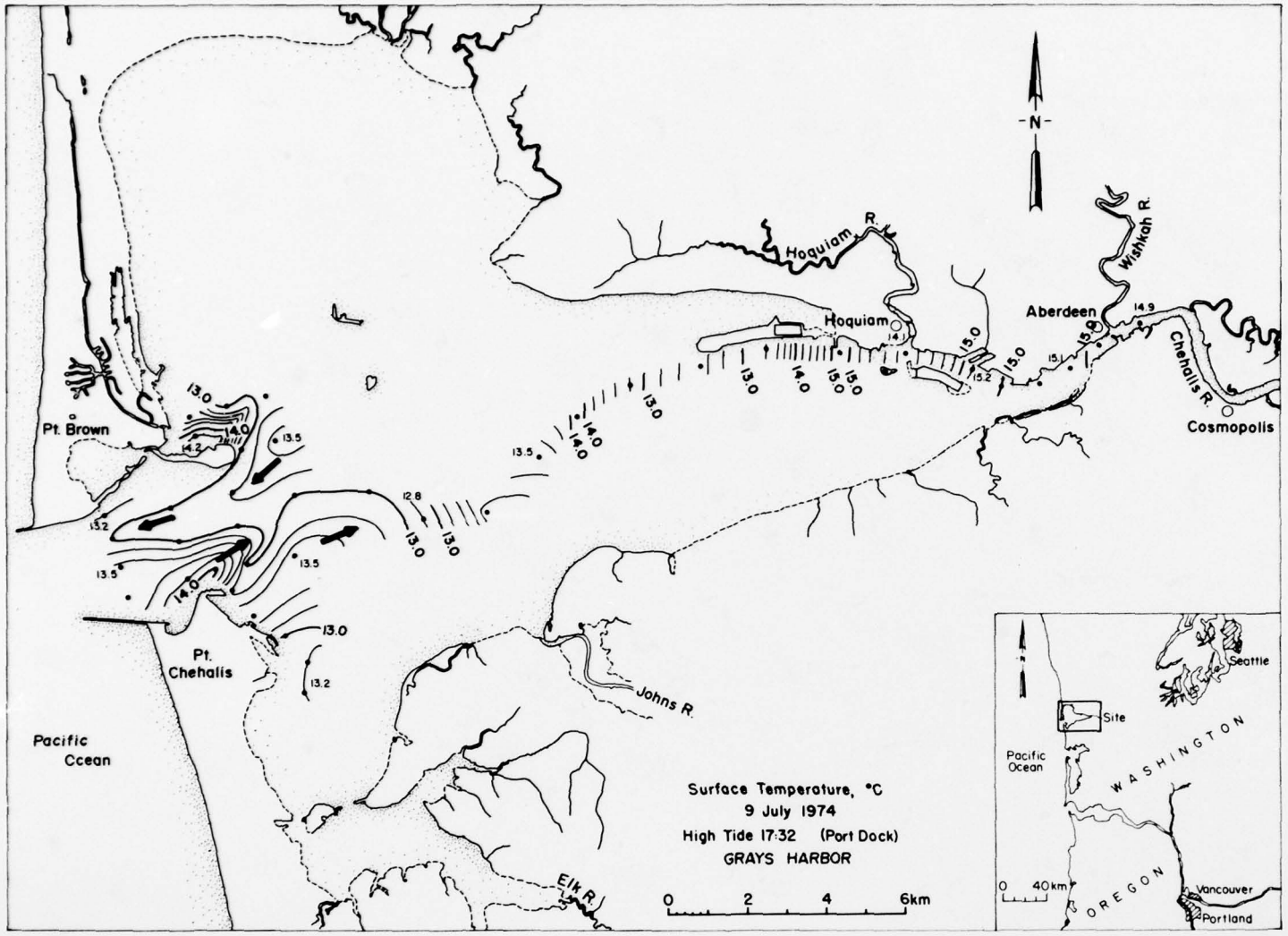

b. Late flood.

Figure 25 (cont'd). Surface temperature distribution, 9 July 1974.

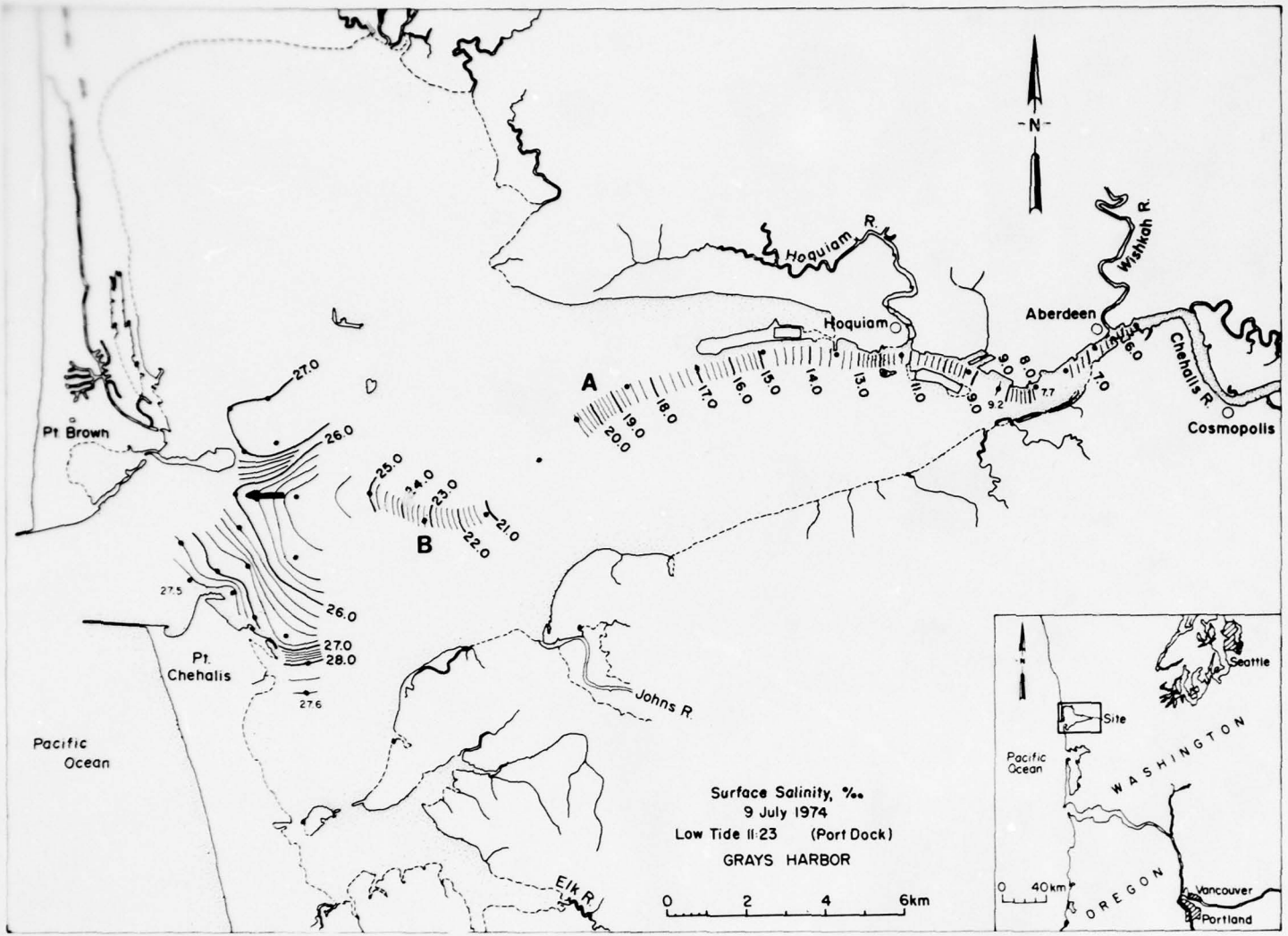

a. Late ebb.

Figure 26. Surface salinity distribution, 9 July 1974.

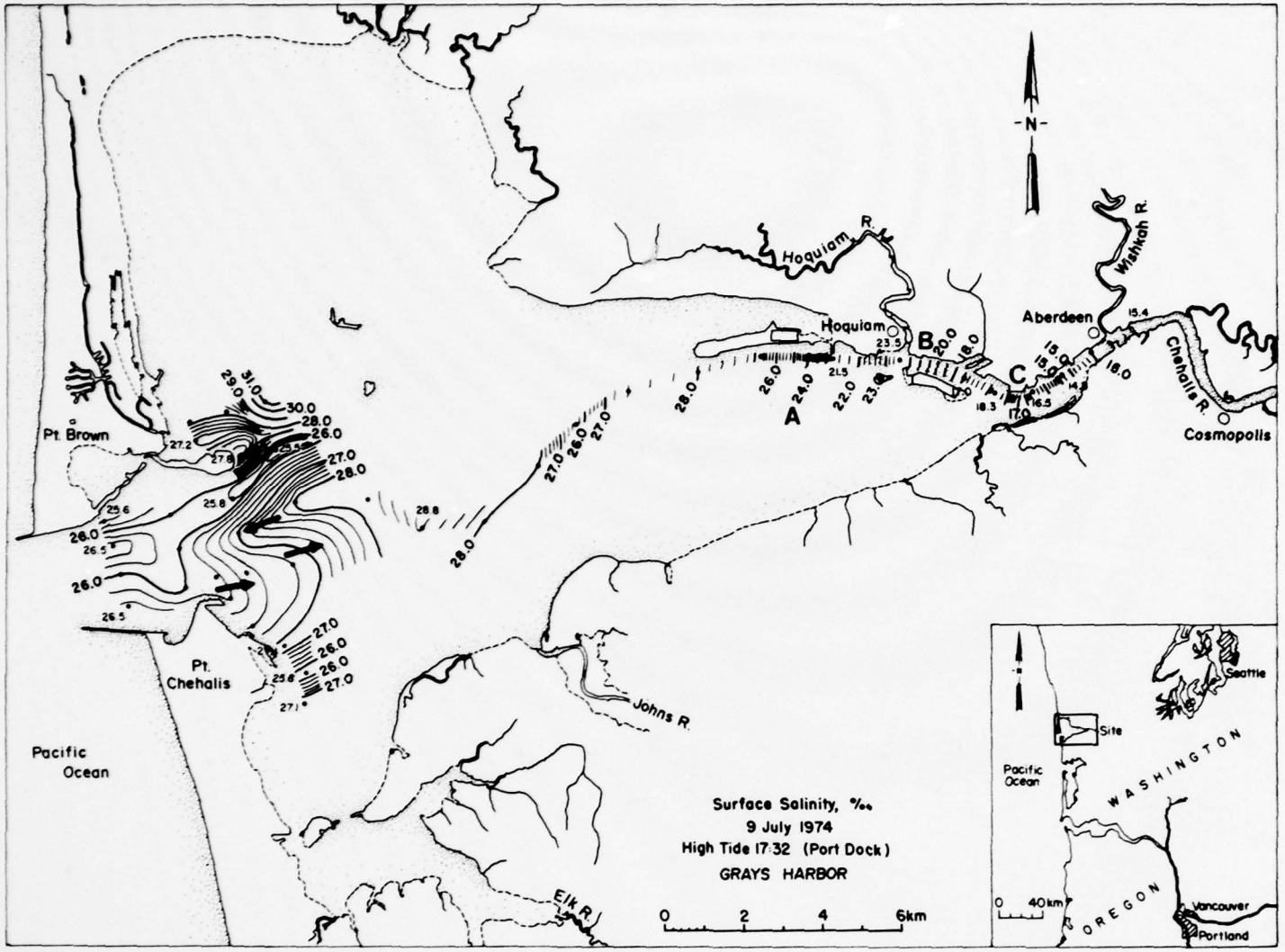

b. Late flood.

Figure 26 (cont'd). Surface salinity distribution, 9 July 1974.

(A) where a rapid salinity change, from 18 to 20.9 ppt, was observed and east of the harbor mouth (B) where salinity changed from 25 to 21 ppt.

During flood (Fig. 26b) the oceanic and mixed water had migrated upstream to the limits of the sampling area. Rapid salinity changes east (C) (16-18 ppt), north (B) (17-23 ppt) and west (A) (22-27 ppt) of Rennie Island suggested that mixing was very active in this area. West of Moon Island to the harbor mouth salinity changes were less pronounced, 26-28 ppt, but variable. Water more saline than observed at the mouth (25.6-26.5 ppt) was found in the area of Crossover Channel (28-28.8 ppt), in southern North Bay (26-31 ppt), and in northern South Bay (27 ppt). These high salinity zones may have been caused by upwelling of subsurface water which is generally more saline. It appeared that the major portion of the flood stream on the surface occupied the central and southern parts of the harbor mouth.

Suspended sediment concentrations were low and distributions were complex. Few discernible circulation patterns were apparent from these ground truth data or from the sediment patterns observed on the NASA photography. During late ebb (Fig. 27a; also see Fig. 1) the lowest concentrations were found north of Rennie Island (6 mg/l), in Cow Pt. Reach (9.1-10.2 mg/l) and south of Damon Pt. (11.4 mg/l). The highest concentrations were found north and northwest of Westhaven Cove. Generally concentrations were higher in the surface water during ebb than during flood (Fig. 27b). The ebb currents in the harbor are usually stronger than the flood currents. The ebb currents may therefore resuspend more sediment from the tidal flats.

Surface temperature distribution during late flood-early ebb (after predicted high water slack and before maximum ebb currents at the harbor entrance) on 10 July 1974 is shown in Figure 28a. This distribution was similar to that in Figure 25b with cooler water, 13.2°-14°C (55.7°-57.2°F), near the harbor entrance and warmer, 15°-16°C (59°-60.8°F), east of Moon Island. Coldest temperatures were found approximately 3 km (4.8 mi) northeast (A) of Westhaven Cove. Water from below the surface may have been brought to the surface by the strong currents and/or because the harbor bottom becomes shallower at this location.

Surface temperature distribution during late ebb-early flood (from 2 hours after maximum ebb currents through low water slack to two hours before maximum flood, Table VIII) on 10 July 1974 is shown in Figure 28b. The warmer water from the eastern harbor had migrated toward the harbor entrance as shown on Figure 25a. Temperatures near the entrance (Fig. 25a and 28b) were also similar, although warmer water, 14°-15.1°C (57.2°-59.2°F), occupied the northern portion of the entrance on 10 July.

Highly variable surface salinities (Fig. 29a) occurred at the harbor entrance (23-27 ppt), in Crossover Channel (23.9-25.5 ppt), south of Moon Island (20.8-23.1 ppt), north of Rennie Island (14.4-19.7 ppt) and in Cow Pt. Reach (11.1-14.1 ppt). Salinities in southwestern North Bay and northwestern South Bay were 3 to 4 ppt higher than at the entrance. More saline bottom water may have been brought to the surface in the shallower zones south of Damon Pt. and north of Westhaven Cove (Fig. 29a). Inferred surface currents tend to be circular during this transition time between ebb and flood.

Salinities during late ebb-early flood (Fig. 29b) were less variable at the harbor entrance than observed in Figure 29a and comparable to those acquired on 9 July (Fig. 26a). Note the two areas (A and B) of rapid salinity change. The only current pattern inferred on Figure 29b was the movement of less saline water (25-27 ppt) across the entrance from Damon Pt. to just north of Westhaven Cove.

Suspended sediment concentrations of the flooding oceanic water (Fig. 30a) are approximately 5-8 mg/l lower than and were less variable than those of the water at the entrance at the end of ebb tide on 10 July 1974 (Fig. 30b). The clearest water near the harbor entrance during flood (Fig. 30a) was observed in the center. Greater concentrations occurred in the shallower areas east of Westhaven Cove, north and east of Damon Pt. and locally along the navigation channels. Lowest concentrations in the harbor were found in the Chehalis River near Aberdeen.

Concentrations during late ebb-early flood (Fig. 30b) were highly variable along the navigation channels and near the entrance. Because the water with highest concentrations generally occurred in the shallower locations, sediment reworking was probably the cause of the observed suspended sediment patterns.

Shipboard data were acquired during late flood-early ebb [from approximately 40 min before high water slack to 2 hours before maximum ebb currents at the harbor entrance (Table

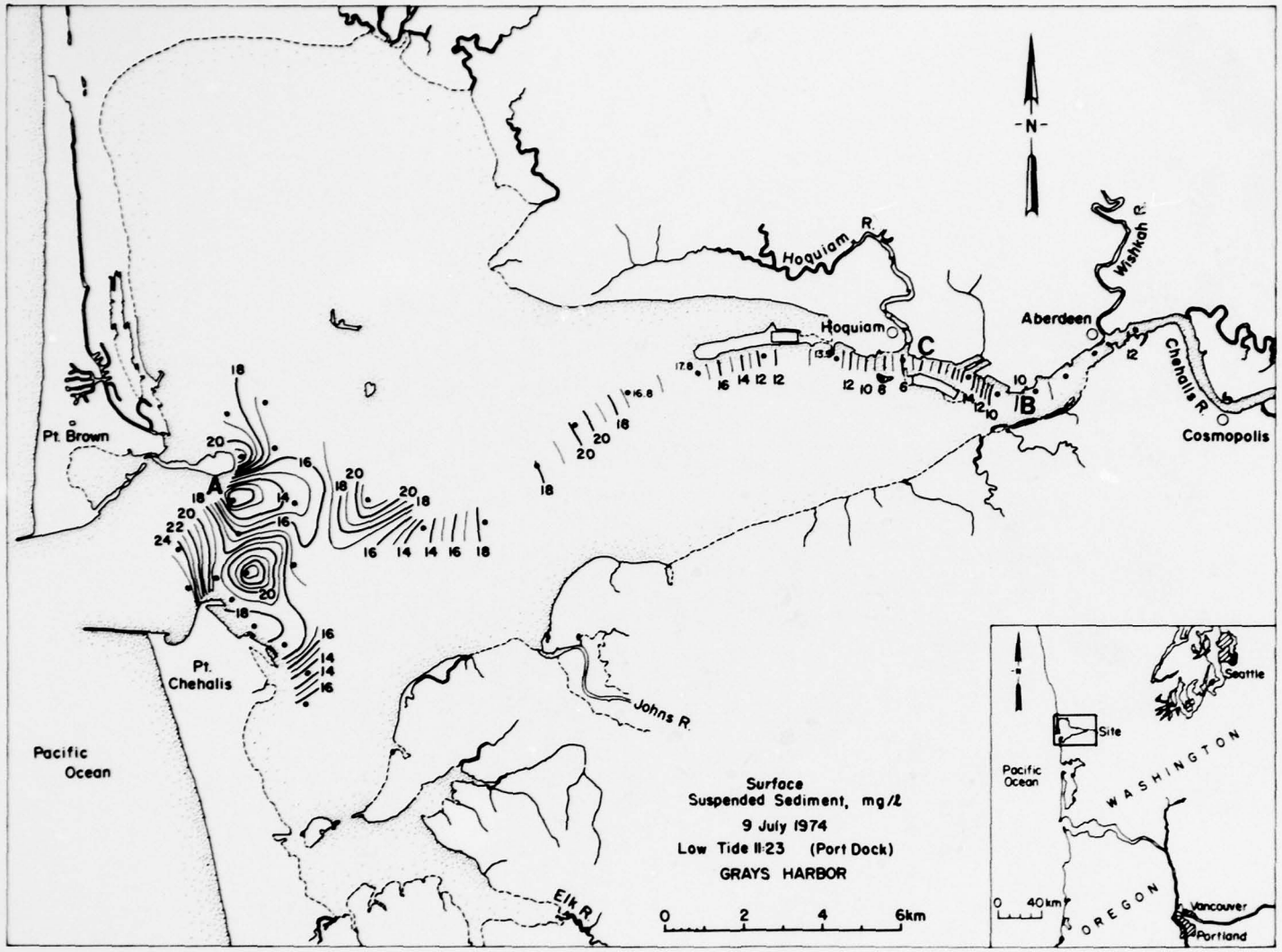

a. Late ebb.

Figure 27. Surface suspended sediment distribution, 9 July 1974.

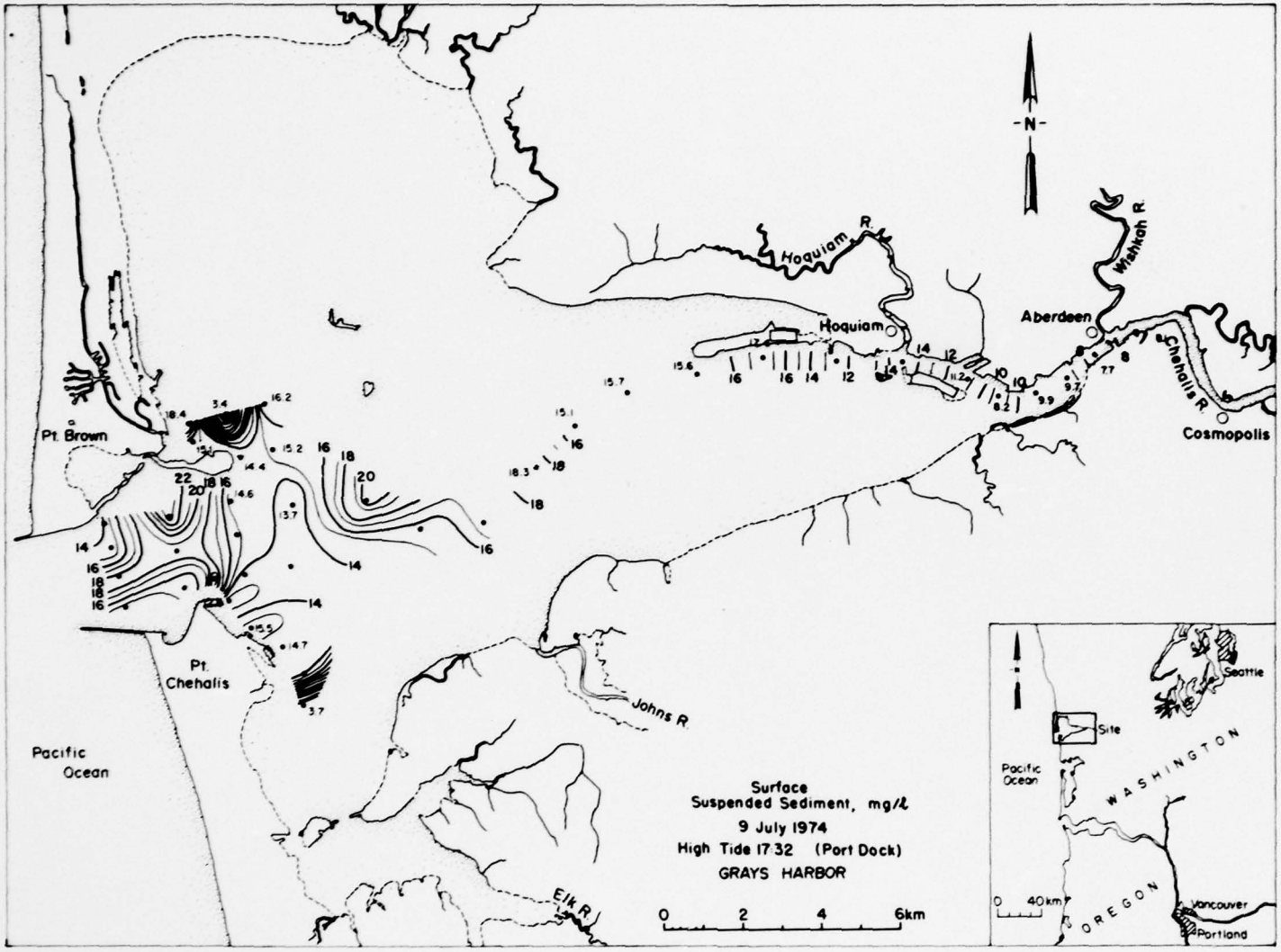

b. Late flood.

Figure 27 (cont'd).

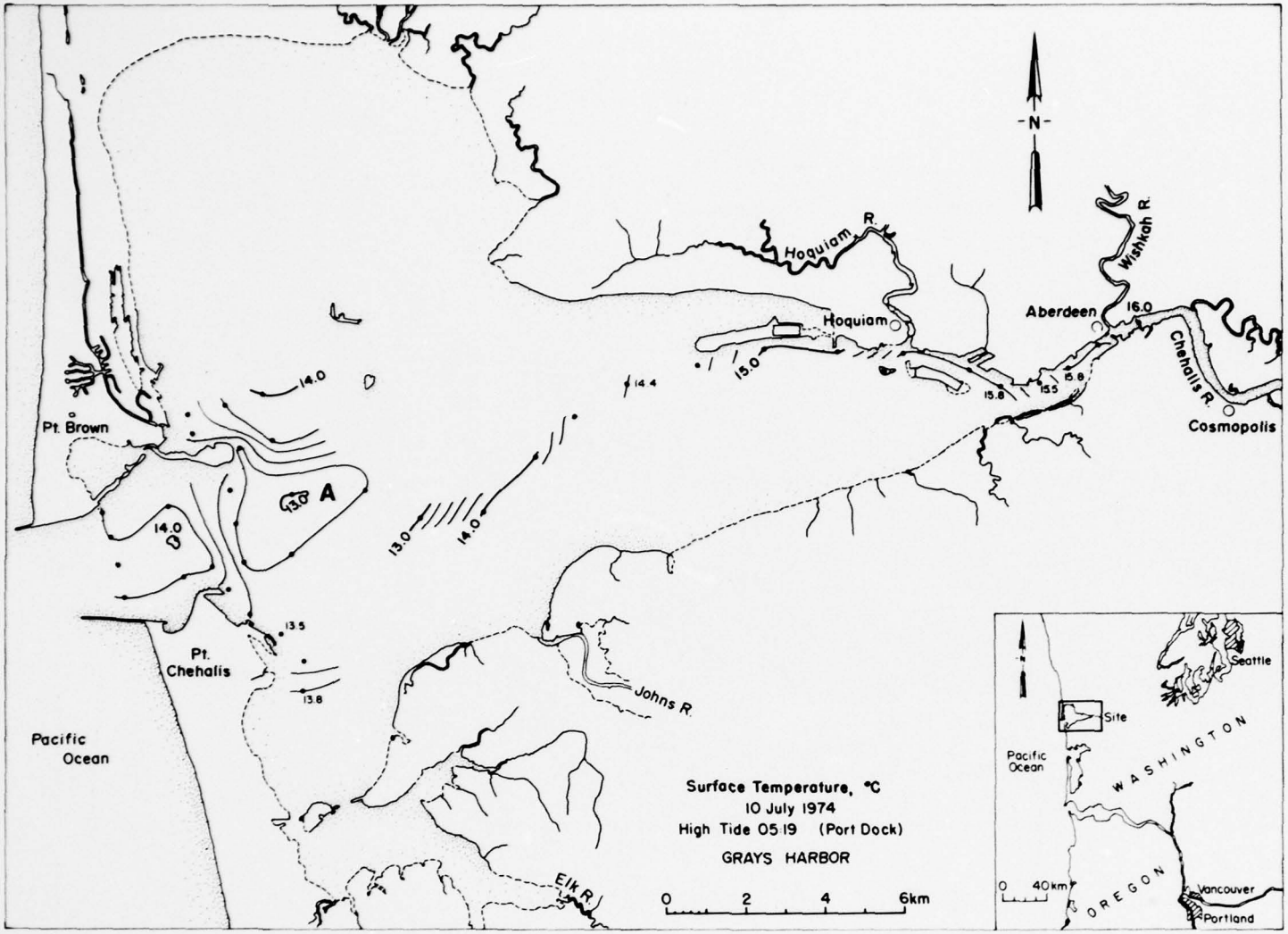

a. Late flood — early ebb.

Figure 28. Surface temperature distribution, 10 July 1974.

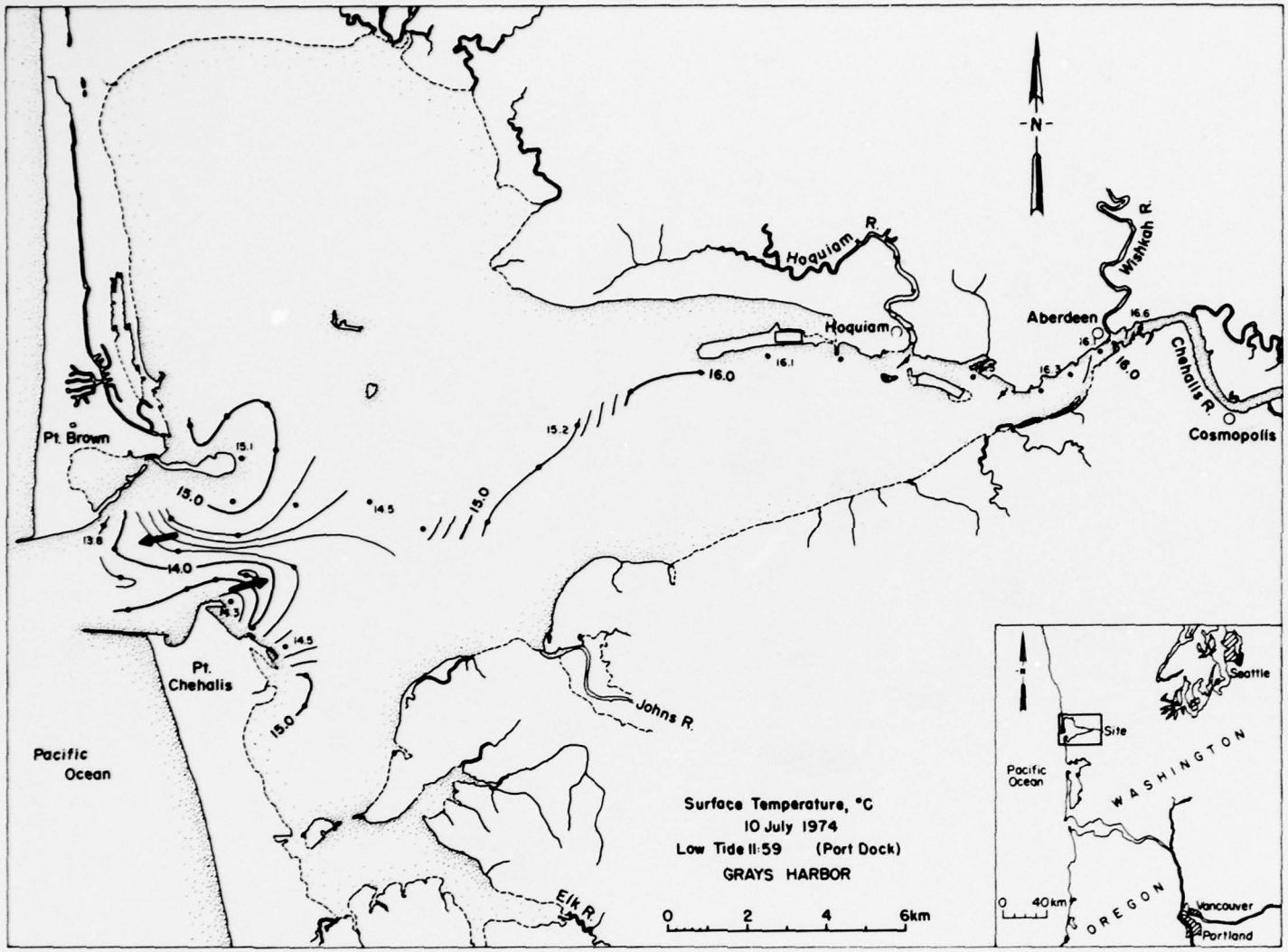

b. Late ebb — early flood.

Figure 28 (cont'd).

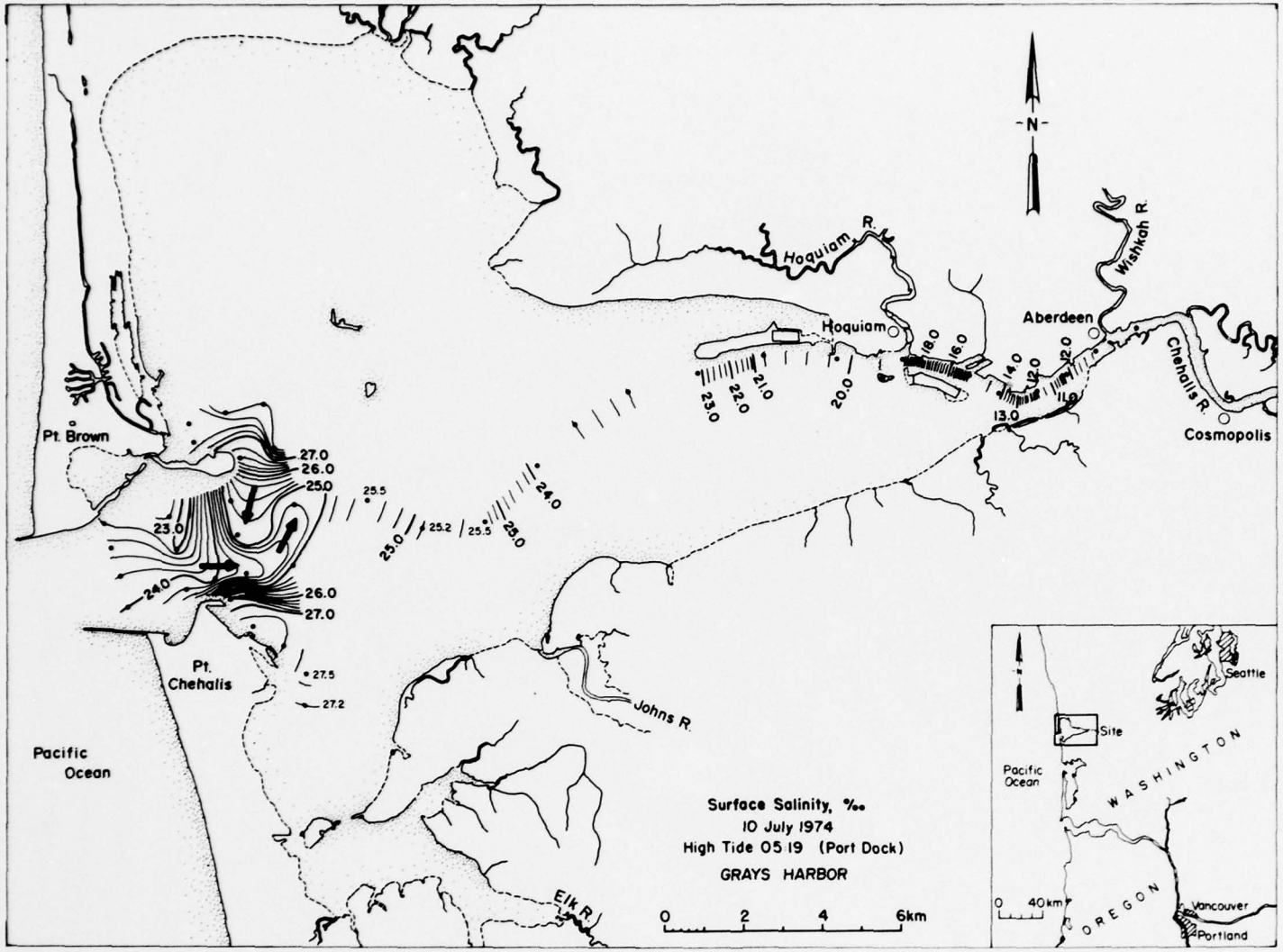

a. Late flood — early ebb.

Figure 29. Surface salinity distribution, 10 July 1974.

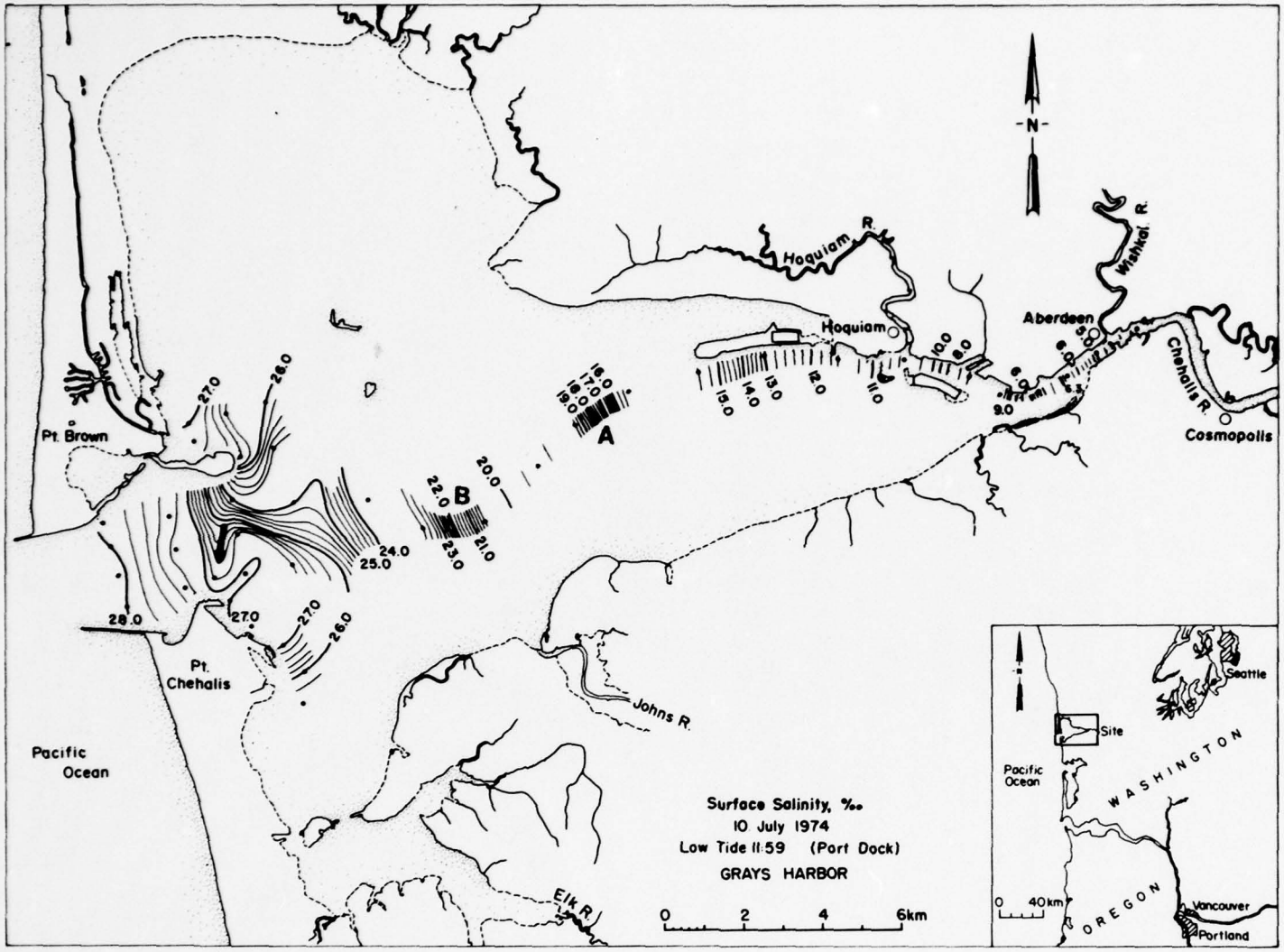

b. Late ebb — early flood.

Figure 29 (cont'd).

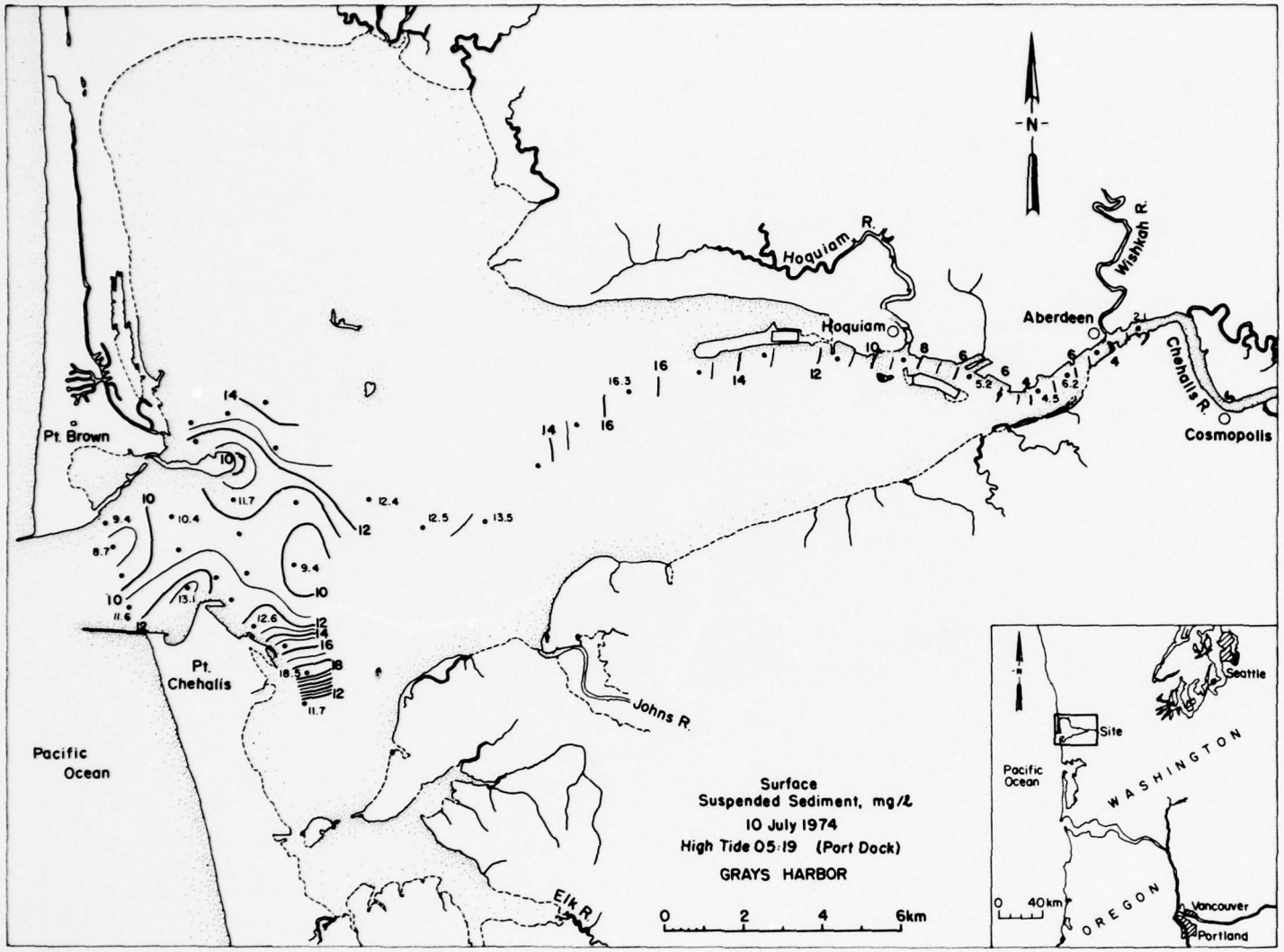

a. Late flood — early ebb.

Figure 30. Surface suspended sediment distribution, 10 July 1974.

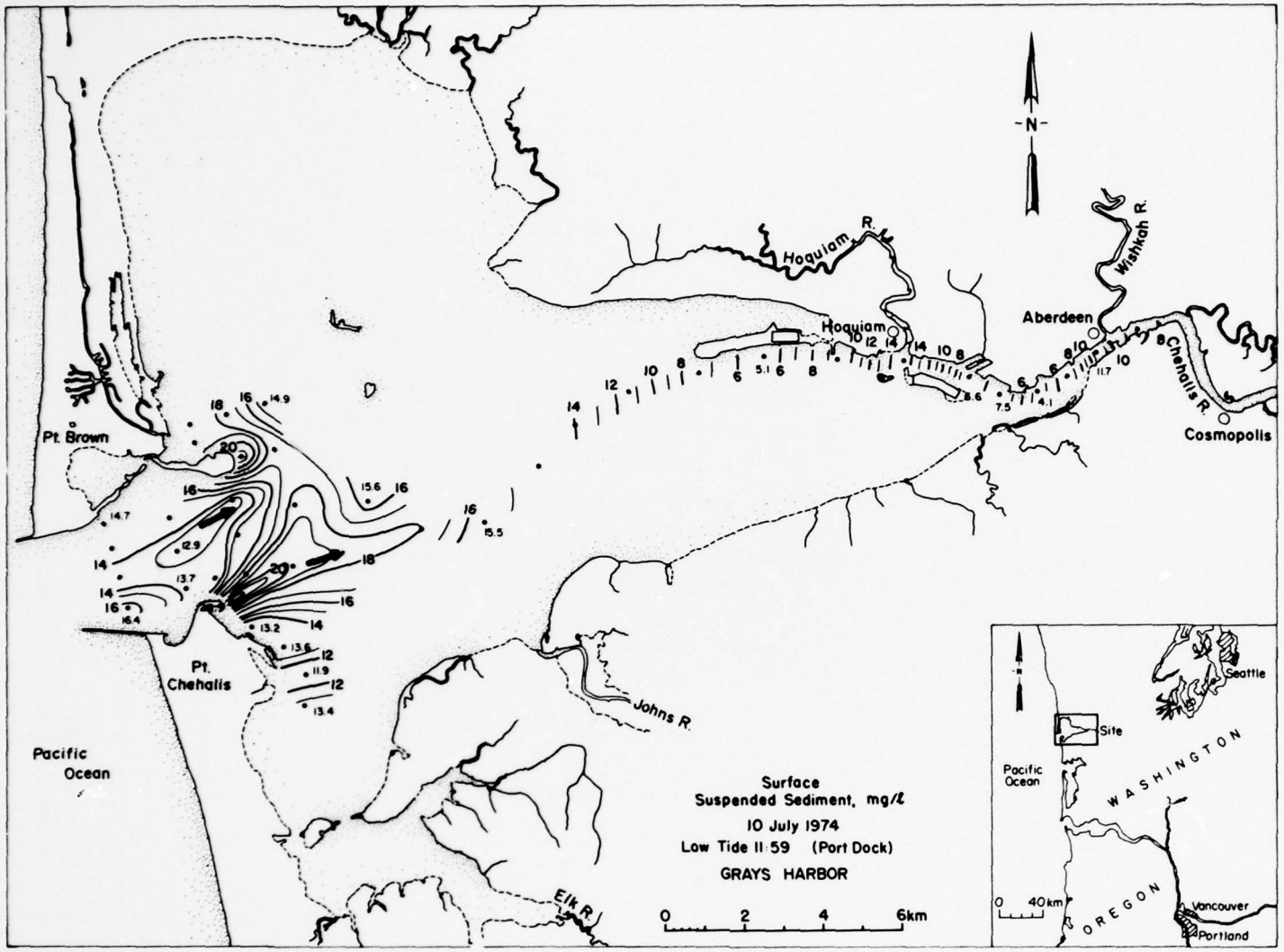

b. Late ebb — early flood.

Figure 30 (cont'd).

VIII)] and during late ebb-early flood [from approximately 1.5 hours before low water slack to 1.2 hours before maximum flood currents at the harbor entrance (Table VIII)] on 11 July 1974. Temperature distribution (Fig. 31a) showed that cooler, 13.5°-14°C (56.3°-57.2°F), flooding oceanic water was entering the harbor in the southern half of the entrance; warmer harbor water, 14°-14.8°C (57.2°-58.6°F), occupied the northern half of the entrance. This distribution may also have indicated that during early ebb harbor water initially flushed through the north side of the entrance. As observed from 9 and 10 July data the warmer temperatures were found in the southwest North Bay, northwest South Bay and east of Moon Island.

Surface temperatures in the harbor during late ebb-early flood (Fig. 31b) were higher than during flood, since the cooler oceanic surface water was flushed and warmer, fresher water migrated into the harbor. Temperatures at the entrance, 14.1°-15.6°C (57.5°-60.1°F), indicated that warmer water in the eastern part of the main harbor and in the upper portions of North and South Bays had migrated to the entrance during ebb.

Salinity data (Fig. 32a) at the harbor entrance showed a well defined interface between surface waters on 11 July 1974: 21.2-23.6 ppt in the northern half, 24-25 ppt in the southern half. High salinities were found in North and South Bays where flooding water had advanced. Rapid salinity decreases occurred southwest of (24.2-22.4 ppt) and south of (20.2-14.3 ppt) Moon Island and north of Rennie Island (13.9-9.3 ppt). During ebb (Fig. 32b) the fresher waters migrated toward the harbor entrance and areas of rapid change were found southwest of Moon Island (14.6-18.9 ppt) and in the vicinity of East Reach (North Channel) (19.2-24.0 ppt). At the entrance an area of lower salinity (23.3-24.8 ppt) was surrounded by more saline water (25-26.1 ppt). Saline water that had flooded into North and South Bays during the previous flood tide remained after ebb since flushing was less active in these embayments. Other than the detection of the western migration of harbor water during ebb and the eastern movement of oceanic water during flood, no additional circulation patterns were inferred from these salinity data.

Suspended sediment patterns (Fig. 33) were complex. The pattern northeast of the south jetty in the vicinity of the hopper dredge disposal area during late flood may have been caused by easterly moving flood water reworking bottom material and producing a zone of high concentration (15-18.3 mg/l). If currents reworked bottom sediments and were observed on the surface, there would have to be upwelling. Salinities shown on Figure 32a and water column data (Fig. 34) do not indicate upwelling. Barrick (1976) reports that upwelling occasionally occurs in local areas (generally near the harbor entrance) when the meteorological conditions are proper. This zone of high concentration could be due to wave action over the inner bar or turbidity from shore. Other general patterns observed include: lower concentrations were found in the middle of the harbor entrance, concentrations were higher nearer the north and south shores, higher concentrations occurred in shallower areas where tidal flat sediments were resuspended, and concentrations were lower farther up the navigation channel towards Aberdeen during flood although greater variability in concentrations occurred during ebb in this area.

Temperature, salinity and suspended sediment data were acquired from the water column stations during early ebb (Fig. 34a) [approximately 0.5 hours after high water slack and 2 hours before maximum ebb currents (Table VIII)] and during late ebb-early flood (Fig. 34b) [from approximately 1 to 0.6 hours before low water slack (Table VIII)] on 10 July 1974. Water column data were also acquired during early ebb (Fig. 35a) [from approximately the time of high water slack to 0.7 hours after high water slack (Table VIII)] and during early flood (Fig. 35b) [from approximately 0.3 hours before to 0.4 hours after low water slack (Table VIII)] on 11 July 1974.

Temperatures showed very little change from the surface to near the bottom at stations 2, 3 and 5 during early ebb (Fig. 34a). At stations 6, 18 and 19 temperatures were more variable at the surface and at depth. Data at station 6 showed a 1°C (1.8°F) drop from the surface to 9.1 m (30 ft), then a 1°C (1.8°F) rise from 9.1 to 16.1 m (30 to 53 ft). The greater variability may have been a result of more mixing between oceanic and harbor water at the more eastern stations. Surface salinities were lower than those at depth at all stations. Variations in suspended sediment concentration were more pronounced, but not consistent, below the surface at stations 2, 5, and 19, where concentrations were lower nearer the bottom. At stations 3, 6, and 18, concentrations were higher nearer the bottom. The highest near bottom concentration (27 mg/l) was found at station 18.

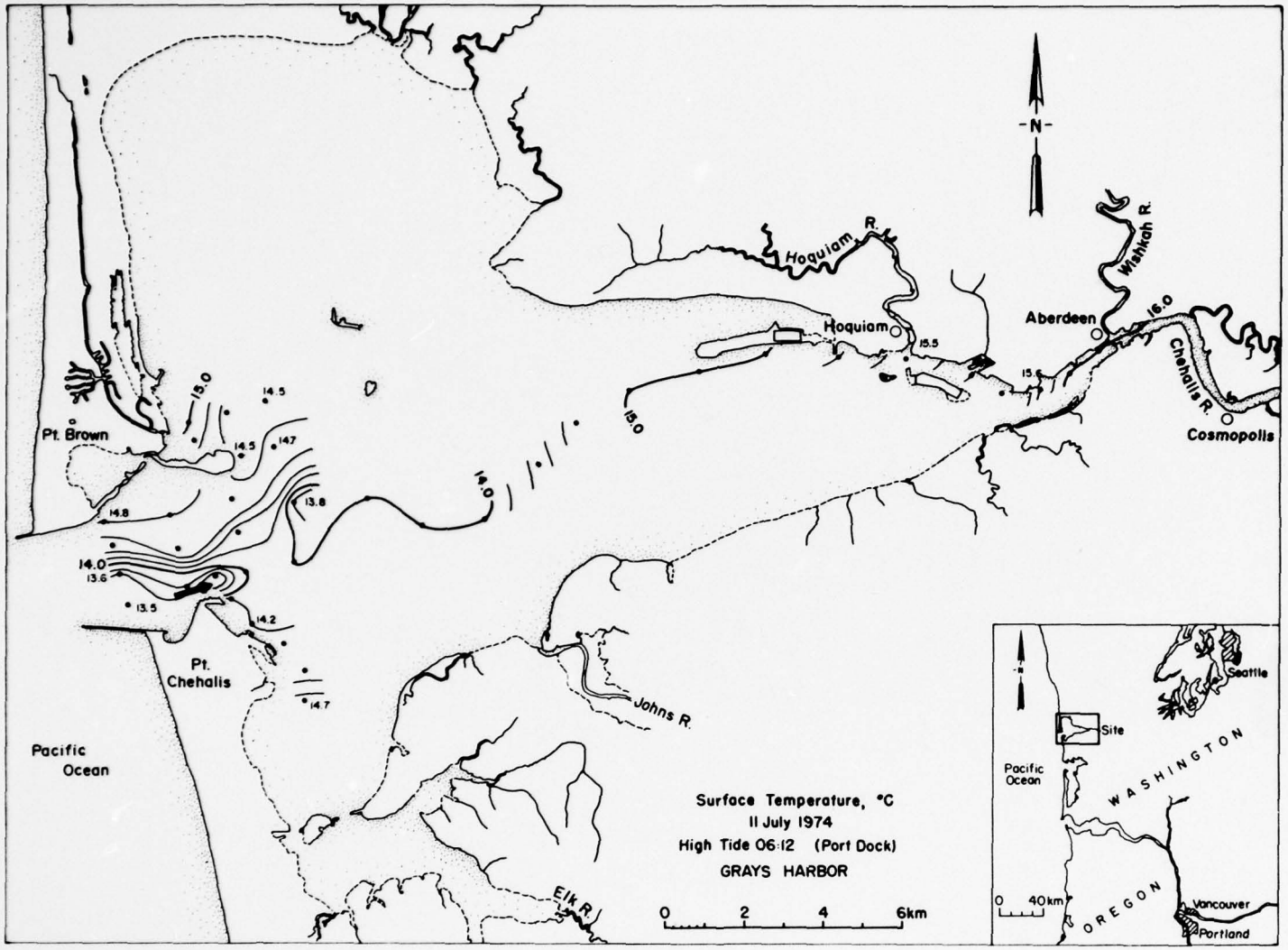

a. Late flood — early ebb.

Figure 31. Surface temperature distribution, 11 July 1974.

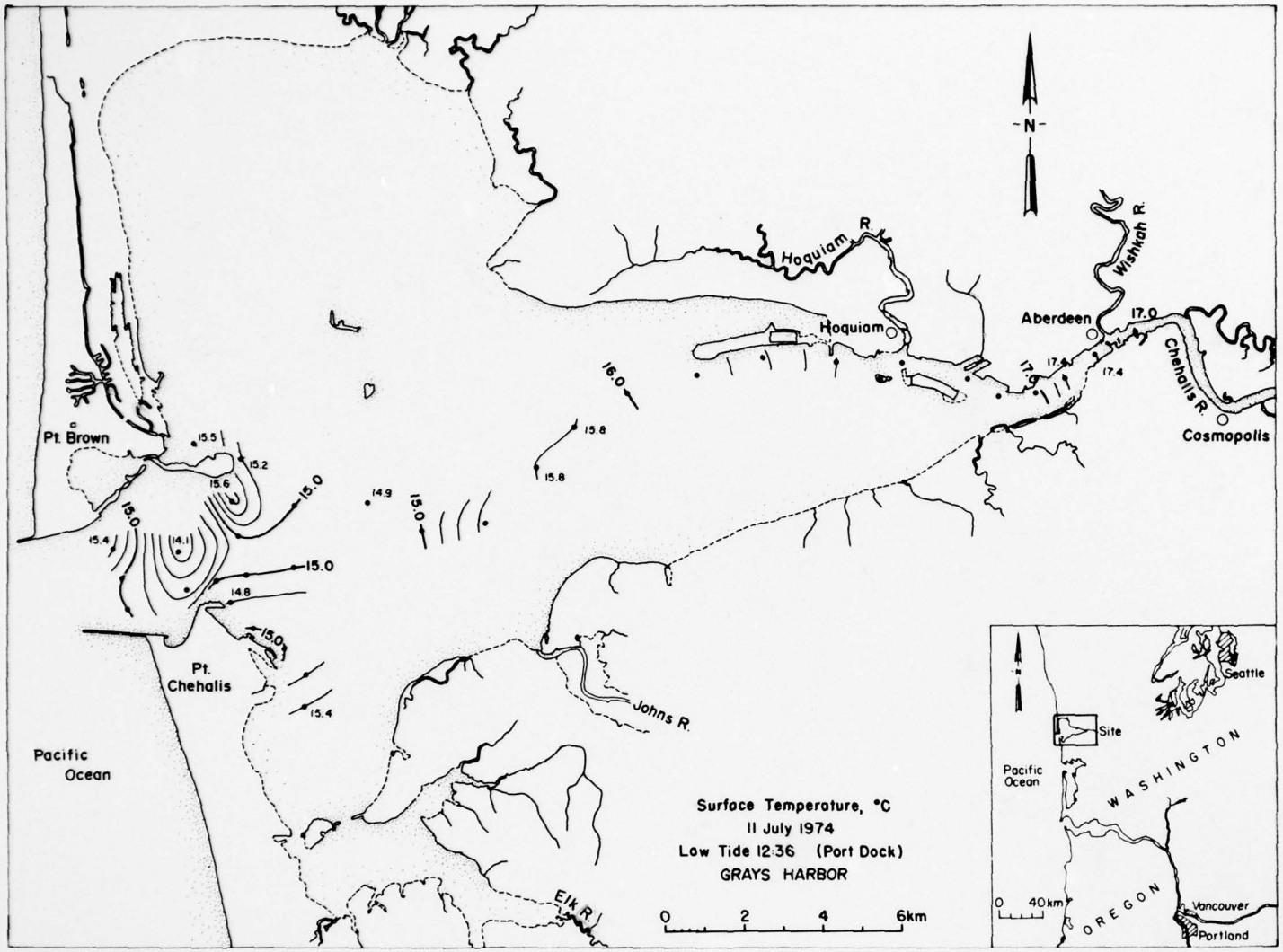

b. Late ebb — early flood.

Figure 31 (cont'd). Surface temperature distribution, 11 July 1974.

AD-A061 823 COLD REGIONS RESEARCH AND ENGINEERING LAB HANOVER N H F/G 14/5
ESTUARINE PROCESSES AND INTERTIDAL HABITATS IN GRAYS HARBOR, WA--ETC(U)
JUL 78 L W GATTO IAO-CWP-S-75-9
UNCLASSIFIED CRREL-78-18 NL

2 OF 2
AD
A061823

END
DATE FILMED
2-79
DDC

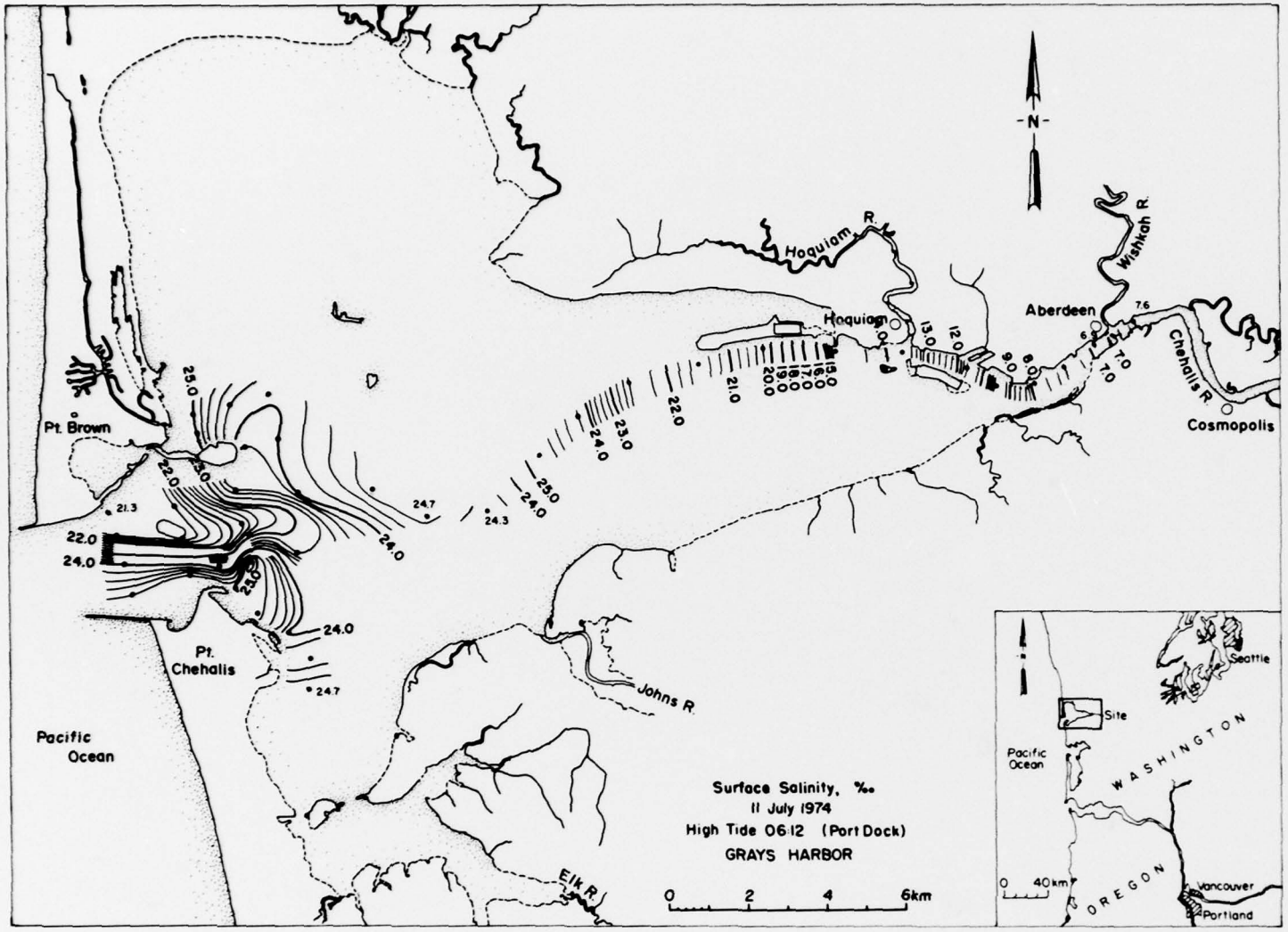

a. Late flood — early ebb.

Figure 32. Surface salinity distribution, 11 July 1974.

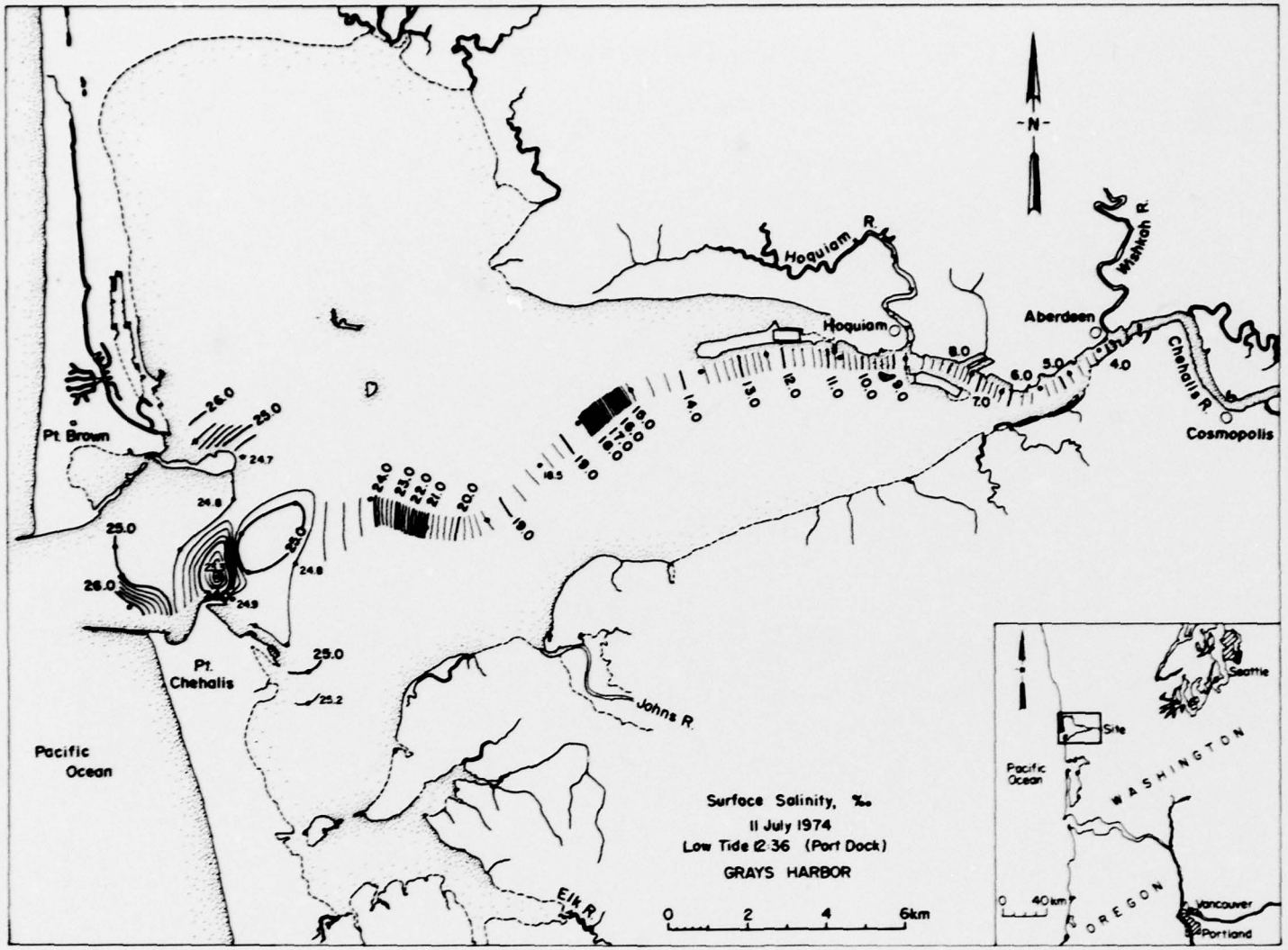

b. Late ebb — early flood.

Figure 32 (cont'd). Surface salinity distribution 11 July 1974.

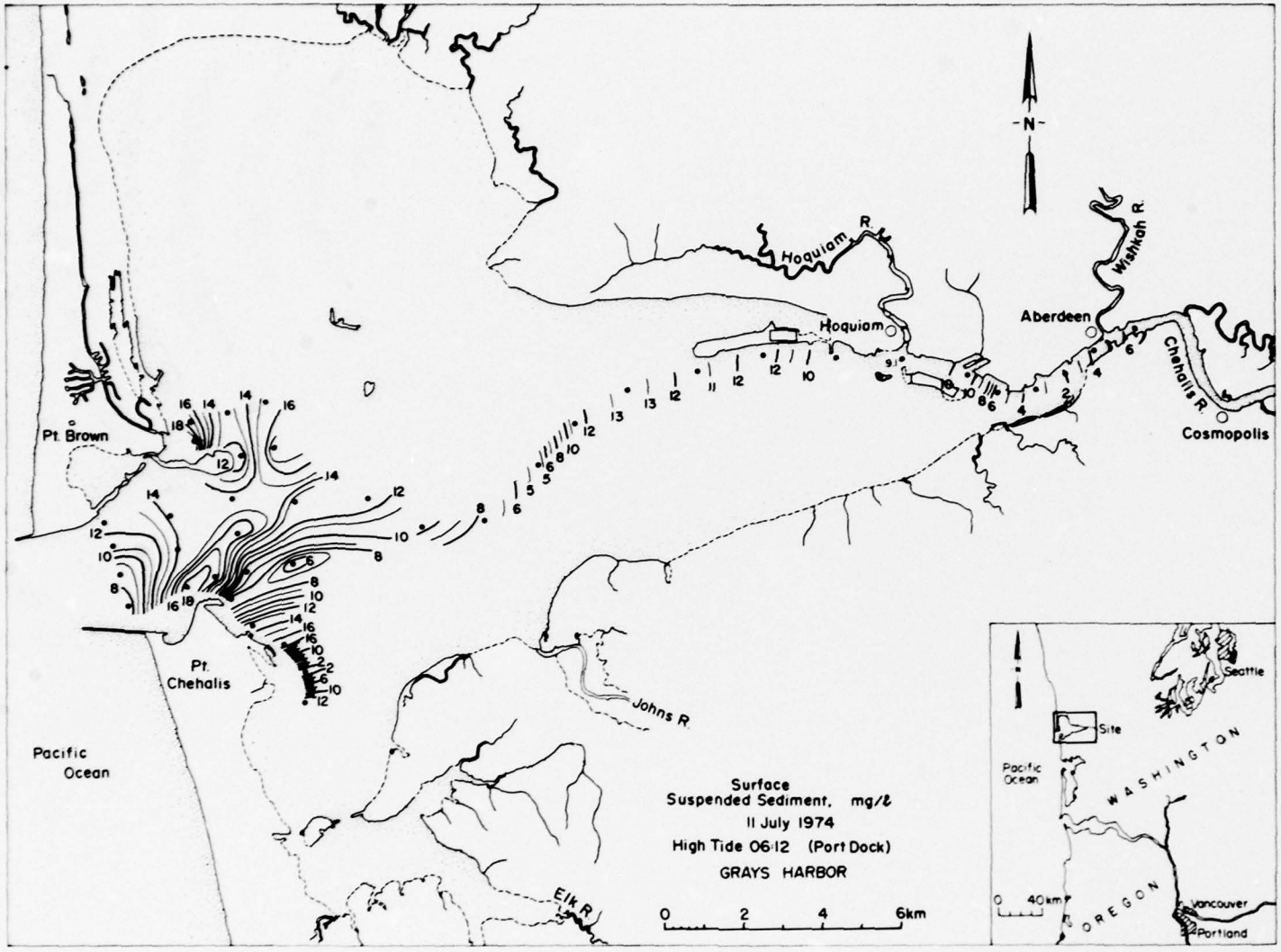

a. Late flood — early ebb.

Figure 33. Surface suspended sediment distribution, 11 July 1974.

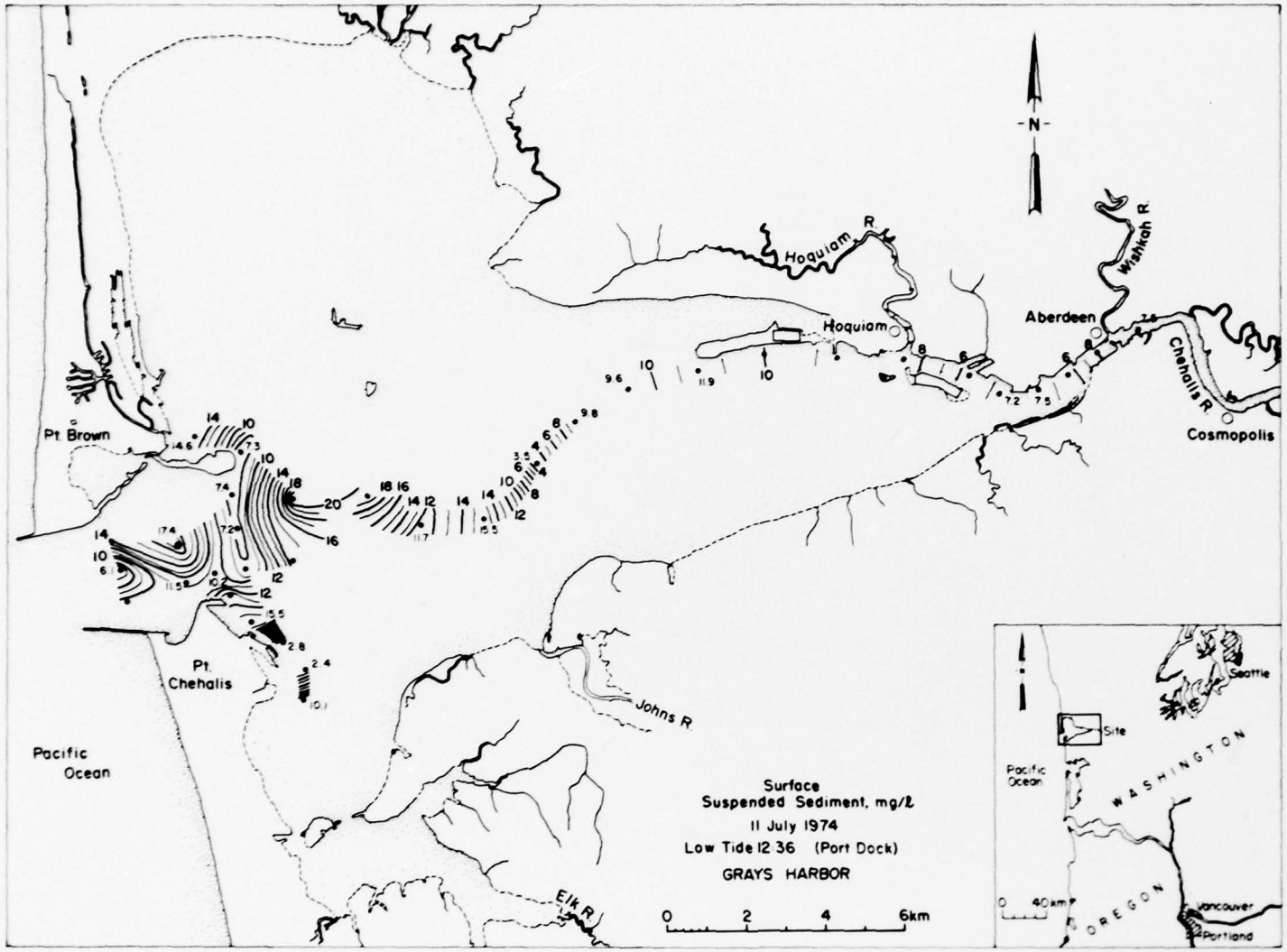

b. Late ebb — early flood.

Figure 33 (cont'd). Surface suspended sediment distribution, 11 July 1974.

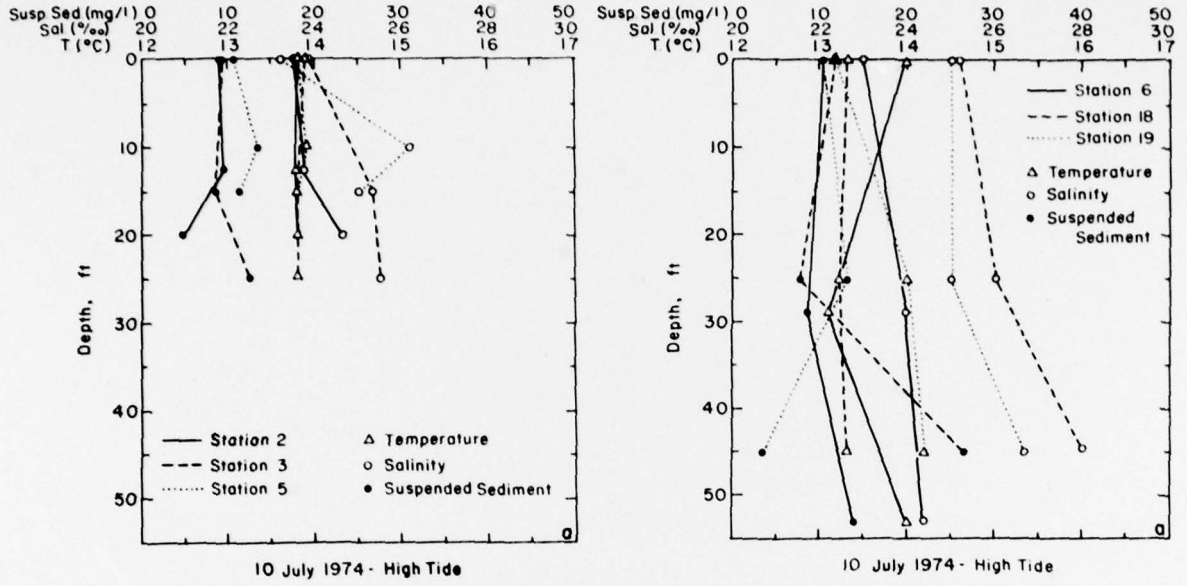

a. Early ebb.

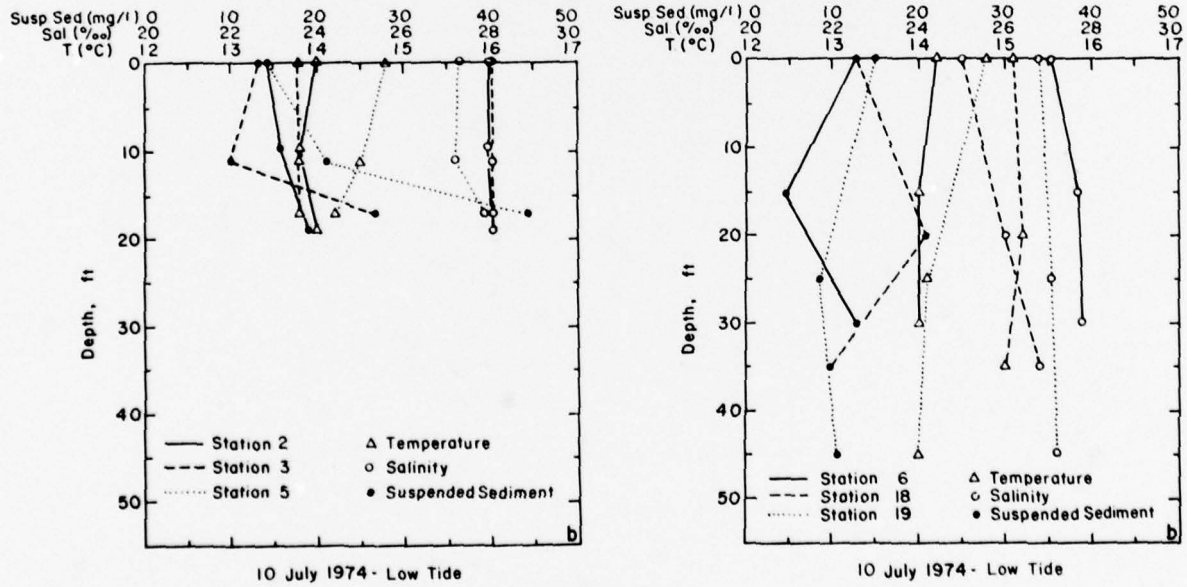

b. Late ebb — early flood.

Figure 34. Water column data, 10 July 1974.

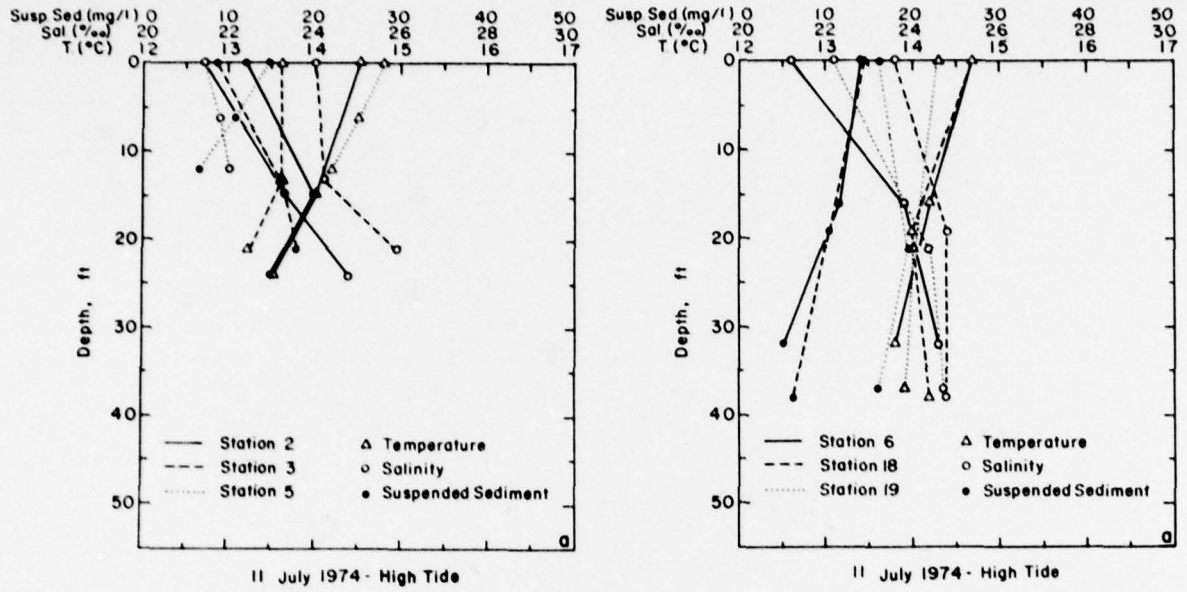

a. Early ebb.

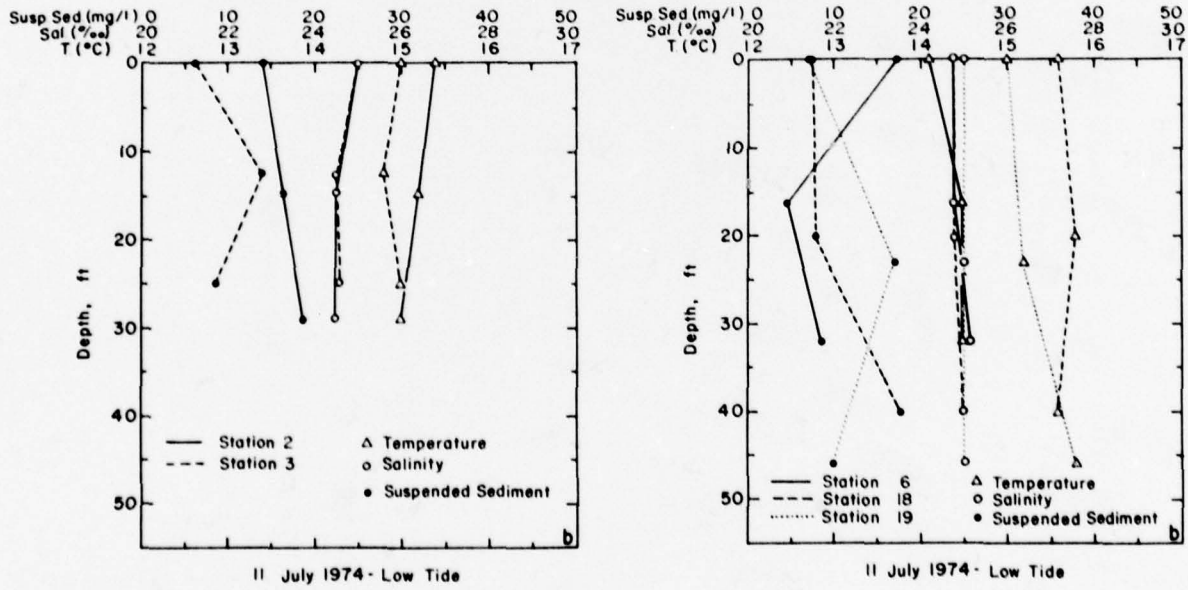

b. Early flood.

Figure 35. Water column data, 11 July 1974.

Temperature variations were greater at the surface and at depth during late ebb-early flood (Fig. 34b) than during early ebb (Fig. 34a). Temperatures varied the most at the eastern stations. All temperatures decreased with depth, although at station 2 the temperatures increased slightly from 3.0 to 6.1 m (10 to 20 ft) after decreasing from the surface to 3.0 m (10 ft). Salinities at stations 2 and 3 were virtually identical with only minor change from surface to the bottom, while salinities between stations located farther into the harbor were more variable. Suspended sediment concentrations with depth were more variable than temperature or salinity. There did not appear to be any discernible relationships or patterns in the concentrations other than high variability below the surface. The concentrations were higher at the bottom than at the surface at stations 2, 3 and 5; at stations 6, 18 and 19 concentrations were equal or less at the bottom.

Water stratification in the harbor entrance was not pronounced although there appeared to be slight changes in temperature and salinity data at depths between 3.0 and 4.5 m (10 and 15 ft) at station 5. The water column generally appeared well mixed at all stations during the different tidal stages.

Data acquired during early ebb (Fig. 35a) on 11 July 1974 were more variable than those acquired on 10 July (Fig. 34a) during the similar tidal stage. Surface temperature and salinity measurements between stations 6, 18 and 19 varied more, while values at depth varied less on 10 July 1974. Suspended sediment values were variable and showed no discernible patterns.

Data from stations 2 and 3 during early flood on 11 July 1974 (Fig. 35b) showed minor differences and variation with depth. Salinities were virtually identical at stations 6, 18 and 19, while more variability in temperature and sediment concentrations was observed between stations at these sites. Stratification was not prominent on 11 July 1974 at the sites although a zone of minor change was defined between 3.6- and 7.6-m (12- and 25- ft) depths. Frequently, surface temperature and salinity values were very similar to those at depth.

Other types of shipboard surveys, not performed for this demonstration project specifically, are tide and current surveys. These provide circulation data for the surface and at depth. These surveys are usually performed with stationary tidal gauges and current meters. Occasionally drifting drogues are used for determination of current velocities and directions. Such surveys are routinely performed by the National Ocean Survey for navigational chart revision and for preparation of tide and tidal current tables. Beverage and Swecker (1969) performed a current survey as part of an environmental quality study of Grays Harbor. Brogdon (1972a) and Brogdon and Fisackerly (1973) reported the results of tide and current surveys accomplished as verification and base tests for the Grays Harbor hydraulic model. These data were used in addition to the temperature, salinity and suspended sediment data in comparing the validity of interpretations made from remote sensing techniques.

Hydraulic modelling

Surface current studies were made of the harbor entrance area with time-exposure photographs of confetti floating on the water surface. Photographs were acquired every hour through a tidal cycle (24.8 hours) and movement of confetti was used to determine current velocities. Dye dispersion studies were also done at various depths and locations to simulate pollutant dispersion.

Surface circulation patterns near maximum ebb in the model (Fig. 36a) were similar to those observed on the RS-14 imagery during the same tidal stage south of Whitcomb Flats, east of Westport and in the eastern South Channel (Fig. 10). Currents in the eastern channels (Fig. 36b) were also comparable. Currents observed during early ebb (2 hours earlier than in Figure 36b) in the eastern harbor are shown in Figure 37. Surface current patterns were apparent only near the north and south jetties on the RC-8 photographs acquired on 13 July 1974 (Fig. 7). Tidal stage was early flood just after low water slack and water movement was minimal. The currents near the ends of the jetties as observed on the photographs were virtually identical to those in the model for a similar tidal stage (Fig. 38). Variations in the color of the surface waters were insufficient to discern circulation elsewhere on the photographs.

Surface currents in the area near the harbor entrance observed on the Zeiss photographs during late flood nearly at high water slack (Fig. 11) were comparable to those shown in the model (Fig. 39a). The areas of minor movement near the north side of the south jetty, just east of Westport, and west of Damon Pt., and currents

a. Near harbor entrance (from Brogdon 1972a).

Figure 36. Surface current patterns in Grays Harbor model at maximum ebb.

b. Eastern harbor (from Brogdon 1975a).

Figure 36 (cont'd).

Figure 37. Surface current patterns in Grays Harbor model during early ebb (from Brogdon 1975a).

Figure 38. Surface current patterns during early flood, Grays Harbor model [from Brogdon (1972a)]

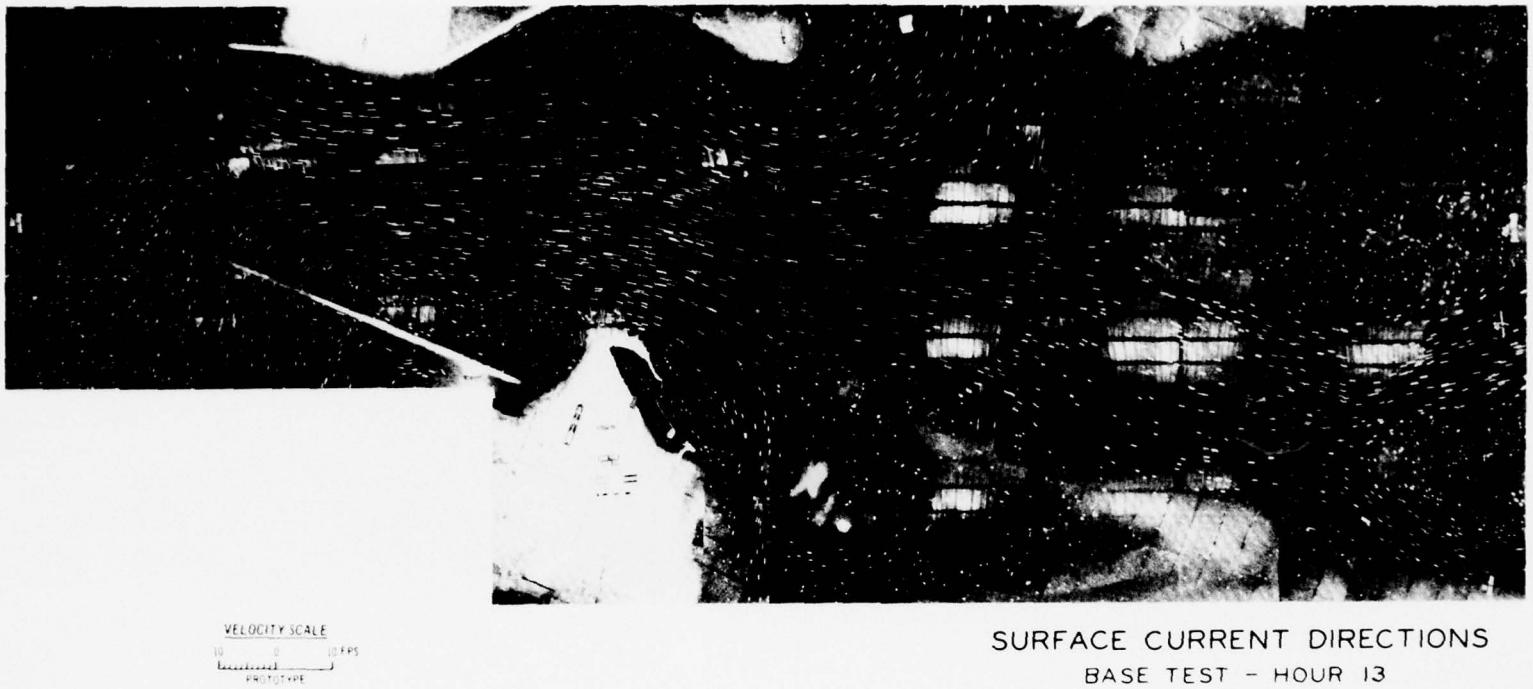

a. Near harbor entrance (from Brogdon 1972a).

Figure 39. Surface current patterns in Grays Harbor model during late flood.

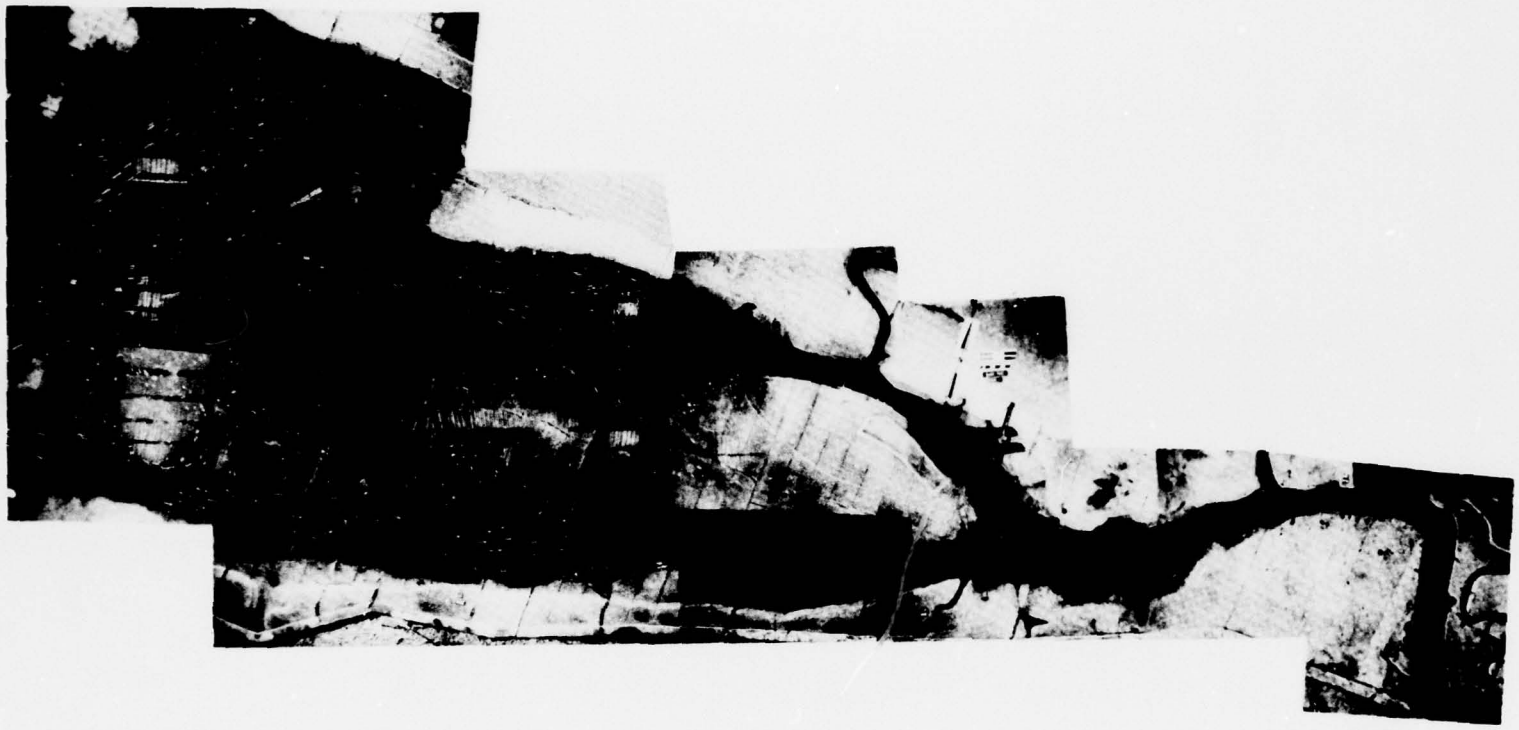

b. Eastern harbor [from Brogdon (1975a)].

Figure 39 (cont'd).

through the entrance (currents observed on photographs were more northeasterly than in the model), into South Bay, and up South Channel were observed on the photographs. The path taken by the flooding water up Crossover channel in the model was not observed on the photographs. The water appeared to move over the tidal flats and did not appear to be directed through the tidal channels as seen in the model. With few exceptions currents in the eastern harbor (Fig. 39b) were generally similar to those observed on the photographs (Fig.11). Currents over the tidal flats southwest of Rennie Island and nearshore westerly currents along the south coast of South Channel which were apparent on the photographs did not form in the model. Seattle District personnel report that there was not enough water in the model at this location for the confetti; also the channel is very narrow here and boundary effects in the model could cause inaccurate patterns.

Surface currents during mid-flood just before the time of maximum flood currents as delineated from M²S imagery (Fig. 14) were comparable to the model results (Fig. 40). The diverging currents just northeast of Westport where a portion goes into the South Channel and the other goes into South Bay at Whitcomb Flats were observed on the imagery (Fig. 40a). The northeasterly currents past the mouth of the Johns River were also delineated. Currents in the eastern harbor (Fig. 40b) were similar except near the Hoquiam Slips 1 and 2. A westerly nearshore current was apparent on the imagery but not formed in the model.

The dye drogues released south of Moon Island (Fig. 16) during the time of maximum flood moved in patterns similar to those on Figure 40b. Dye streams from stationary buoys and the patterns in which the dye drogues moved at the harbor entrance during maximum flood and ebb were also comparable to the model surface current directions for similar tidal stages (Fig. 40a and 36a, respectively), except that model flow was more eastward than northeasterly as shown on the photographs. Near the south jetty the dye drogues moved westerly along the jetty during ebb as did the confetti in the model (Fig. 36a). During flood the drogues moved northeasterly out of the quieter area near the jetty into the main flood stream. This was also comparable to the patterns formed in the model (Fig. 40a).

Comparison of results

Data reliability

The most useful remote sensing data products for circulation studies were the low altitude photographs of the stationary dye streams and drifting dye drogues, and the night thermal imagery. The RC-8 or Zeiss 22.86-cm × 22.86-cm (9-in. × 9-in.) color and CIR photographs were most useful for mapping the distribution of intertidal habitats. The data on current velocities and directions acquired from the dye studies compared favorably with the data acquired from shipboard surveys and published reports. The maps of circulation patterns prepared from the NASA photographs were not as reliable as those prepared from the thermal imagery because there was not sufficient difference in surface water color (due to turbidity) to trace water movement. However, thermal differences and surface patterns apparent on the night imagery served as adequate indicators of surface circulation. Current velocity data were not acquired from this imagery but the current patterns mapped from the thermal imagery were generally comparable to those observed in the hydraulic model.

The circulation patterns inferred from the maps of surface temperature, salinity and suspended sediments in the area near the harbor entrance (stations 1-25) were generally not comparable to the current patterns observed on the imagery. This may be due to rapid mixing of surface waters that have distinct temperature-salinity characteristics prior to mixing. Because current velocities are high in this area the various water types become indistinguishable and temperature-salinity distributions are variable and surface current patterns are difficult to infer.

The LANDSAT-1 imagery was not useful for analysis of surface circulation. Surface water color differences were so small that it was difficult to differentiate water patterns from patterns resulting from bottom reflection effects by photointerpretation techniques. Computer analysis of the radiometric data may provide more information. Coastal patterns north and south of Grays Harbor were readily apparent and the regional physical setting and geomorphology could easily be delineated, but the harbor appeared small and the 70-m (231-ft) resolution on the satellite imagery proved inadequate for addressing the objectives of this project.

a. Near harbor entrance [from Brogdon (1972a)]

Figure 40. Surface current patterns in Grays Harbor model during mid-flood.

b. Eastern harbor [from Brogdon (1975a)].

Figure 40 (cont'd). Surface current patterns in Grays Harbor model during mid-flood.

The following are some of the requirements that must be met for successful use of remote sensing techniques in mapping salt marsh vegetation and eelgrass:

(1) Photo flights must be made during lowest possible tide.

(2) For coastal estuaries, remote sensing data should be gathered between about 1 June and mid-July for eelgrass mapping. This will minimize confusion in interpretation caused by growth of benthic algae on tidal flats.

(3) Ground truth data collection costs and time can be minimized by contracting with investigators who are thoroughly familar with the study area.

(4) Mapping of underwater vegetation will not be possible with standard usage of aerial infrared film with Wratten 12 filter. Use of a filtering system designed specifically for underwater resolution will probably reduce resolution of upland vegetation types.

Three types of aerial photographs were used in mapping Grays Harbor intertidal habitats: NASA color infrared, color (Washington Department of Game), and black and white. The black and white photographs were most readily available and were of sufficient quality to be useful for detailed study. However, the CIR photographs provided the best means of mapping eelgrass, although they were acquired during a +0.9 m (3 ft) low tide when much of the *Z. marina* beds were inundated. CIR photographs would have been ideal for mapping and determining eelgrass extent in Grays Harbor if taken under precisely the right tidal conditions (during an extreme low water tidal stage).

The CIR photographs also provided the most discernible views of salt marsh vegetation. Very subtle changes in plant species composition were detected. However, a major difficulty in mapping with the CIR photographs was caused by the wide range of exposures encountered between photographs. This made it very difficult to develop signatures for particular marsh types based on shades of color. In other words, on any one photograph salt marsh species composition changes were easily discerned. Problems were encountered in observing areas from one photograph to another as varying degrees of exposure caused color shifts.

Color photographs were not useful for eelgrass mapping, and were not used for this purpose. For classification and mapping of salt marsh vegetation they were comparable to CIR photographs. They had the added advantage of not showing the effects of variable exposure between photographs. Signatures were much easier to develop and were useful on all color photographs.

Estimates of the amount of time required to prepare a map (Fig. 24) of eelgrass and marshlands without aerial photographs indicate that the approach discussed here was more cost effective and would take considerably less time: for eelgrass mapping, 20 man-days with aerial photographs, 90 man-days without; for marshland mapping, 35 man-days with photographs, 135 man-days without.

Two estimates of the extent of Whitcomb Island vegetation were made. One estimate, 0.02 km^2 (5.2 acres), was derived using a polar planimeter and the NASA CIR photographs. An estimate for 1975 was determined by pacing the vegetation area. The area was 411.58 × 45.73 m (1350 × 150 ft) or 0.018 km^2 (4.6 acres). There were approximately 0.02 km^2 (5 acres) of dune vegetation developed on Whitcomb Island by 1975.

According to USACE topographic data for 1968 there are 0.057 km^2 (14 acres)above +2.1 m (7 ft) but none over +2.7 m (9 ft). The 0.02-km^2 (5-acre) dune area in 1975 was estimated to be above +3.9 m (13 ft). It was estimated by pacing that approximately 0.06 km^2 (15 acres) were above the highest driftwood line.

An estimate of the effort needed to complete the eelgrass and salt marsh mapping with and without aerial photographs was provided to evaluate the two approaches. These estimates are only approximations since only the method using aerial photographs was used during the study. Costs of equipment were not considered.

For mapping of eelgrass, approximately 10 man-days were required in the field to check eelgrass conditions with the photographs. An additional 10 man-days were required to transfer information from photographs to the map. In contrast, it was estimated that to produce a comparable map of eelgrass in Grays Harbor using boat and field survey techniques would require at least 80 man-days for the field work. Transferring field notes to the map would probably require at least an additional 10 man-days.

Approximately 20 man-days were required for field work to develop and verify the photographic signatures required in mapping salt marsh vegetation from the aerial

Table XVI. Characteristics of and estimated costs for the two methods of data collection.

Remote sensing	*Conventional shipboard*
Aircraft rental: $200-$1000/hr*	Boat costs, $100-$300/day†
Image processing: $1500/200 exposures**	Data collection can take 5-7 times longer
Limited sea-truth data collection with a small boat; boat costs, $100-$300/day	Data reduction/analysis, variable man months††
Imagery analysis, variable man-months††	Data not synoptic, show only site conditions
Shows regional relationships, a synoptic view and large area	Data more accurate, but processes between data stations must be extrapolated***
Local differences between processes are observed	

*Depends on aircraft size; aircraft would be selected based on area to be covered, altitude requirements and types of imagery to be acquired.

†Depends on boat size and whether an operator is included.

**For 22.86-cm×22.86-cm (9-in.×9-in.) format film transparencies; less for smaller format photographs; high altitude processed imagery was provided by NASA as part of the project.

††Depends on amount of imagery or data acquired.

***The accuracy requirement must be determined for the particular applications.

photographs. Another 15 man-days were required to map and calculate extent of the various types. Mapping the salt marshes completely from the ground would probably require at least 120 man-days in the field (minimum of 4 trained people for a 3-month field season). Calculating extent of various types from the completed map would require 15 man-days.

Estimated accuracy of the vegetation mapping is ± 0.0041 km² (± 1 acre) for each discrete marsh or eelgrass bed mapped. A vegetational unit of less than 1 acre in size is not shown on Figure 24. Personnel at the Seattle District consider the reliability of the mapping to be excellent. The reliability of most maps is directly related to familiarity of the investigators with the study area; i.e., the better and more comprehensive the ground truth information, the better the reliability of photointerpretations.

Costs benefits

A cost comparison between data collection techniques from aboard ship and from an aircraft and/or satellite is difficult to make because specific project requirements would determine the most appropriate methods of obtaining data. This project was designed to demonstrate the utility of remote sensing techniques in acquisition of circulation data and in mapping intertidal habitats. Aircraft imagery proved to be a reliable tool in obtaining a synoptic view of the dynamic surface water currents and in mapping habitat distributions.

For comparison purposes, Table XVI shows some generalized characteristics of and estimated costs for the two methods of data collection. It is extremely important to realize that remote sensing techniques must be used in conjunction with conventional ground surveys. It is likely, depending on project requirements, that the number of ground surveys can be reduced when remote sensing techniques are used as a tool along with the standard techniques. Remote sensing techniques are most useful when circulation studies are made in large areas, when repetitive data are required, and when regional synoptic relationships are investigated.

CONCLUSIONS

Advantages and disadvantages

Remote sensing techniques have several advantages. The dynamic processes on and near the water's surface within a large area can be observed simultaneously. Thermal imagery proved to be very useful in providing an overview of the circulation within a large area and in conducting a reconnaissance type circulation study. Color photographs of dye dispersion and drogue movement were the most useful in providing detailed site specific circulation information. Comparisons of the processes between locations can be made for a particular instant. More detail is available than on maps prepared from field data and shipboard techniques can

only provide data for a specific location at an instant. Processes active between stations must be extrapolated or assumed. When used together, the remote sensing and ground survey techniques provide data that allow a fuller view of the processes or area under investigation than would be observed using only one approach. Imagery can be acquired repetitively in less time than repetitive shipboard surveys. Remote sensing provides a permanent record of the processes at the time of image acquisition. In addition, the processes active during varying tidal and seasonal conditions can be readily observed.

There are several disadvantages of using remote sensing techniques. Geometric distortions and scale variations are inherent in the imagery. These limitations should be considered in determining linear distances from photographs. Since scale variations and geometric distortions increase from the central to the peripheral portions of an image, if geometrically corrected photographs are not available, measurements can be made in the middle portion of the image where distortions are minimal. However, utilizing geometrically corrected and rectified imagery to greatly reduce the measurement errors that result from distortions is the best approach. Acquisition of useful aerial photographs is restricted to clear weather or scattered cloud conditions. In addition, when weather conditions are windy, acquisition of useable photographs is increasingly more difficult. However, in windy conditions acquisition of data during ship surveys may also be restricted or eliminated. During data collection (9-11 July 1974) by personnel from Grays Harbor College, surface conditions were windy and several stations near Damon Pt. could not be reached because of high breakers and excessive surface roughness. Generally, data collected from imagery may not be as accurate as data acquired from ship surveys. Also, the types of remote sensing data evaluated during this investigation are limited to surface conditions,while data acquired in shipboard surveys are not. Therefore, the requirements and objectives of an investigation must be considered in determining the application of remote sensing techniques. These techniques can be convenient and useful tools in accomplishing project objectives.

Table XVII. Applications of aircraft and satellite imagery.

A. Use in developing a data base for:
1. Preliminary site selection
2. Coastal zone management decisions
3. Channel and harbor maintenance schedules
4. Regional environmental interpretations
5. Ecosystem protection decisions
6. Environmental impact statements
B. Augment preparation and revision of hydrographic and navigation charts
C. Acquire engineering design data
D. Interpret coastal processes
E. Improve thematic mapping
F. Monitor:
1. Estuarine circulation
2. Dispersion of pollutants
3. Movement of sea ice
4. Sediment distribution
5. Fish migration

Applications

A number of applications in earth resources studies for which data acquired by aircraft and satellites could be used were recognized during this investigation (Table XVII). Additional references to proven applications in a wide variety of earth resources investigations are numerous in the literature. Rather than cite these references, the following list gives a few of the Congressional acts which form the basis for the principal civil works mission responsibilities of the Corps of Engineers for which remote sensing data may be useful:

1. Water and land conservation:
   Federal Water Project Recreation Act, 1965
   Land and Water Conservation Act, 1965
   Outdoor Recreation Act, 1963
   Estuarine Study Act — Inventory of Estuaries, 1968
2. Environmental impacts:
   National Environmental Policy Act, 1969
3. Maintenance of waterways, shorelines and beaches:
   River and Harbor Act, 1962-1968
   Coastal Zone Management Act, 1972
4. Water quality:
   Clean Water Restoration Act, 1966
   Fish and Wildlife Coordination Act, 1946-1958
   Federal Water Pollution Control Act, 1948-1972
   Water Quality Act, 1965
   Marine Protection, Research and Sanctuaries Act, 1972

The utility of aircraft and satellite imagery in meeting some of these responsibilities has been demonstrated or suggested by this or related investigations.

RECOMMENDATIONS

Based on the results of this demonstration project, one primary recommendation is warranted. Remote sensing techniques can provide a regional perspective not obtainable with surface shipboard surveys alone. The data acquired from interpretation of imagery can be as useful as data obtained from extensive field surveys. Therefore, these techniques should be seriously considered and, when determined appropriate, used to augment conventional techniques in the collection of data for operational Corps of Engineers projects.

LITERATURE CITED

Barrick, R.C. (1976) Hydrodynamics of Grays Harbor estuary, Washington, Appendix A. In *Maintenance dredging and the environment of Grays Harbor, Washington*. U.S. Army Engineer District, Seattle, Washington, June, 95 p.

Beverage, J.P. and M.N. Swecker (1969) *Estuarine studies in* upper Grays Harbor, Washington. U.S. Geological Survey, Water Supply Paper 1873-B, 90 p.

Brogdon, N.J., Jr. (1972a) Grays Harbor estuary, Washington, *Report 1, Verification* and base tests. U.S. Army Engineer Waterways Experiment Station (USAE WES), Vicksburg, Mississippi, Technical Report H-77-2, April, 275 p.

Brogdon, N.J., Jr. (1972b) Grays Harbor estuary, Washington, Report 2, North jetty study. USAE WES, Technical Report H-72-2, September, 153 p.

Brogdon, N.J., Jr. (1972c) Grays Harbor estuary, Washington, *Report 3, Westport small-boat basin study*. USAE WES, Technical Report H-72-2, September, 159 p.

Brogdon, N.J., Jr. (1972d) Grays Harbor estuary, Washington, Report 4, South jetty study. USAE WES, Technical Report H-72-2, September, 301 p.

Brogdon, N.J., Jr. (1975a) Grays Harbor estuary, Washington, Report 5, Maintenance studies of 35 ft deep navigation channel. USAE WES, Technical Report H-72-2, October, 208 p.

Brogdon, N.J., Jr. (1975b) Westport small-boat basin, revision study. USAE WES Miscellaneous Paper H-75-8, November, 169 p.

Brogdon, N.J., Jr. (1976) Grays Harbor estuary, Washington, Report 6, 45-ft msl (40-ft mllw) navigation channel improvement studies. USAE WES Technical Report H-72-2, April, 429 p.

Brogdon, N.J., Jr. and G.M. Fisackerly (1973) Grays Harbor estuary, Washington, Report 1, Verification and base tests, Appendix A: Supplementary base test data. USAE WES, Technical Report H-72-2, 324 p.

Cameron, H.L. (1952) The measurement of water current velocities by parallax methods. *Photogrammetric Engineering*, vol. 18, no. 1, p. 99-104.

Cameron, H.L. (1962) *Water current and movement measurement* by time-lapse air photography, An evaluation. *Photogrammetric Engineering*, vol. 28, no. 1, p. 158-163.

Cameron, H.L. (1965) Currents and photogrammetry. In *Oceanography from space*. Woods Hole Oceanographic Institution, Woods Hole, Massachusetts, Reference 65-10, April, p. 29-36.

Cooper, A.W. (1974) Salt marshes. In *Coastal ecological systems of the United States*, vol. 2. Conservation Foundation, Washington, D.C., p. 55-98.

Cowardin, L.M. and V.I. Myers (1974) Remote sensing for identification and classification of wetland vegetation. *Journal of Wildlife Management*, vol. 38, no. 2, 313 p.

Duhaut, J. (1972) Photogrammetry for marine studies. *Photogrammetric Record*, vol. 7, April, p. 273-294.

Gatto, L.W. (1976) Baseline data on the oceanography of Cook Inlet, Alaska. CRREL Report 76-25, July, 83 p. AD A029358.

Green, T. and R.E. Terrell (1978) The surface temperature structure associated with the Keweenaw current in Lake Superior. *Journal of Geophysical Research*, vol. 83, no. C1, p. 419-426.

Hefner, J., W. Brown and F.J. Wobber (1974) *Aerial* photography for coastal wetlands management. *Photographic Applications in Science, Technology, and Medicine*, vol. 9, no. 6, p. 24-29.

Huebner, G.L. (1975) The marine environment. In *Manual of remote sensing*, Falls Church, Va.: American Society of Photogrammetry, vol. 2, chapter 20, p. 1553-1622.

Jefferson, C.A. (1975) Plant communities and succession in Oregon coastal salt marshes. Xerox University Microfilms, Ann Arbor, Michigan.

Keller, M. (1963a) Growth and distribution of eelgrass (*Z. marina L.*) in Humboldt Bay, California. Humboldt State College, M.S. Thesis, 53 p.

Keller, M. (1963b) Tidal current surveys by photogrammetric methods. U.S. Coast and Geodetic Survey, Washington, D.C., Technical Bulletin 22, October, 20 p.

Lillesand, T.M., F.L. Scarpace and J.L. Clapp (1975) Water quality in mixing zones. *Photogrammetric Engineering and Remote Sensing*, vol. 41, no. 3, March, p. 285-298.

MacDonald, K.B. and M.G. Barbour (1974) Beach and salt marsh vegetation of the North American Pacific coast. In *Ecology of halophytes* (R.J. Reimold and W.H. Queen, Editors), New York: Academic Press, p. 175-235.

McRoy, C. (1966) The standing stock and ecology of eelgrass (*Zostera marina L.*) in Izembek Lagoon, Alaska. University of Washington, M.S. Thesis, 138 p.

Messmer, L. (1971) A partial list of the vascular plants of the "sink" on the Oyhut Peninsula. Washington Department of Game, unpublished manuscript, Olympia, Washington, 5 p.

Meyer, W. and R.J. Welch (1975) *Water resources assessment*. In *Manual of Remote Sensing*, Falls Church, Va., American Society of Photogrammetry, vol. 2, chapter 19, p. 1479-1551.

Munday, J.C., C.S. Welch and H.H. Gordon (1978) Outfall siting with dye-buoy remote sensing of coastal circulation.

Photogrammetric Engineering and Remote Sensing, vol. 44, no. 1, p. 87-96.

National Aeronautics and Space Administration (1972) Earth observations aircraft remote sensing handbook. 3 volumes. Manned Spacecraft Center, Houston, Texas, MSC-04810, April, p. 5-110.

National Ocean Survey (1972a) Tidal current tables, 1973. National Oceanic and Atmospheric Administration, Rockville, Maryland, 254 p.

National Ocean Survey (1972b) Tide tables, 1973. National Oceanic and Atmospheric Administration, Rockville, Maryland, 222 p.

National Ocean Survey (1973) Tidal current tables, 1974. National Oceanic and Atmospheric Administration, Rockville, Maryland, 254 p.

National Ocean Survey (1973 and 1974) Tide tables, 1974 and 1975. National Oceanic and Atmospheric Administration, Rockville, Maryland, 222 p.

Parker, R. (1975) Waterfowl habitat inventory, eelgrass survey. Washington State Game Department, Game Management Div. Proj. no. W-27-R-27.

Phillips, R.C. (1974) Temperate grassflats. In *Coastal ecological systems of the United States* (H.T. Odum, B.J. Copeland and E.A. McMahan, Editors), vol. II. The Conservation Foundation, Washington, D.C., p. 244-299.

Phipps, J.B. (1977) Environmental summary maps of Grays Harbor, Washington. Grays Harbor College, Aberdeen, Washington, 23 p.

Ramey, E.H. (1968) Measurement of ocean currents by photogrammetric methods. U.S. Coast and Geodetic Survey, Rockville, Maryland, Technical Memorandum 5, May, 18 p.

Scheidegger, K.F. and J.B. Phipps (1976) Dispersal patterns of sand in Grays Harbor estuary, Washington. *Journal of Sedimentary Petrology*, vol. 46, no. 1, p. 163-166.

Smith, J.L., D.R. Mudd and L.W. Messmer (1976a) Impact of dredging on the vegetation in Grays Harbor, Appendix F. In - *Maintenance dredging and the environment of Grays Harbor, Washington*. U.S. Army Corps of Engineers District, Seattle, Washington, June, 122 p.

Smith, J.L., D.R. Mudd and L.W. Messmer (1976b) Impact of dredging on the vegetation in Grays Harbor. Washington Department of Game Final Report prepared for the Corps of Engineers, Seattle District, January, 122 p.

Stroud, L. and A.W. Cooper (1968) Color-infrared aerial photographic interpretation and net primary productivity of a regularly flooded North Carolina salt marsh. Water Resources Institute, University of North Carolina, Report no. 14.

Thayer, G.W., D.A. Wolfe and R.B. Williams (1975) The impact of man on seagrass systems. *American Scientist*, vol. 63, no. 3, May-June, p. 288-296.

Thomas, M.L.H. and J.R. Duffy (1968) Butoryethanol ester of 2,4-D in the control of eelgrass (*Zosterma marina* L.) and its effects on oysters (*Crassostrea virginica* Gmelin) and other benthos. *Proceedings, Northeastern Weed Control Conference*, vol. 22, p. 186-194.

U.S. Army Corps of Engineers, North Pacific Division, Seattle and Portland Districts (1971) Columbia-North Pacific Region: National Shoreline Study, Inventory report, August, 80 p.

U.S. Army Corps of Engineers, Seattle District (1975) Grays Harbor and Chehalis River navigation project, operation and maintenance: Final Environmental Impact Statement, Seattle, Washington, June, 260 p.

Waddell, J.E. (1964) The effect of oyster culture on eelgrass (*Zostera marina* L.) growth. Humboldt State College, M.S. Thesis, 48 p.

White, R. and M. Knowles (1976) *Underwater investigation of* hopper disposal vicinity, Appendix D. In *Maintenance dredging and the environment of Grays Harbor Washington*. U.S. Army Corps of Engineers District, Seattle, Washington, June, 6 p.

Welch, C.S. and J.C. Munday (1977) An aerial strategy for studying frontal structures in coastal waters (abstract). *EOS, Transactions, American Geophysical Union*, vol. 58, no. 9, September p. 801. Presented at Chapman Conference on Oceanic Fronts, New Orleans, Louisiana, 11-14 October 1977.

In accordance with letter from DAEN-RDC, DAEN-ASI dated 22 July 1977, Subject: Facsimile Catalog Cards for Laboratory Technical Publications, a facsimile catalog card in Library of Congress MARC format is reproduced below.

Gatto, Lawrence W.
Estuarine processes and intertidal habitats in Grays Harbor, Washington - A demonstration of remote sensing techniques / by Lawrence W. Gatto. Hanover, N.H.: U.S. Cold Regions Research and Engineering Laboratory; Springfield, Va.: available from National Technical Information Service, 1978.
vi, 85 p., illus.; 27 cm. (CRREL Report 78-18.)
Prepared for Directorate of Civil Works - Office, Chief of Engineers by Corps of Engineers, U.S. Army Cold Regions Research and Engineering Laboratory under Project Nos. CWP-S-75-9 and CWR-S-74-16.
Bibliography: p. 78.

see NEXT CARD

Gatto, Lawrence W.
Estuarine processes...
1978 (Card 2)

1. Aircraft photography. 2. Data acquisition. 3. Ecology. 4. Estuaries. 5. Grays Harbor, Washington. 6. Ground truth data. 7. Intertidal habitats. 8. LANDSAT imagery. 9. Remote sensing techniques. 10. Water surface circulation. I. United States. Army. Corps of Engineers. II. Series: Army Cold Regions Research and Engineering Laboratory, Hanover, N.H. CRREL Report 78-18.